Changjiang Delta in the Anthropocene

Multi-scale hydro-morphodynamics and management challenges

Guo, Leicheng; Zhu, Chunyan; Xie, Weiming; Xu, Fan; Wu, Hui; Wan, Yuanyang; Wang, Zhanghua; Zhang, Weiguo; Shen, Jian; Wang, Zheng Bing

DOI
10.1016/j.earscirev.2021.103850

Publication date
2021

Document Version
Final published version

Published in
Earth-Science Reviews

Citation (APA)
Guo, L., Zhu, C., Xie, W., Xu, F., Wu, H., Wan, Y., Wang, Z., Zhang, W., Shen, J., Wang, Z. B., & He, Q. (2021). Changjiang Delta in the Anthropocene: Multi-scale hydro-morphodynamics and management challenges. *Earth-Science Reviews*, *223*, Article 103850. https://doi.org/10.1016/j.earscirev.2021.103850

Earth-Science Reviews 223 (2021) 103850

Contents lists available at ScienceDirect

Earth-Science Reviews

journal homepage: www.elsevier.com/locate/earscirev

Changjiang Delta in the Anthropocene: Multi-scale hydro-morphodynamics and management challenges

Leicheng Guo [a,*], Chunyan Zhu [a,b], Weiming Xie [a], Fan Xu [a], Hui Wu [a], Yuanyang Wan [c], Zhanghua Wang [a], Weiguo Zhang [a], Jian Shen [d], Zheng Bing Wang [b,e], Qing He [a]

[a] State Key Laboratory of Estuarine and Coastal Research, East China Normal University, Shanghai 200241, China
[b] Civil Engineering and Geosciences faculty, Delft University of Technology, PO Box 5048, Delft 2600 GA, the Netherlands
[c] Shanghai Estuarine and Coastal Research Center, Shanghai 201201, China
[d] Virginia Institute of Marine Science, College of William & Mary, Gloucester Point, Williamsburg, VA 23062, USA
[e] Deltares, PO Box 177, Delft 2600 MH, the Netherlands

ARTICLE INFO

Keywords:
Delta
Tide
Sediment
Morphology
Human activities
Changjiang

ABSTRACT

The Changjiang Delta (CD) is one of well-studied large deltas of critical socio-economical and ecological importance regionally and global representativeness. Cumulated field data and numerical modeling has facilitated scientific understanding of its hydro-morphodynamics at multiple spatial and time scales, but the changing boundary forcing conditions and increasing anthropogenic influences pose management challenges requiring integrated knowledge. Here we provide a comprehensive synthesis of the multi-scale deltaic hydro-morphodynamics, discuss their relevance and management perspectives in a global context, and identify knowledge gaps for future study. The CD is classified as a river-tide mixed-energy, muddy and highly turbid, fluvio-deltaic composite system involving large-scale land-ocean interacted processes. Its hydro-morphodynamic evolution exhibits profound temporal variations at the fortnightly, seasonal, and inter-annual time scales, and strong spatial variability between tidal river and tidal estuary, and between different distributary channels. As the river-borne sediment has declined >70%, the deltaic morphodynamic adaptation lags behind sediment decline because sediment redistribution within the delta emerges to play a role in sustaining tidal flat accretion. However, the deltaic channels have become narrower, deepened and growingly constrained under cumulated human activities, e.g., extensive embankment and construction of jetties and groins, possibly initiating a decrease in morphodynamic activities and sediment trapping efficiency. Overall, the CD undergoes transitions from net sedimentation and naturally slow morphodynamic adaptation to erosion and human-driven radical adjustment. A shift in management priority from delta development to ecosystem conservation provides an opportunity for restoring the resilience to flooding and erosion hazards. The lessons and identified knowledge gaps inform study and management of worldwide estuaries and deltas undergoing intensified human interferences.

1. Introduction

Deltas are globally densely populated regions in the land-to-ocean interface and are of essential socio-economical and ecological importance (Muis et al., 2016). However, they are also facing high risks of erosion, flooding, loss of habitats and associated ecosystem owing to changing climate, sea-level rise (SLR), and human activities (Syvitski et al., 2009; Tessler et al., 2015). Human activities have become a primary force in modulating earth system at varying spatial and time scales, leading to the initiation of an Anthropocene Epoch since the mid-20th century, which is characterized by unprecedented anthropogenic influences in changing climate, altering river discharge and sediment load, disturbing landscape and altering biogeochemical cycles and biodiversity (Waters et al., 2016; Syvitski et al., 2020). Management and restoration of deltas need integrated perspectives and long-term vision that involves multiple stakeholders and comprises. Basic knowledge of deltaic dynamics in specific cases and/or that of general implications is needed for optimized management strategy and better restoration opportunity.

The Changjiang Delta (CD), also called Yangtze Delta, is one of the

* Corresponding author.
E-mail address: lcguo@sklec.ecnu.edu.cn (L. Guo).

https://doi.org/10.1016/j.earscirev.2021.103850
Received 6 July 2021; Received in revised form 28 October 2021; Accepted 1 November 2021
Available online 5 November 2021

largest well-studied deltas in the world in terms of the magnitude of river discharge (4620–92,600 m^3/s), the huge amount of riverine sediment supply (85–678 Mt. yr^{-1}), the strength of tides (maximal tidal range up to 5.9 m), and its geometric size (~650 km of inland tidal propagation and a mouth width of ~90 km). In terms of forcing strength and size, the CD is only second to the Amazon Estuary, which is ~1100 km in length and forced by a river discharge up to 270,000 m^3/s (Gallo and Vinzon, 2005; Nittrouer et al., 2021), and the Ganges-Brahmaputra-Meghna delta complex (Wilson and Goodbred Jr., 2015). However, the former is located in the Amazon rainforest where human development, management demand and scientific researches are relatively minor. In that sense, the CD renders an excellent example of a large-scale fluvio-deltaic system with outstanding human development and management challenges and accumulated knowledge in the subject of the estuary and delta sciences. Note that both Changjiang Estuary and Changjiang Delta were used to refer to the river mouth zone of the Changjiang River in different subjects. In this study, CD is preferred because it encompasses both the subaerial and subaqueous zones.

The CD is located at the land-ocean interface where the Changjiang River, also called Yangtze River, with a main river length of ~6300 km, meets the East China Sea (ECS), an epi-continental marginal shelf sea in the west of the Pacific Ocean (Fig. 1). The river's silt-laden water brings a huge amount of sediment and builds up the mega CD beyond Nanjing since 8000 aBP (Chen et al., 1985; Li et al., 2002; Song et al., 2013a; Wang et al., 2018c). The CD hosts a cluster of large cities (including the metropolis Shanghai) and is home to a total population of ~237 million (~6% of Chinese people). The annual GDP output in the CD was ~90 trillion RMB (~20% of the national GDP in 2018), implying its fundamental socio-economical importance. The CD is also of profound ecological significance given that the brackish water environment is home to important species like the *Chinese Sturgeon*, and the tidal wetlands provide valuable habitats for migratory birds in East Asia. The saltmarshes in the coastal ecosystem of CD also play a role in dissipating waves, trapping sediment, and stimulating tidal flat accretion, which is beneficial to coastal defense from flooding and erosion.

Knowledge of the hydro-morphodynamics in the CD is a prerequisite for better management and sustainable development. One of the urgent management challenges is the delta adaptation in response to changing conditions such as the regulated river flow and declined sediment load, SLR, and increasing human activities. These changing conditions affect saltwater intrusion and threaten freshwater supply for >10 million people in Shanghai, affect the maintenance of the golden navigational waterway stretching thousands of kilometers inland from the delta, endanger conservation of saltmarshes and associated habitats and ecosystems, and challenge coastal defense against delta erosion and typhoon-enhanced compound flooding risk. Therefore, a comprehensive understanding of deltaic hydro-morphodynamics is pivotal for regional management and strategic planning.

Studies of the hydro-morphodynamics in the CD have a history of >70 years since the 1950s (Chen, 1957). Historically, 'dominated by huge river flow and macro-tides and moderate wave, the sheer size of the Changjiang Estuary, plus variations in river flow, tidal stage and phase, as well as the bifurcations of flow through various channels, combine to create a complex hydrographic and sedimentologic environment, which are only being understood in a semi-quantitative sense' (pp. 37, Milliman et al., 1985). New knowledge has accumulated in the recent four decades as long-time series of data available and new instrument and modeling methods deployed. But there still lacks a comprehensive synthesis of the achievements and remained knowledge gaps. Scientific knowledge of hydro-morphodynamics in river- and tide-controlled mixed-energy deltas and estuaries is comparably less than that acquired on river−/wave-dominated deltas and tide-dominated estuaries. In this contribution, we provide a synthesis of the multi-scale hydro-morphodynamics in the CD, discuss their importance and implications in a global context, provide a conceptual development model for fluvio-deltaic systems, and identify research questions for future study. Such understandings may shed lights on coastal science and management in general.

2. System setting and data

2.1. Brief introduction to the CD

The present CD has a length of ~650 km in which more than one tidal wave (wavelength of ~400 km for M_2 tide given a mean water depth of 10 m) can be accommodated. Datong is the limit of tidal wave propagation in the dry season, where river discharge is regularly monitored (Fig. 1); Jiangyin is the limit of tidal current reversal (~405 km downstream of Datong) upstream of which tidal currents cease to reverse in direction. Based on the longitudinal variations in river and tidal forcing strength, the CD is divided into three segments: a tidal river between Datong and Jiangyin, a tidal estuary between Jiangyin and the mouth zone, and a nearshore reach seaward of the mouth (Shen and Pan, 2001; Fig. 1).

River discharge and tides are the most important primary forces in the CD, leading to predominant partial stratification in its mouth zone, while monsoon-driven wind, waves and storm events, and shelf currents are of comparatively secondary importance, The CD is a highly turbid and muddy environment with high suspended sediment concentrations (0.5 kg/m^3 on average but occasionally up to 100 kg m^{-3} in the near bottom layer under energetic conditions in the turbidity maximum zone) and subtle fine sediment transport dynamics (Wan et al., 2014; Lin et al., 2021). Morphologically, the CD is a fluvio-deltaic composite system (Fig. 1b), with multiple bifurcations into the North Branch, North Channel, North Passage, and South Passage. Nowadays the South Branch (the reach between Xuliujing and Wusong) receives a major portion of subtidal ebb flow compared with the North Branch; the latter is presently a tide-dominant environment with little fluvial influence. The North Channel, North Passage, and South Passage occupy the mouth zone, also called the turbidity maximum (TM). Broad tidal flats and shoals develop between the branches in the mouth zone, such as the eastern Chongming flat, the eastern Hengsha flat, the Jiuduan shoal and the Nanhui flat (Fig. 1c).

The mouth zone of the CD is wide and shallow. Its channel depth is usually <7 m below the reference datum, i.e., the lowest low tide, which is the theoretically lowest low tidal water levels. The shallow channels behave as transverse bars between the inner delta and the outer sea (Fig. 1), called mouth bars (Chen et al., 1979, 1985). The mouth bars hinders navigation of increasingly larger containers and cruise ships that require larger water depth. Extensive regulations and dredging were then implemented in the selected main waterway, the North Passage, to keep deep channels and promote shipping industry. Moreover, extensive reclamation of tidal flats in the past seven decades has enlarged the subaerial delta area (see Section 6.2).

2.2. Data and methods

We collected and compiled a series of data in terms of river discharge, sediment load, tidal height, suspended sediment concentrations, bathymetry, and satellite images from literature, public database, and our own measurements, which complemented literature review. The yearly and monthly streamflow and sediment load data were from Guo et al. (2018, 2019) and published bulletins (http://www.mwr.gov.cn/sj/tjgb/zghlnsgb/; China Water Resources Committee (CWRC), 2010, China Water Resources Committee (CWRC), 2020). Daily river discharge data were collected from the hydrology bureau of the Changjiang Water Resources Commission (http://www.cjh.com.cn/sqindex.html).

Hourly tidal height data throughout the delta were collected from the water resources departments of Anhui and Jiangsu Provinces (http://yc.wswj.net/ahsxx/LOL/public/public.html; http://221.226.28.67:88/jsswxxSSI/Web/Default.html?m = 2). Subtidal water levels

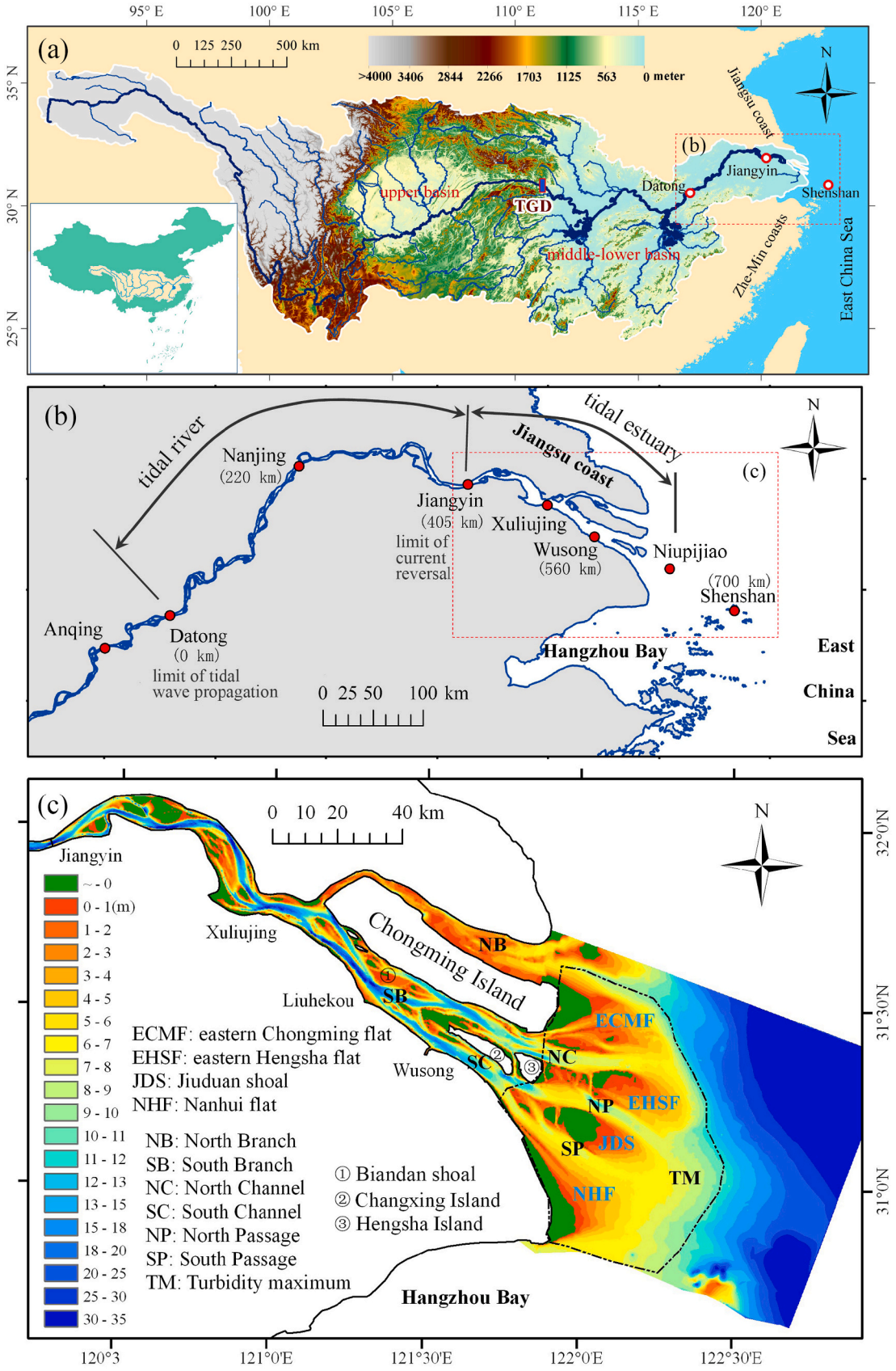

Fig. 1. (a) The DEM of the Changjiang River basin, (b) a top view of the river course of the CD, and (c) the bathymetry in 1997 in the delta regions seaward Jiangyin. The water depth in (c) is referenced to the lowest low tide.

were estimated using a high-pass filter. To calculate the time-varying tidal ranges, the hourly tidal height data were first high-pass filtered to remove variations at subtidal frequencies and then interpolated into 6-min intervals. Tidal ranges were estimated by the differences between the minimum and maximum water levels using a moving 27-h window (Guo et al., 2015). Amplitudes and phases of individual tidal constituents were resolved by harmonic analysis (Pawlowicz et al., 2002). More details of the tidal analysis methods are referred to Guo et al. (2015, 2020).

Sediment concentration and composition data were collected from Liu et al. (2010a) and Yang, Li, Zhang, Qiao, Liu, Bi, Zhang, and Zhou (2020a, Yang, Luo, Temmerman, Kirwan, Bouma, Xu, Zhang, Fan, Shi, Yang, Wang, Shi, and Gao, 2020b). Usually water samples of 600 ml were collected at six layers vertically each hour for 27 h (representing a full tidal cycle) and suspended sediment concentrations were obtained by filtering the water through the Millipore filter membrane and then dried and weighed. Sediment composition was analyzed using Coulter LS 100Q grain-size analyzer (Liu et al., 2010a).

Bathymetry data since 1958 were collected from Zhao et al. (2018) and Zhu et al. (2019), and the recent survey data were from the management departments of the navigation waterway. These data were georeferenced and corrected to the same datum, the lowest low tide, which enables studies of decadal morphodynamic changes and the erosion-deposition patterns. These data mainly covers the regions downstream of Xuliujing, while discussion of the erosion and deposition changes in the river reaches between Datong and Xuliujing was based on literature (Wang et al., 2009; Zheng et al., 2018b).

Satellite images from 1974 were obtained from Landsat source (https://www.usgs.gov/core-science-systems/nli/landsat) and georeferenced to reveal large-scale changes in coastline and human activities. We also collected and compiled historical geography maps showing the topography of the delta in the period before instrumental data was available, e.g., the period prior to 1900, from the library of the University of Texas library (http://legacy.lib.utexas.edu/maps/historical/), the Virtual Shanghai website (https://www.virtualshanghai.net), the David Rumsey Map Collections (https://www.davidrumsey.com), and the United States Library of the Congress (https://www.loc.gov). Assemble of these data helps to put up an integrated picture of the forcing conditions and the deltaic physics.

3. Changing forcing conditions

3.1. Fluvial forces

3.1.1. River discharge changes

The long-term (1953–2020) averaged river discharge is ~28,500 m^3/s at Datong, and the recorded maximal river discharge was 92,600 m^3/s (on 1 Aug 1954) and the minimum was 4620 m^3/s (on 31 Jan 1979) (Zhang et al., 2003). Under the influence of the Asian monsoon, the river discharge exhibits profound seasonal and inter-annual variations (Fig. 2b), with a hydrograph that is typical for large subtropic rivers. Both catastrophic river floods (e.g., in 1954, 1998, and 2020) and severe droughts (e.g., in 1978 and 2006) are likely to happen (Fig. 2a). To control big floods and facilitate hydropower generation, water usage and navigation, a series of large dams, including the Three Gorges Dam (TGD) (Fig. 1a), were constructed in the upstream main river since the 1990s, profoundly altering the river discharge and sediment load regime (Guo et al., 2019).

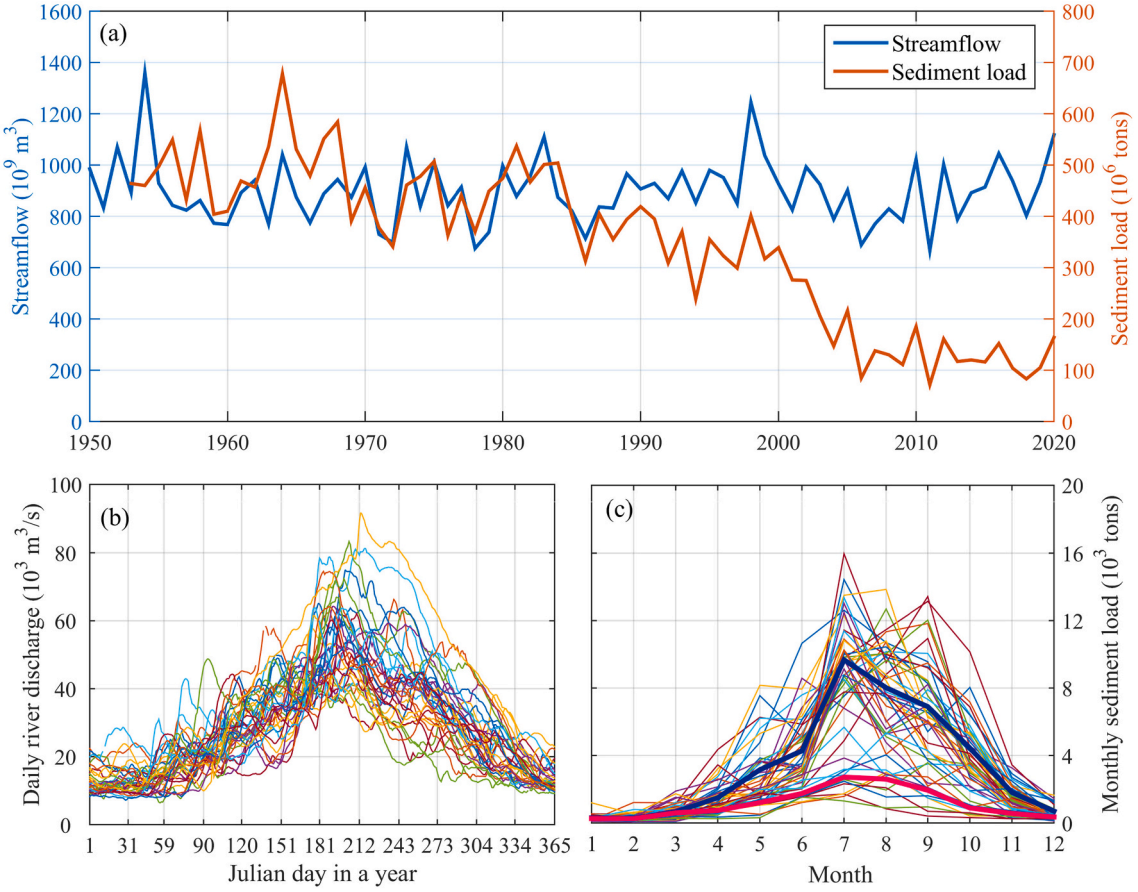

Fig. 2. River discharge and sediment load changes at Datong: (a) annual streamflow and sediment load since the 1950s, (b) daily river discharge hydrographs, and (c) monthly sediment load based on data in 1953–2020. The two thick lines in (c) indicate the mean value in the periods of 1953–2002 (blue) and 2003–2020 (red). (For interpretation of the references to colour in this figure legend, the reader is referred to the web version of this article.)

The TGD, the large dam constructed between 1994 and 2009 in the main river approximately 1220 km upstream Datong, has a storage capacity of 36.3 km^3, and could reduce the flood peak discharge by maximally 30,000 m^3/s in the wet seasons and flush 500–3000 m^3/s more water downstream in the dry seasons (Guo et al., 2018). At the decade to century time scales, the annual streamflow at Datong has not exhibited directional increasing or decreasing trend (Fig. 2a), other than a reduction change point detected in 1954 (Guo et al., 2018; Fig. S1 in the Supporting Information, SI). It is noteworthy that water withdrawal along the delta downstream of Datong might be considerable (Zhang et al., 2003), which could reduce the actual river discharge in counteracting saltwater intrusion in the dry seasons. Global climate change and increasing water consumption within the river basin may alter the river discharge regime in the future, e.g., possibly more concentrated precipitation and larger peak flood discharge (Nakaegawa et al., 2013).

3.1.2. Sediment load reduction

The Changjiang River supplies significant amounts of (suspended) sediment load to the river mouth in stimulating delta development. In the long term, the riverine sediment load 2000 years ago was estimated to be much smaller than the present-day value based on interpretation of accumulated sediment volume in the delta (Wang et al., 2013a, 2018c). Since then a small increase in sediment load was detected due to increased population and human activities in the watershed, followed by a fast increase in the recent ~800 years owing to accelerated human activities and land-use changes (Chen et al., 1979; Wang et al., 2008, 2011). Field monitoring of sediment flux started in the early 1950s and the data suggested a mean sediment load of 470.4 Mt. yr^{-1} between 1950 and 1985 at Datong (Fig. 2a). The sediment load exhibited stepwide decreases since 1985, owing to the combined influences of reforestation, soil conservation and hydropower dams within the river basin (Yang et al., 2006, 2011; Xu and Milliman, 2009; Guo et al., 2019). The TGD accelerated the decrease since 2003, and the yearly sediment load has approached a temporal low level of 122.8 Mt. yr^{-1} in 2006–2020, which was ~26% of the mean value in 1950–1985. Sediment replenishment from channel erosion downstream of TGD and increased sediment output from the tributaries and lakes partially explained the sediment load recovery, when comparing with more striking reduction at Yichang (from 530 Mt. yr^{-1} in 1950–1985 to 24 Mt. yr^{-1} in 2006–2020), the gauge ~40 km downstream the TGD (Guo et al., 2019; Tian et al., 2021).

Intra-annually, more than 87% of the sediment load was delivered in the wet seasons between May and September (Fig. 2c). The reduction in sediment load in the wet seasons was much more profound in the post-TGD decades (Xu and Milliman, 2009; Guo et al., 2018). Although sediment transport rates are expected to be exponentially larger for high river discharge in theory, the suspended sediment concentrations in the middle-lower river did not increase apparently for river discharge >50,000 m^3/s (Yin and Chen, 2009), which was ascribed to a deficiency in fine sediment, i.e., a source-limited condition. This sediment deficiency is to be exacerbated in the post-TGD era considering declined sediment source from the upper basin and downstream bed texture changes as a result of channel degradation (Lai et al., 2017).

The suspended sediment reaching the delta was composed of clay and silt, with a median grain size of ~27 μm in the pre-TGD period, while the bed sediment was sandier, with median grain size of ~166 μm at Datong (Shen, 2001; Liu, 2009). Along with sediment load reduction, the suspended sediment becomes finer downstream of the TGD (Luo et al., 2012; van Maren et al., 2013; Li et al., 2017), with the median grain size decreased to ~11.7 μm between 2000 and 2020. The bed sediment becomes coarser downstream of the TGD, and the consequent armoring effect plays a role in slowing down fluvial morphodynamic adjustment and sediment replenishment might eventually diminish (Lai et al., 2017). Considering the combined effects of the series of large hydropower dams in the upper main river and the armoring effect along the downstream river, the river-supplied sediment to the delta is likely to persist at a low value in the coming 100–400 years, and the subsequent impact on the deltaic morphodynamics arises management concern (see Section 5.2).

3.2. Variability of tidal dynamics

Tidal waves propagating into the CD mainly consist of progressive waves stemming from the ECS, with a mean direction of 305° (Shen et al., 1989a; Fig. S2). This tidal wave direction, together with the Coriolis force, was ascribed to control the overall alignment of channel development and the south-eastward extending axis of the CD (Chen et al., 1979; Shen et al., 1989a). However, the role of tidal wave direction and the Coriolis effect in causing asymmetric delta development has not been soundly validated.

The tides acting in the CD have a mixed diurnal and semi-diurnal regime, with M_2 the most important constituent, followed by S_2, O_1, and K_1. The mean tidal range is 2.7 m at the mouth zone while the maximal tidal range is 5.9 m (Guo et al., 2015). Temporally, tidal ranges exhibit strong fortnightly (spring-neap), monthly (perigee-apogee), semi-annual (March and September equinox) and inter-annual (due to river discharge) variations (Fig. 3c). The tidal ranges during the perigean spring tides in September (when the mean sea level is also higher, see Fig. 4b) are the largest within a year course. Spatially, the tidal ranges are larger in the North Branch than in the South Branch; and tidal bores may form in the inland regions of the North Branch owing to its convergent planform (Chen, 2003). The tidal ranges are maximal in the seaward front of the mouth zone, e.g., at Niupijiao, and predominantly decay inland owing to the combined influence of friction and river discharge, albeit the width convergence seaward of Jiangyin (Fig. 3d). At the decadal time scale, the tidal ranges exhibited limited changes since 1990 (Zhu et al., 2021), whereas longer-term (decadal to centennial time scale) changes were limitedly reported owing to scarcity of long-term tidal data, although strong morphological changes and human activities have occurred.

River discharge plays a significant role in modulating tidal wave propagation in the CD. River discharge leads to a significant increase in the river stage, from ~4 m (Wusong Datum, the lowest tidal water level at Wusong gauge based on data in 1871–1900, which is used as the reference for river stage and land elevation) in the dry seasons to ~16 m in the wet seasons at Datong (Figs. 3b and S3). A higher mean water level and a larger longitudinal water level gradient enhance stronger tidal damping in the wet seasons, particularly along the tidal river (Cai et al., 2014). River discharge also enhances tidal wave deformation by shortening the rising tidal period and prolonging the falling tidal period. The falling tidal period increases landward from 6.2 h at Niupijiao to 8.6 h at Nanjing at the spring tide in the dry season. The tidal duration asymmetry is further confirmed by a significant M_4 overtide detected inside the delta (Guo et al., 2015). Given the energy of M_4 is mainly derived from M_2, its amplitude is larger in the mouth zone in the wet season and decays landward (Fig. 3e). Moreover, a significant fortnightly component MSf is detected in the tidal river, which induces lower low water and mean water level at neap tides than spring tides (Figs. 3b and f). This frequency-dependent behavior confirms that large estuaries behave as frequency filters: the long-period low-frequency oscillations with larger wavelengths dampen more slowly and travel further inland compared with the astronomical diurnal and semi-diurnal tides (Godin, 1999). The inland penetration of the low-frequency oscillations also suggests more landward tidal influence than the wave limit of astronomical tides, which possibly increases the river stage and induce fluvial-tidal compound flooding risk along tidal rivers (Guo et al., 2020).

The tidal prism (~10^9 m^3) was reported to be an order of magnitude larger than the river streamflow (~10^8 m^3 during a tidal cycle) in the CD (Shen et al., 1989a). The tidal prism is expected to have decreased over time given reduced channel volumes as a result of sediment deposition and tidal flat embankment, but it remains an open question to what

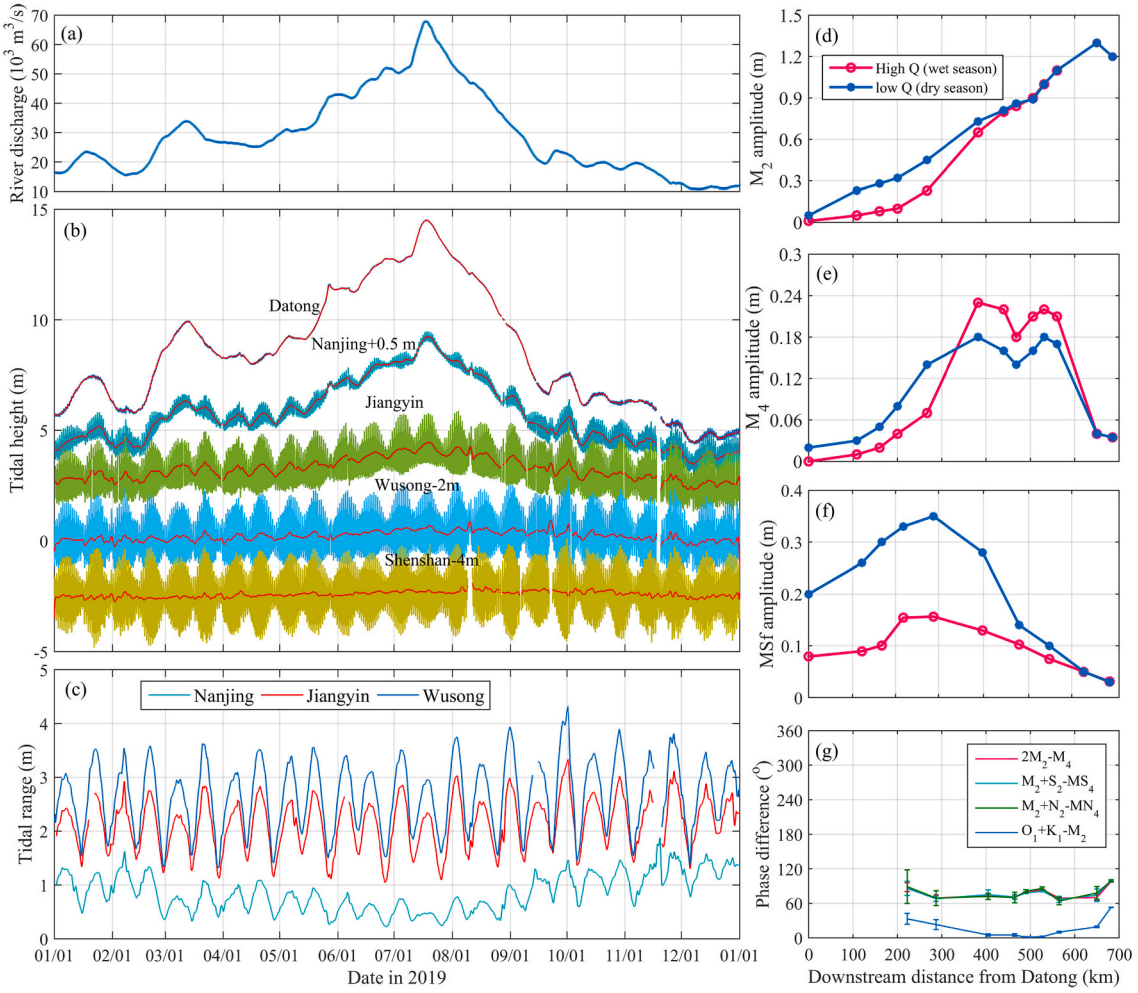

Fig. 3. Tidal dynamics in the CD based on data in 2019: (a) river discharge at Datong, (b) hourly tidal water levels with subtidal levels (red lines), (c) temporal changes in tidal ranges, and longitudinal variations of the amplitude of (d) M_2, (e) M_4, and (f) MSf during low and high river flow conditions, and (g) the phase differences of the selected constituents leading to tidal asymmetry. The data in panels (d), (e), and (f) are from Guo et al. (2020) and that in panel (g) is from Guo et al. (2014). The numbers following Nanjing, Wusong, and Shenshan in panel (a) indicate the offset of the water levels to get rid of overlapping. (For interpretation of the references to colour in this figure legend, the reader is referred to the web version of this article.)

degree the reduction is. Tidal current velocities are up to ~3 m/s and the ebb currents are overall stronger than flood currents owing to the influence of river discharge. The river-enhanced ebb dominance benefits seaward sediment flushing. The surface tidal currents exhibit a rectilinear pattern within the delta because of the confined channel boundary, whereas it is rotating currents in the open coastal ocean outside the delta (see Figs. S2b and S4). Tidal currents cease to reverse in direction and the mean water levels tend to be lower at neap tide than spring in the reaches between Datong and Jiangyin, which is defined as the tidal river (river as the dominant forcing, with unidirectional currents and higher mean water level at spring tide); accordingly, the reaches seaward Jiangyin are called tidal estuary (tides as the dominant forcing, with bidirectional currents) (Guo et al., 2015).

The subtidal flow partition rates between the branches in the CD are uneven and induce spatial variations in hydrodynamics. The present North Branch is a tide-dominated channel with a subtidal flow partition <5% compared with the South Branch (Yun, 2004). The North and South Channels have an approximate half-half division of subtidal flow, and the partition rate between the North and South Passages was equal before the North Passage was regulated with jetties and dikes. However, the subtidal flow partition rate towards the North Passage has reduced to ~40% owing to increased flow resistance, and the left 60% goes towards the South Passage. Overall, the South Branch-North Channel has the largest river influence and least saltwater intrusion, whereas the North Branch undergoes comparably less river influence and the most severe saltwater intrusion. The regime of the subtidal flow partition partly explains sediment import in the North Branch (Guo et al., 2021a, 2021b) and landward residual currents in the seaward part of the South Passage (Wu and Zhu, 2010; see Fig. 6a).

3.3. *Changes in other marine forcing*

Although river and tides are the most important primary forces in the CD, other marine forcing, including mean sea level variations, wind and waves, and shelf currents, also affect the deltaic hydromorphodynamics. The impact of marine forcing is particularly substantial in the mouth zone, leading to profound stratification, density currents and strong circulations.

3.3.1. *Mean sea level changes*

Sea level controls the accommodation space for delta development at the millennial time scales. Since the mean sea level had reached a high stand close to the present sea level ~ 8000 cal aBP (Zhao et al., 1996; Song et al., 2013a; Wang et al., 2018c). In the recent decades, the SLR rate was 0.3–4 mm yr^{-1} between the 1980s and 1990s along China's coasts (ESDCAS, 1994), while the mean SLR rate in the CD was ~1 mm

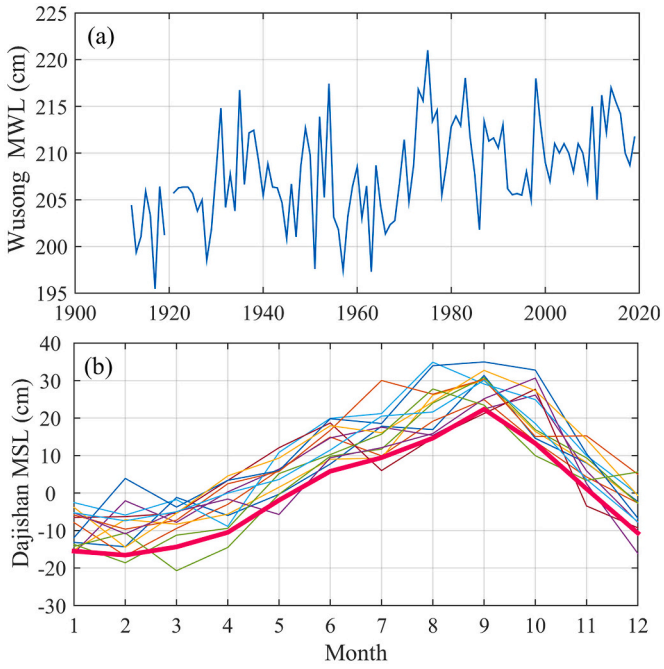

Fig. 4. (a) Inter-annual changes of mean water level (MWL) at Wusong since 1912, and (b) monthly changes of mean sea levels (MSL) at Dajishan in the period of 2007–2019. Data in (a) are from Chen (1991), Xu (1995), and Chen et al. (2018), and data in (b) are from the annual bulletins of sea-level changes on China's coasts published by the Ministry of Natural Resources of PRC (http://www.mnr.gov.cn/sj/sjfw/hy/gbgg/zghpmgb/; SOA, 2020). The data in (a) are referenced to the Wusong Datum, and the records in (b) are referenced to the long-term mean sea level, which is 2.09 m above the Wusong Datum. The thick line in (b) indicates the mean value between 1975 and 1993.

yr^{-1} between 1912 and 1993 (Qin and Li, 1997) and increased to 2.4 mm yr^{-1} in 1981–2015 (Wang et al., 2018b; Fig. 4a). The mean water level at Wusong was 0.14 m higher during 2009–2019 compared with that in 1910–1930 (DMMW, 2021). Considering land subsidence (Xu, 1995; see Section 6.4), the relative SLR is expected to be 6–17 cm as to 2050 when taking the mean sea level in the period of 1980–2020 as a reference (DMMW, 2021).

The mean sea level also exhibits strong seasonal variations along the coasts of ECS (Fig. 4b). The mean water level is 0.2–0.5 m higher in the summer seasons (July-September) than in the winter seasons (December-February; Guo et al., 2015, 2020), which is ascribed to higher water temperature, shelf circulations, and winds over the marginal ECS (Liu et al., 2010c). This seasonal variation in mean sea level height has profound impact on flooding management and deltaic hydrodynamics as it controls the inundation depth over tidal flats and the overflow of the dikes and jetties that affects lateral water exchanges.

3.3.2. *Wind and waves*

The mean wind speed is 4–7 m/s in the mouth zone (Zhu et al., 1984). Governed by the monsoon climate, south-easterly wind prevails in summer and north-westerly wind dominates in winter, while the latter is usually stronger during cold-air outbreaks. Extreme storms such as strong typhoons may generate local wind up to 50 m/s in the summer-autumn season, enhancing water mixing and driving significant sediment transport nearshore (Yang et al., 2019; Ren et al., 2021).

Both wind waves and swells are important in the CD (Shen et al., 2003). The mean significant wave height and wave period are 0.9 m and 4.0 s, respectively, while the maximal wave height is up to 6.2 m when typhoon events pass by or make landfall (Zhu et al., 1984). The extreme water level tends to be significantly higher during typhoon events at spring tides in summer (when the mean sea level is higher and river discharge is larger), which substantially challenges coastal flood defense (Wang et al., 2018a). The wind waves decay fast when approaching the delta and their dynamic influences are confined to the nearshore and delta front regions.

Wind and waves can induce considerable irregular variations in the deltaic dynamics. At the daily time scale, strong wind plays a profound role in modulating saltwater intrusion (Li et al., 2012a; Zhu et al., 2020) and the effluent and plume dispersion off the delta (Chao, 1991; Chang and Isobe, 2003; Lee et al., 2017; Wu et al., 2018a). Large waves stimulate the formation of near-bottom hyper-concentrations and fluid mud in the mouth zone (Li and Zhang, 1998; Wan et al., 2014; Lin et al., 2021), which may enhance siltation in the navigational waterway along the North Passage (Wan et al., 2014). Although waved-induced morphological features like barrier islands and sand spits are absent in the CD, there is ample evidence implying wave influences, e.g., the historical relic cheniers in the southern delta plains (see Section 3.3; Liu and Walker, 1989), concave-up tidal flat profiles in the delta front region (Yang et al., 2020a, 2020b), and coarser sediment over tidal flats than that in the channels in the mouth zone (Hu et al., 2009). However, the impact of waves on the deltaic hydro-morphodynamics is insufficiently understood because of a lack of wave data. The CD is also vulnerable to episodic typhoon events in summer and the extreme events may enhance sediment transport and induce severe erosion, particularly in the delta front regions (Ren et al., 2021). Big waves associated with strong typhoons are capable to induce bed liquefaction, which endangers the infrastructure like dikes and jetties, and reworks sediment over the shallow tidal flats, resulting in short-term tidal flat erosion (Fan et al., 2006; Zhu et al., 2014). The long-term effect of episodic storm events on the large-scale deltaic morphodynamics was, however, insufficiently examined owing to the scarcity of field data during strong events.

3.3.3. *Coastal ocean dynamics*

The CD is subject to strong influence of alongshore coastal and shelf currents in the marginal sea. The effluent of the Changjiang River interacts with the coastal and shelf currents, and the interaction controls the seaward dispersion of the Changjiang diluted water, transport and fate of the river-supplied sediment. The ECS is a river-influenced marginal sea lying on a broad (width $>$ 500 km) and shallow (depth $<$ 130 m) epi-continental shelf (bed slope less than 1/1000) (Liu et al., 2006; Fig. 5a). In summer, the Changjiang plume extends north-eastward like a jet, with another branch flowing southward along the Zhe-Min coasts (Mao et al., 1963; Beardsley et al., 1985; Eisma et al., 1995; Fig. 5b), which is driven by the inertia of high river discharge, buoyancy, vortex stretching, bottom friction (Beardsley et al., 1985), and upwelling-favorable wind (Chao, 1991) (Fig. 5a). The diluted water from the Changjiang may even reach the Korean Peninsula in summer (Watanabe, 2007; Chang et al., 2014). In winter, the Changjiang plume is confined to a narrow band (west of 123.5°E) hugging the Zhe-Min coasts to the south of the delta, which is mainly driven by northerly wind and shoreward Ekman drift (Beardsley et al., 1985; Chao, 1991; Wu, 2015).

The shelf currents play a role in modulating the river plume and seaward sediment dispersion (Liu et al., 2021). To the north of the CD, the Subei Currents are perennially southward, which can drive sediment transport from the abandoned Yellow River delta towards the CD, supplying sediment in building up the northern delta plains (Wang et al., 2020; Shang et al., 2021), even to the depocenter zone (Liu et al., 2010b). A recent monitoring and modeling study, however, suggests northward penetration of a branch of Changjiang plume in summer, to the shoreward of the Subei Currents (Wu et al., 2018a). The driving mechanism of the southward sediment transport from the abandoned Yellow River delta towards the CD thus needs further explanation. To the south, the Zhe-Min Coastal Currents are southward in winter and northward in summer (Beardsley et al., 1985; Lee and Chao, 2003). Collectively, southward dispersion of the river-borne sediment prevails and leads to the formation of inner-shelf mud deposition as south as to the Taiwan Strait (Hu and Yang, 2001; Liu et al., 2006, 2007; Fig. 5a).

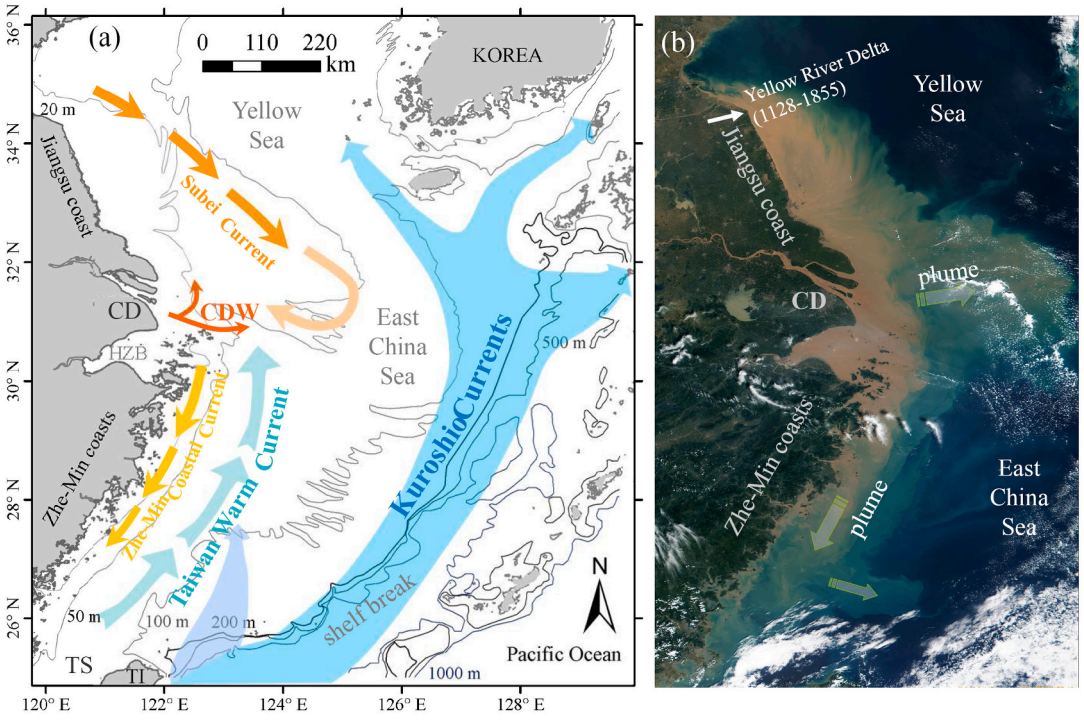

Fig. 5. (a) Topography of the CD, East China Sea, the Yellow Sea with depth contours, and sketches showing the coastal and shelf currents, and (b) a satellite image showing the river plume with surface turbidity. TS and TI mean Taiwan Strait and Taiwan Island, respectively. CDW is Changjiang diluted water. The satellite image in (b) is from the USGS website, which was acquired on 16 Sep. 2000. (For interpretation of the references to colour in this figure legend, the reader is referred to the web version of this article.)

Satellite images showing surface turbidity confirm the southward sediment dispersion (Shi and Wang, 2012; Shen et al., 2013; Fig. 5b). In the mid-shelf zone, a small branch of the Kuroshio Current (the northward current along with the shelf break) heading north into the shelf sea is called the Taiwan Warm Current, which would reach the submarine river valley off the CD. It constrains the Changjiang plume and associated sediment dispersion within the inner shelf zone, although cross-shelf penetration occurs occasionally (Guo et al., 2003; Wu, 2015; Liu et al., 2021).

The shelf morphology plays a role in modulating the shelf currents and circulations. The oceanic influence was interpreted to be more significant when the CD started to develop from an incised valley ~8000 aBP, with a much wider and convergent planform (Uehara et al., 2002; Song et al., 2013a; Wang et al., 2018c). Stronger tidal amplification and more inland impact of the oceanic forcing at that time benefited deposition of fluvial sediment within the incised valley. A recent numerical modeling study suggested that the coastal and shelf currents will exhibit a very different pattern if the inner shelf mud deposition was removed from the morphology (Wu, 2021), suggesting the morphological controlling impact. Extensive tidal flat reclamation along the coasts of China and Korean Peninsula modified the coastline morphology and induced changes in the tidal wave propagation in the semi-closed Yellow Sea and ECS, which possibly exerted remote impact on the CD (Song et al., 2013c).

3.4. Estuarine stratification and circulations

The hydrodynamics within the CD exhibit strong spatial-temporal variability under the interactions between the fluvial and marine forcing. Freshwater flushes seaward near the surface and saltwater intrudes landward near the bottom, forming a salt wedge stretching approximately 60 km inland (up to the division zone between the North and South Passages, other than the saltwater intrusion in the North Branch). The mouth zone is predominantly partially-mixed (60–70% of the time) with gravitational circulations (Fig. 6b), while well-mixed or highly-stratified situations occur when river discharge is comparatively low at spring tides or high at neap tides, respectively (Chen et al., 1999). This is consistent with the classical two-layer stratification theory, but note that a major part of the delta is well-mixed and density stratification only occupies a relatively short reach of the delta (Fig. S5).

Seasonal variations in river discharge (dry vs. wet season) and fortnightly variations in tidal range (spring vs. neap tides) induce changes in the scale and strength of saltwater intrusion and stratification, with the most severe saltwater intrusion occurred at spring tides in the dry seasons (low river discharge). Spatially, saltwater intrusion is comparatively more severe in the North and South Passages, and less in the North Channel, while saltwater may occupy the entire North Branch and even overspill into the South Branch. But note that northerly wind in the winter seasons would induce landward Ekman currents which enhance saltwater intrusion (Wang et al., 2010; Li et al., 2012a). For example, strong northerly wind persisting for weeks in February 2014 (dry season) enhanced saltwater intrusion in the North Channel, resulting in unusually higher salinity surrounding the Qingcaosha Reservoir (see Fig. 11b; Zhu et al., 2020). Occasional saltwater intrusion along North Channel and North Branch threatens freshwater intake and supply (Shen et al., 2003; Xue et al., 2009; Wu et al., 2010). There were plans to construct a barrier at the mouth of North Branch to mitigate saltwater intrusion and overspill, but its potential impact on the ecosystem and sustainable development of the delta remains an open question.

Residual currents induced by river discharge prevail in the South Branch and landward reaches, while density currents, wind-driven currents, and coastal currents are of regional importance in the mouth and nearshore zones (Shen et al., 1989a, 1989b). Other than the vertical density currents, the mouth zone is also featured by horizontal subtidal circulations driven by tide-induced Stokes transport (Wu et al., 2010), i.e., the seaward subtidal currents in the North Channel and North Passage and landward subtidal currents in the seaward part of the South Passage. The high jetties in the North Passage have largely blocked the

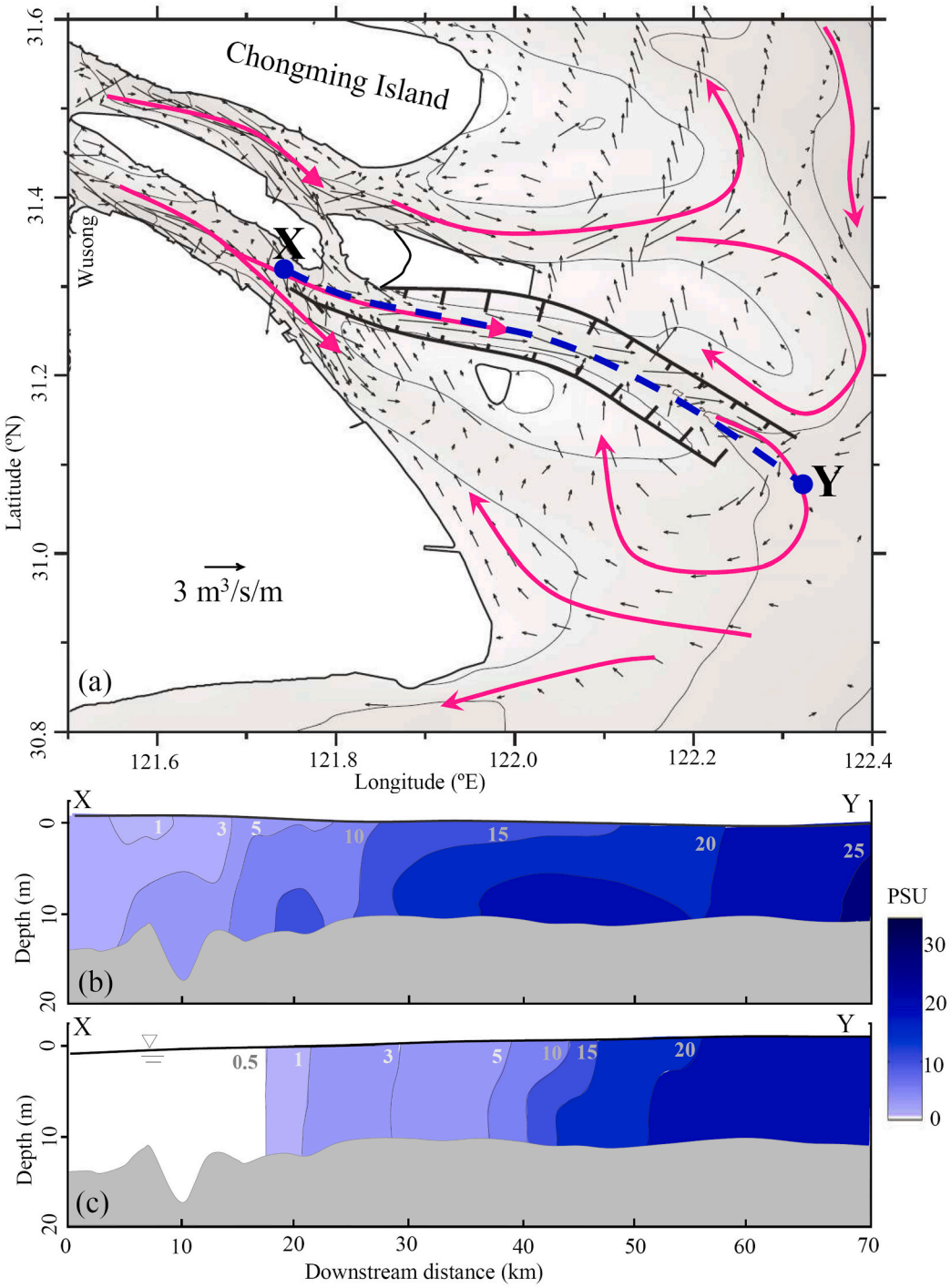

Fig. 6. (a) Horizontal distribution of the depth-averaged subtidal water flux under the post-regulation condition; longitudinal variations of salinity along the North Passage (the blue dash line in a) during (b) high water slack and (c) low water slack at spring tide under a river discharge of ~17,000 m^3/s at Datong. Panel (a) was the model result modified from Wu et al. (2010); panels (b) and (c) were modified from Wu and Zhu (2010). (For interpretation of the references to colour in this figure legend, the reader is referred to the web version of this article.)

inter-channel exchanges and significantly altered the horizontal circulations as well as the in-channel vertical circulations (Zhu et al., 2018; Chen et al., 2020).

In-channel lateral currents are another factor contributing to horizontal circulations considering large lateral water depth variations. In the surface, water and sediment transport converges towards the main channels while near-bottom water and sediment transport are diverged towards the surrounding flats, creating a shear front between the deep channels and tidal flats (Chen et al., 1999). This shear front benefits shoreward sediment transport and tidal flat accretion. Asymmetric tidal mixing is another important contribution to the circulations and sediment transport in the mouth zone (Jiang et al., 2013; Song et al., 2013b).

The in-channel lateral circulations adjust with the jetty-altered horizontal circulation, i.e., with enhanced stratification in the North Passage (Zhu et al., 2018; Zhou et al., 2019; Chen et al., 2020; Fig. S6). Knowledge of the density currents has been well established, whereas their interactions with horizontal (inter-channel) and lateral (in-channel) circulations are incompletely understood.

4. Sedimentary dynamics

4.1. Sediment transport regime

Suspended load transport is the dominant form of sediment

movement in the CD, while bedload transport is comparably limited. However, near-bottom mass transport may occur, particularly in the South Branch and upstream reaches, which is evidenced by moving bed forms like sand waves (Zheng et al., 2018a) and the seaward migration of the sand bars (Yun, 2004). The bed sediments have a larger content of sand than the suspended sediment, with the median grain sizes in the range of 30–300 μm and 5–20 μm, respectively (Liu et al., 2010a). Longitudinally, the bottom sediment in the TM zone is smaller in grain size than that in the landward and seaward regions. Laterally, the bottom sediment is finer over the shallow flats than in channels inside the delta, e.g., the South Branch, but it is coarser over flats than that in channels in the mouth zone (Hu et al., 2009). These differences are attributed to the tidal forcing dominance inside the delta and wave influence in the mouth zone.

The CD is a highly turbid system because of the excessive riverine supply of fine sediment and strong currents. The suspended sediment concentrations (SSC) is the highest in the mouth zone, i.e., the turbidity maximum (Fig. 7a). The position of the primary TM is coincident with the saltwater wedge because the gravitational circulation induces sediment transport convergences and is one of the main governing mechanisms of TM formation (Shen and Pan, 2001; Liu et al., 2010a, 2011). Inside the North Branch, there is a secondary turbidity maximum owing to the strongly amplified tidal forcing (Fig. 7a). Vertically, the SSC is much larger near the bottom than that in the surface layer. The near-bottom sediment concentration, monitored by tripod systems, is up to 10–100 kg/m^3 in the TM (Liu et al., 2011; Wan et al., 2014; Lin et al., 2021; Fig. 7c). Near-bottom hyper-concentrations and fluid mud with a thickness of ~1–2 m are frequently monitored in the channels at spring tides (Li and Zhang, 1998; Wan et al., 2014; Ge et al., 2020; Lin et al., 2021). The formation and maintenance of the TM and the near-bottom hyper-concentrations are a composite result of salinity-induced stratification and density circulations, shear-induced resuspension, flocculation-enhanced settling, and high SSC-induced drag reduction, and a possible supply of reworked sediment from surrounding tidal flats under energetic storms (Li and Zhang, 1998; Wan et al., 2014; Lin et al., 2021). A positive feedback mechanism is established once high sediment concentration forms, because the SSC-enhanced stratification causes turbulence damping and drag reduction, which benefits maintenance of the high sediment concentration in the bottom layer (Lin et al., 2021). An in-depth study about the fluid mud dynamics and its role in sediment transport processes are still needed given the relevance to navigation channel siltation and maintenance dredging (Wan et al., 2014).

The SSC in the CD also displays strong temporal variations. Intratidally, high SSC occurs 1–2 h after the flood and ebb peak when tidal current velocities are large. At the seasonal time scale, the SSC is higher in summer (wet season) and lower in winter (dry season) inside the delta owing to higher riverine sediment supply in summer, whereas it is higher in winter and lower in summer outside the delta, because the northerly wind and shelf currents in winter rework more bottom sediment and leads to higher SSC (Chen et al., 2006; Shen et al., 2013). Interannually, the surface SSC in the South Branch and outside the delta shows a decreasing trend in the recent decade in response to riverine sediment load decline (Li et al., 2012b), which is confirmed by surface SSC derived from satellite images (Shen et al., 2013). However, the decrease in SSC is less apparent in the TM compared with that in the South Branch and offshore (Fig. 7b), owing to strong sediment resuspension under strong tidal currents (Yang et al., 2020a, 2020b). Continued monitoring is needed to inform the future trend in SSC changes.

The cohesiveness of the fine sediment plays an important role in

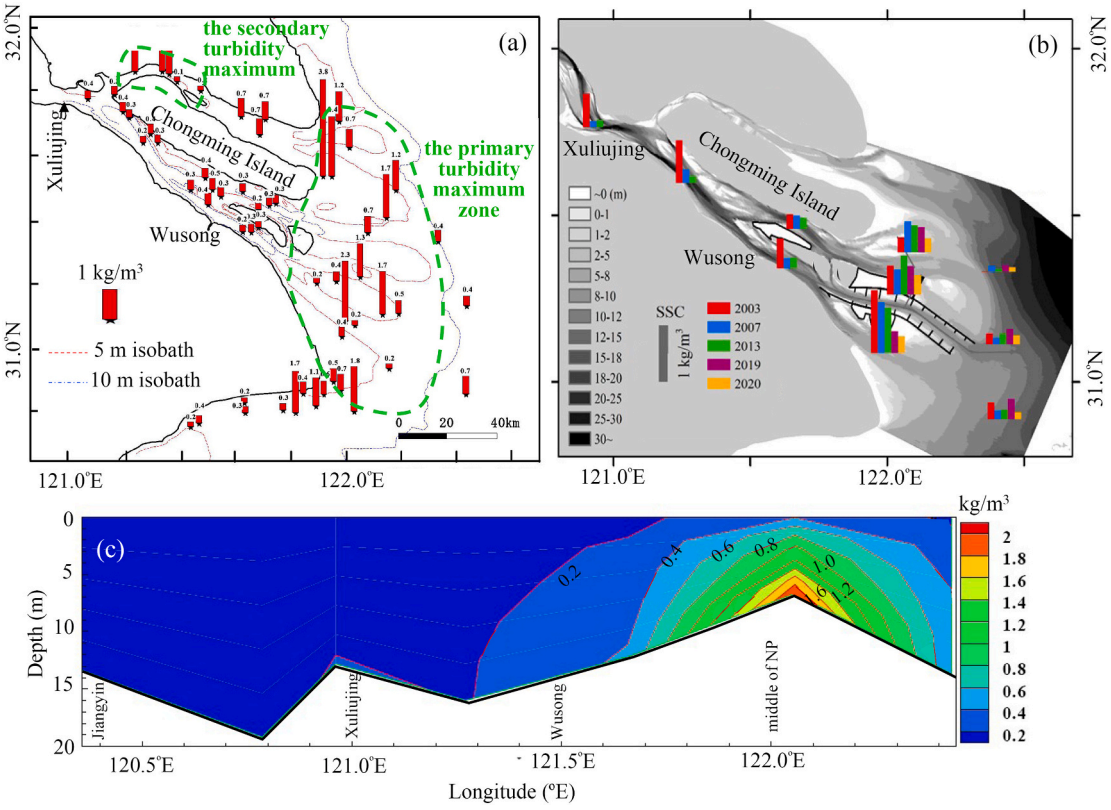

Fig. 7. (a) Spatial distribution of tide- and depth-averaged suspended sediment concentration with a turbidity maximum zone identified, (b) changes of the averaged suspended sediment concentrations over the recent 17 years, and (c) longitudinal variations of the tide-averaged suspended sediment concentration along Jiangyin-Xuliujing-Wusong-middle North Passage (NP). Panels (a) and (c) were modified from Liu (2009) based on depth- and tidally-averaged SSC data collected at spring tides in the wet seasons of between 2004 and 2005. Panel (b) was modified from Zhu et al. (2021) based on tidally- and depth-averaged SSC in the wet seasons (see Section 2.2).

sediment transport dynamics. Silt and clay are the dominant content of the suspended sediment in the delta, with the median grain size predominantly in the range of 5–20 μm (Liu et al., 2010a). The fine sediment aggregates into flocs with much larger sizes than the primary particles, i.e., median floc size reaching 30–250 μm based on in-situ instruments like LISST (Tang, 2007; Guo et al., 2017), and larger settling velocities up to 4 mm s^{-1} (Shi and Zhou, 2004; Tang, 2007; Guo et al., 2017). Although salinity is widely recognized as a factor stimulating flocculation, flocculation of fine sediment was also detected in the freshwater river upstream of Datong, owing to the cohesiveness nature of fine sediment and partially the influence of biochemical material (Guo and He, 2011). The influence of turbulence shear and biochemical material on flocculation processes is particularly critical as they may even stimulate flocculation under low SSC conditions (Deng et al., 2019, 2021). The continuous flocculation processes in the river-delta continuum suggest that the river provides 'parent flocs' to the delta in which increased salinity and SSC enhance the flocculation processes, whereas stronger currents and turbulence in the delta might have opposite effects (Guo et al., 2017; Deng et al., 2019).

The critical shear stress for erosion and deposition are other essential parameters in fine sediment transport dynamics, particularly the critical stress for erosion and its spatial variations. Over shallow water tidal flats, direct measurement of the critical erosion stress is possible using erosion instruments like the Cohesive Strength Meter (Tolhurst et al., 2000), whereas it is technically challenging to do that underwater. An alternative method is to infer the erosion parameter through detection of water content of the bottom surface sediment based on soil mechanics (Winterwerp et al., 2012). In practice, Qiao (2019) mapped the spatial distribution of the critical erosion stress in the CD based on ~180 bottom sediment samples with measurements of sediment composition, wet density, and water content. However, point measurements are time consuming and 180 samples are far from enough to get a high-resolution map for large systems like the CD where spatial variability of the erosion stress is significant. Another initiative is to infer the erosion stress via the plasticity index method based on surface SSC from remote sensing and hydrodynamic modeling (Ge et al., 2015). Incorporation of such data in sediment transport modeling could improve model performance in terms of intra-tidal and spatial variations of SSC. Note that as erosion continues, the erosion parameter changes as sub-surface sediments with different composition and degree of compaction are exposed. Geological survey with core data may help to reveal the changes in sediment property and associated erosion stress over time. Overall, a combination of point measurements, field interpretation, geological cores and numerical modeling might do a better job in mapping the critical shear stress and merit future effort.

The net sediment transport flux, the tidally-averaged product of current velocity and SSC, is predominantly seaward in the CD owing to strong river forcing. Regional variability includes landward transport near the bottom in the TM zone due to the density currents, and landward transport in the seaward part of the South Passage (which is consistent with landward subtidal water flux therein), and sediment import in the North Branch owing to the tide-controlled flood-dominance. The sediment transport convergence in the TM zone leads to the formation of mouth bars. Landward flux in the seaward part of the South Passage is partially responsible for the fast accretion of the Jiuduan shoal. Moreover, the lateral sediment transport from the Jiuduan shoal towards the North Passage, the navigational channel, was detected as a source of siltation, but was later impeded by the raised jetties. Landward sediment transport in the North Branch induces channel infilling and shrinkage in the past century (Guo et al., 2021a, 2021b).

4.2. Long-term sedimentation and sediment budget

Study of net sediment accumulation informs large-scale morphodynamic evolution. The North Branch was continuously filled and became shallower in the past century, owing to sediment import (Yun, 2004, 2010; Guo et al., 2021a, 2021b). In the South Branch, sand bar movement and channel migration occurred frequently (see Section 5.2), owing to prevailing near-bottom mass sediment transport (Yun, 2004). The bed sediment is much sandier and larger in grain size than the suspended sediment in the South Branch, suggesting limited exchange between near-bottom suspended and bed sediments, in other words limited settling and deposition of suspended sediment and resuspension of bed sediment (Liu et al., 2010a). In the mouth zone, the gravitational circulation stimulates net sediment trapping and the formation of the mouth bars (Liu et al., 2011; Wan et al., 2014). Over the submerged shoals and sand bars, the constructive tidal forcing favors onshore sediment transport and net accretion of tidal flats (Zhu et al., 2014).

The nearshore regions seaward of the North and South Passages, approximately between the 5 m and 20 m isobath, are the place where the river-supplied sediment temporally deposits and is later reworked and transported away by wave-driven currents and alongshore currents. Short-term deposition rate in these nearshore regions is up to 4 cm per month in the wet seasons, whilst the long-term (up to millennial time scales) sediment accumulation rate is an order of magnitude less, i.e., approximately 1–5 cm yr^{-1} (McKee et al., 1983; DeMaster et al., 1985; Xu et al., 2012; Jia et al., 2018; Fig. 8a). Core data also suggest a thick layer (up to ~30 m) of mud deposition (clay and silt with little sand) therein (Liu et al., 2010b; Wang et al., 2018c; Su et al., 2020). These evidences suggest that the subaqueous regions off the South Passage were a sink of river-supplied sediment, called the depocenter or 'mud bank'. However, the bed slope seaward of the North and South Passages remains much smaller compared with that seaward of the North Branch and North Channel (see Fig. 10), suggesting a low net deposition rate. The exchange rates between near-bottom suspended sediment and bed sediment were detected to be high in the depocenter zone, also suggesting strong resuspension and deposition processes therein (Fig. 8b; Liu et al., 2010a). One explanation of these sedimentary and morphological phenomena is a seasonally alternated sediment deposition and erosion pattern. Specifically, a major portion of the river-supplied sediment temporally deposits outside the North and South Passages, predominantly in the wet seasons, whereas the deposited sediment is reworked and transported southward in the dry seasons (Yang et al., 1992; Liu et al., 2006). As a result, the intra-annual balance leads to relatively smaller net deposition at the decadal time scale. The jetties in the North Passage and the aggressive reclamation over the Nanhui flat have changed the circulation patterns in the mouth zone (Wu et al., 2018b; Chen et al., 2020), which as a result might alter the sedimentary dynamics in the subaqueous delta front regions.

Only a part of the river-supplied sediment deposits in the CD and knowledge of the sediment trapping efficiency has implications for delta management. The sediment deposition rate in the CD was interpreted to vary in the range of 99–224 Mt. yr^{-1} based on the reconstructed strata and deposition volume changes in the late Holocene (Wang et al., 2018c). A majority of similar studies based on interpretation of the deposition rates and channel volume changes in the delta and inner shelf zone suggested that approximately 40–68% of the Changjiang River-supplied sediment was trapped and deposited in the CD at the centennial to millennial time scales (McKee et al., 1983; Nittrouer et al., 1984; DeMaster et al., 1985; Milliman et al., 1985; Liu et al., 2007, 2010b; Xu et al., 2012; Deng et al., 2017; Jia et al., 2018). The remaining part of the river-supplied sediment was transported out of the delta and deposited nearshore in forming the subaqueous delta (Chen et al., 1985) and partly further southward by alongshore coastal currents in forming the inner shelf mud belt (Fig. 8c; Niino and Emery, 1961; Liu et al., 2007; Xu et al., 2012; Gao et al., 2019). Other than the near-surface sediment plume, eastward cross-shore sediment transport was thought to be small (Sternberg et al., 1985; Milliman et al., 1989), although gravity currents can enhance cross-shelf transport (Wright and Friedrichs, 2006; Wu et al., 2016) and a small percentage of the riverine sediment may even have reached the shelf break (Katayama and Watanabe, 2003).

Note that the inferred sediment trapping efficiency of 40–68%

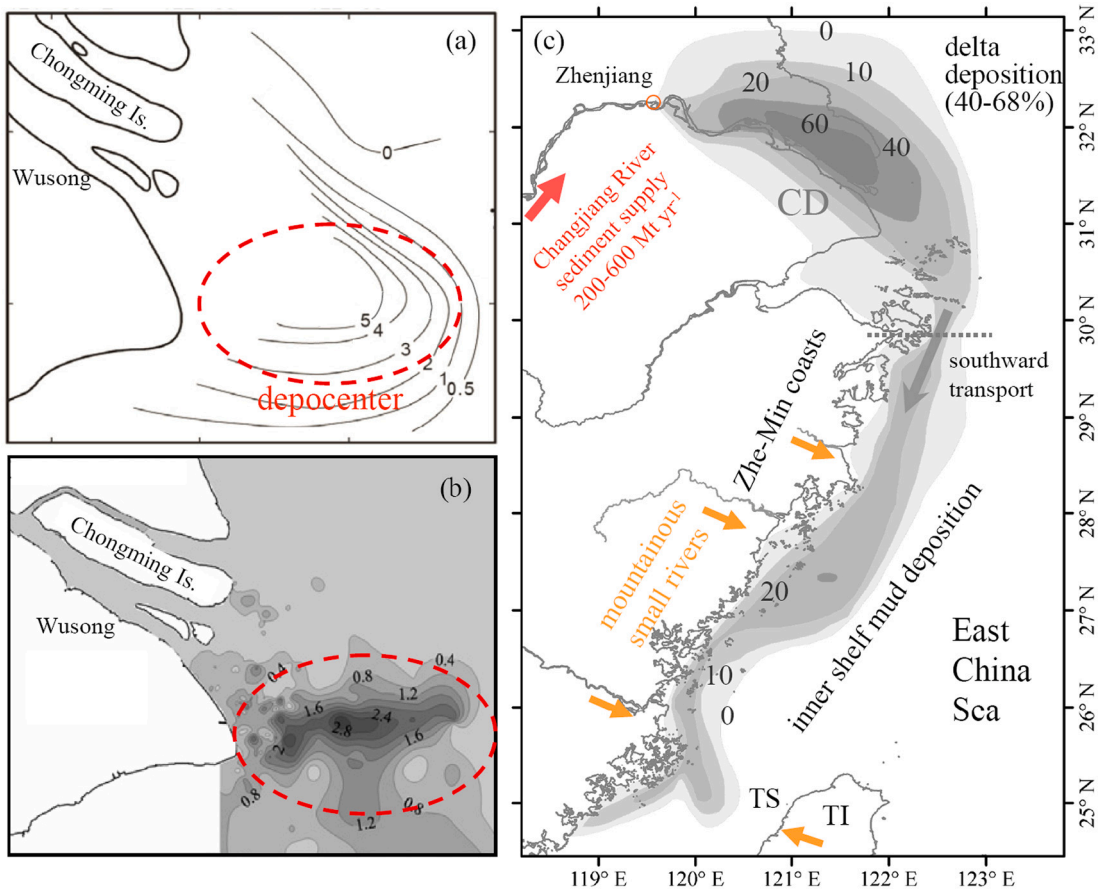

Fig. 8. Sedimentation in the delta-sea continuum: (a) sedimentation rate (cm yr^{-1}), (b) sediment exchange rate (cm yr^{-1}) in the mouth zone of the Changjiang River with the depocenter identified, and (c) spatial distribution of the thickness (meters) of the Holocene deposition stretching from the Changjiang Delta (CD) to the inner shelf zone. Panel (a) was modified from Yun (2004) in which the sedimentation rates were estimated using the radioisotope Pb^{210}; panel (b) was modified from Liu et al. (2010a) in which the sediment exchange rates were interpreted by comparing the composition between the near-bottom suspended sediments and bottom sediments; and panel (c) was modified from Liu et al. (2007) based on seismic profile surveys. TS and TI mean Taiwan Strait and Taiwan Island, respectively.

reflects the mean value at time scales >100 years, whereas the actual trapping efficiency may vary with delta development and sediment source availability over time. The paleo-incised valley was wide and deep in the mid-Holocene, in which the incoming tides were more amplified and likely to be stronger than the present situation (Uehara et al., 2002). The stronger tides benefited sediment deposition and valley infilling since ~8000 aBP (Hori et al., 2001; Chen and Zhu, 2012), leading to a larger sediment deposition rate during the initial stage of delta development (Wang et al., 2018c). Afterwards, the sediment trapping efficiency decreased slightly in response to the increasingly filled valley and reduced sediment source resulting from climate fluctuation. The sedimentation rate increased in the recent 2000 years owing to expanding human activities in the watershed and increased riverine sediment load. In the recent three decades, the river-supplied sediment declined again (see Section 3.1) and accordingly the deposition rates in the delta slowed down (Yang et al., 2011). However, the sediment trapping efficiency in the CD (the percentage of sediment deposited in the delta compared with the river-supplied total sediment) was not necessarily to decrease, which may even possibly become larger considering the inherent deltaic hydro-morphodynamic adaptation and buffering capacity (see Section 5.2). Verifying this hypothesis (i.e., increased sediment trapping efficiency in response to sediment source decline) needs to consider the impact of human activities, which, by contrast, may reduce deltaic morphodynamic activities and alleviate sediment trapping (see Section 6.2). Overall, future study is still needed to figure out more details about the millennial deltaic sedimentation processes and rates. It is also challenging to quantify the sediment budget and sediment trapping efficiency at the decadal time scales, because of incomplete information about sediment dredging and dumping, sediment deposition in the embanked regions, and the spatially varying erosion and deposition (Guo et al., 2021a, 2021b).

Other than the Changjiang River-supplied sediment, marine sediment also contributed to the development of the CD. The Yellow River was once the world most sediment-laden river (sediment load up to 1.63 Bt yr^{-1}) and it delivered a huge amount of sediment to the Jiangsu coast and stimulated shoreline advance between 1125 and 1850 (Liu et al., 2010b). Part of the Yellow River-delivered sediment was transported southward by the Subei Currents, supplying an amount of 30–70 Mt. yr^{-1} sediment in building up the northern CD plains (Zhou et al., 2014; Jia et al., 2018), particularly when the Yellow River discharged into the Yellow Sea at a place ~320 km to the north of CD (Shang et al., 2021; Fig. 5b). The Yellow River sediment source to CD was confirmed by indicators including magnetic properties, clay minerals, rare earth elements, and isotope fingerprints, although the quantity remains understudied (Liu et al., 2010b; Wang et al., 2020; Shang et al., 2021). As the Yellow River shifted its river course far north after 1855, the abandoned Yellow River delta underwent erosion and the eroded sediment may still reach the CD and impose some influences.

5. Deltaic morphodynamics

5.1. Millennial delta development

Reconstruction of the millennial geomorphologic evolution of the CD

based on a large number of cores and dating data show that the delta apex was around Nanjing, which was 420 km further inland than the present delta shoreline (Chen et al., 1985; Song et al., 2013a). The river had incised the bed during the low sea-level conditions, forming a huge, elongated, deep-incised valley as the initial topography for delta development since the mid-Holocene (Li et al., 2002; Wang et al., 2018c; Jiang et al., 2020). This extensive and low-gradient environment captured a major portion of the river-supplied sediment, forming deposition >60 m in thickness (Fig. 9; Chen et al., 1985; Li et al., 2002). Continued valley infilling led to development of a series of mid-channel and bank-attached sand bars and tidal flats, which were eventually merged into the northern delta plain. As a result, the valley was narrowed and the delta apex moved seaward, with new sand bars formed in the further seaward regions (Li et al., 2000, 2002; Saito et al., 2001; Hori et al., 2002). This cyclic development of basin infilling, sand bar development and merging, and seaward shoreline movement may have repeated six times since 6000 years ago until recently the sand bars like the Jiuduan shoal took shape in the 1950s (Fig. 9a; Li et al., 2002).

The delta progradation became faster in the recent 2000 years, owing to increased riverine sediment supply (Chen et al., 1979; Hori

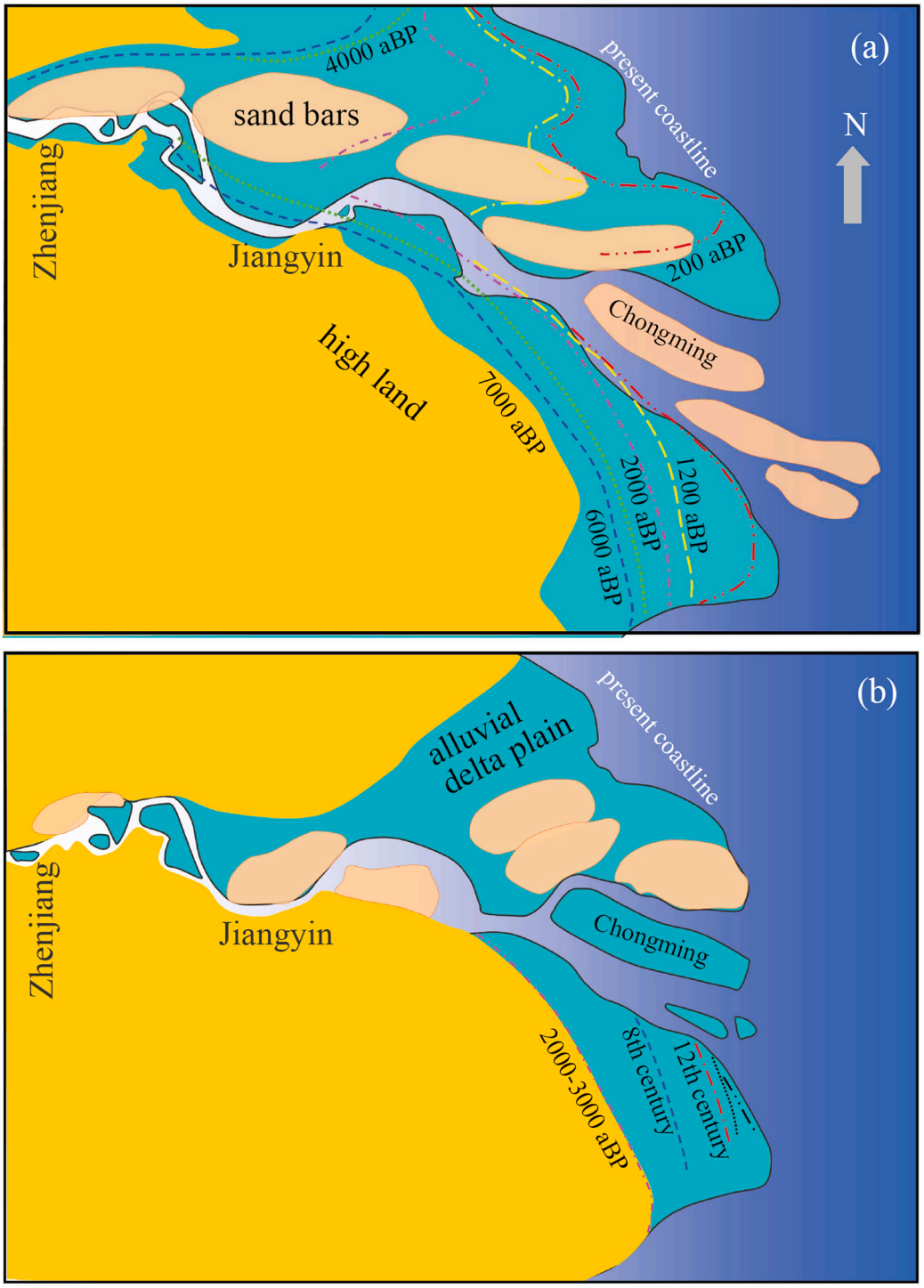

Fig. 9. Millennial time scale evolution of the CD: (a) delta development model since 7000 aBP (modified from Li et al., 2002), and (b) delta development in the recent 2000 years (modified from Chen et al., 1979).

et al., 2001; Wang et al., 2018c). The apex of the delta moved seaward to Zhenjiang and the mouth was as wide as 180 km 2000 aBP (Chen et al., 1979). Within the river valley, distributary channels and elongated sand bars were aligned in the same direction as the river channel. Inter-tidal flats spread extensively along the delta front region (Fig. 9b; Chen et al., 1985; Hori et al., 2002; Yun, 2004). Overall, the delta development processes in the recent 2000 years were summarized as 'tidal flats fringing the south bank, merging of linear sandbanks with the northern bank, successive filling and narrowing of the estuarine embayment, a resultant seaward migration of the river mouth, and the maturing of the estuarine channels' (Chen et al., 1979, 1985).

It is noteworthy that the above two delta development models in Li et al. (2002) and Chen et al. (1985) lack details about the spatial scale and number of the sand bars. The historical sand bars may be smaller in scale and larger in number than the patterns suggested in Fig. 9, as revealed in recent studies (Jiang et al., 2020; Su et al., 2020) and the historical geography maps (Fig. S7). Both elongated sand bars and tidal sand ridges may be present during the delta development processes. Wang et al. (2018c) provided a series of historical morphology of the delta and estimations of the sedimentation rate since 12,000 aBP and suggested that the millennial delta development processes were not linear but varied with changes in Asian monsoon, riverine sediment supply and mean sea levels. Overall, the long-term morphodynamic development processes of the CD are essentially different from that of river-dominated deltas such as the Yellow and Mississippi River deltas, in which large-scale river course migration has led to the formation of sub-delta lobes (Saito et al., 2001; Blum and Roberts, 2012).

The northern and southern CD plains displayed distinctive formation processes. The paleo-terrain was higher in relief in the southern delta, where the river flowed over the northern delta to the sea (Chen and Yang, 1991; Jiang et al., 2021). The northern delta plains developed south-eastwardly by merging sand bars and were once a main sink of river-supplied sediment. In the southern delta plains, the remains of chenier ridges consisting of well-sorted fine-grained sand and shell fragments, and the relic remains of historical dikes, demonstrated the position of ancient coastlines and their advancement (Liu and Walker, 1989; Li et al., 2002). The delta was realigned south-eastwardly at the millennial time scales (Xu and Chen, 1995; Hori et al., 2002; Jiang et al., 2020). The asymmetric development of the southern and northern delta plains was attributed to the combined effect of the Coriolis force (Chen et al., 1979; Li et al., 2011), the prevailing north-westward tidal wave propagation (Yun, 2004), the spatially non-uniform sediment compaction and a southward movement of the depocenter (Chen and Yang, 1991; Jiang et al., 2020), and southward coastal currents. However, no consensus was reached as regards which factor abovementioned played a dominant role.

While the delta development processes were increasingly clarified, the governing mechanisms and the controlling role of the fluvial and marine forces, however, were only limitedly understood. Modeling studies of the paleo-tidal regime suggested that tidal ranges were slightly larger 6000 years ago than present (Uehara et al., 2002). Ancient Chinese literature showed that tidal waves may propagate ~220 km more upstream than Datong in the 3rd to 5th century, and tidal bores were observed around Zhenjiang in the 2nd to 8th century (Chen et al., 1979), suggesting larger tides before the incised valley was filled and narrowed to a major degree. The interactions between river flow and strong tide led to convergent sediment transport inside the delta and may explain fast sediment deposition and build-up of the delta (Chen and Zhu, 2012; Guo et al., 2014). Future study is needed to better understand and identify the controls on the northward merging of sand bars, the progressive advance of the southern delta shoreline, and the role of marine sediment. Long-term hydro-morphodynamic modeling tools may help to validate the millennial delta evolution processes based on the reconstructed historical morphology, particularly in exploring the governing mechanisms.

5.2. Decadal to centennial morphodynamic evolution

Historical maps and bathymetric data available since the 1840s facilitated studies of the centennial delta evolution in a quantitative way, e.g., the multiple bifurcations and formation of the branches (see Fig. S7). The latest bifurcations between the South and North Channels, and between the South and North Passages occurred in the 1860s and 1950s, respectively (Chen et al., 1985; Yun, 2004). Since the late 1950s, the CD took its shape by four main outlets with alternated large islands and shoals.

A majority of past hydro-morphodynamic studies were devoted to the regions seaward of Xuliujing, while research interest in the tidal river was only emerging in recent years. In general, the tidal river (Datong-Jiangyin) displays a uniform channel width, larger sinuosity, and seaward increasing channel depth (Gugliotta and Saito, 2019), in contrast to width convergence and seaward decreasing depth in the tidal estuary part (seaward of Jiangyin). Over time, the river reach between Nanjing and Xuliujing underwent a shift from sedimentation to erosion in the 1980s, in response to sediment decline (Wang et al., 2009). More severe channel erosion was detected in the river between Datong and Wusong in 1998–2013, e.g., an erosion volume of 1.85 billion m^3 (Zheng et al., 2018b). However, Mei et al. (2021) estimated that the net deposition continued in the Datong-Xuliujing reaches in the periods of 1992–2002 and 2008–2013, while erosion occurred between 2002 and 2008. The inconsistency in these studies may be ascribed to the differences in data period and river reaches. Overall, the morphodynamic adjustment along the 405-km long tidal river has a buffering impact on the sediment flux to the tidal estuary, e.g., tidal river erosion possibly leads to larger sediment flux at Xuliujing than that at Datong.

The Xuliujing segment was 15.7 km in width in 1958 but reduced to 5.7 km in the 1970s owing to the embankment of the sand bars close to the northern bank (Yun, 2004). The narrowed and stabilized Xuliujing segment became a controlling transect of the division between the North and South Branches (Chen and Li, 2002; Yun, 2004). The North Branch was once a wide channel where meandering channels and sand bars developed and had a subtidal partition rate up to 25% in the 1910s (Yun, 2004). However, its inflow section width reduced from 15 km in 1842 and to 5.8 km in 1915 as a result of the narrowed Xuliujing segment and embankment of surrounding flats, with subtidal partition rate decreased to ~5% since the late 1950s (Yun, 2004). The North Branch then became a convergent and tide-dominated channel in which linear tidal sand ridges replaced the meandering channel-shoal pattern (Guo et al., 2021a, 2021b). Flood dominance and associated sediment import enhanced the sedimentation and channel shrinkage, which continues until nowadays.

The Jiangyin-Xuliujing-Wusong reach once had a straight planform with a nearly uniform width in the 1860s, whereas accretion and embankment of sand bars along the Jiangyin-Xuliujing reach reduced the channel width (Yun, 2004), and width convergence established downstream of Jiangyin (Guo et al., 2014). The South Branch has a stabilized southern bank due to historically constructed dikes and groins, but a highly erodible northern bank that had retreated 1–4 km between 1860 and 1900 (Chen and Xu, 1981). Later, the northern bank of the South Branch was protected by groins and dikes and became stabilized since the 1970s as well. The sand bars in the South Branch, e.g., the Baimao shoal, the Biandan shoal, and the Zhongyang shoal, grew rapidly owing to excessive fluvial sediment supply. Sand bar movement and channel migration occurred frequently (see Fig. S8), while the overall channel-shoal configuration persisted (Yun, 2004; Guo et al., 2011; Wang et al., 2013b).

The Changxing and Hengsha Islands (see Fig. 1) formed based on merging of a series of small mid-channel sand bars (see Fig. S7). Human activities like diking and reclamation accelerated the merging and stabilization processes (Chen et al., 1985; Yun, 2010). To the east of Hengsha Island, a big triangular-shaped shoal (namely Tongsha shoal) occupied the mouth zone in 1842. Mutually evasive ebb and flood

channels cut into the Tongsha shoal and the reconnection of the ebb and flood channels led to the initial formation of the North Passage since the late 1950s (Fig. S9; Yun, 2004, 2010). The ever recorded biggest river flood occurred in 1954 was thought to play a role in stimulating the formation of the North Passage. Since then, the channel configuration consisting of North Branch, North Channel, North Passage, and South Passage became mature with straightened alignment and accreted shoals (Wang et al., 2013b; Zhao et al., 2018).

Quantitative analyses of the channel volume changes based on comprehensive bathymetric data since 1958 suggested alternative net erosion and deposition before riverine sediment supply had drastically reduced (Wang et al., 2013b; Luan et al., 2016; Zhao et al., 2018). The South Branch was eroded by a volume of 0.97 billion m^3 while the mouth zone was deposited by 1.8 billion m^3 in the period of 1958–2010 (Zhao et al., 2018). The magnitude of erosion and deposition in the South Branch was extraordinary because of the frequent channel migration and seaward sand bar movement; the latter suggested seaward sediment flushing (Fig. 10; Wang et al., 2013b). The net deposition in the mouth zone mainly occurred over the shoals, i.e., the Jiuduan shoal and Hengsha flat, suggesting tidal flat accretion (Zhu et al., 2019). Moreover, the bare subtidal flats and the vegetated inter- and super-tidal flats underwent erosion and deposition, respectively (Zhu et al., 2014), and concave-up tidal flat profiles took form (Yang et al., 2001; Yang et al., 2020a, 2020b). The vegetation over the high tidal flats has an effect in dissipating incoming waves, trapping sediment, and stimulating deposition (Yang et al., 2012; Zhu et al., 2014).

Severe erosion is expected to occur in the CD in response to striking sediment decline. For instance, the subaqueous regions outside the North Channel had undergone net erosion since the 1970s (see Fig. 10c; Yang et al., 2011, Yang et al., 2020a, 2020b; Luo et al., 2012). A shift from accretion to erosion emerged in the subaqueous delta (Luan et al., 2021) and the Jiuduan shoal and Hengsha flat since ~2010 (Zhu et al., 2019). Severe erosion of the delta front zone around 5–15 m isobath was detected between 1997 and 2013, which was ascribed to the influence of jetties in the North Passage (Zhu et al., 2016). Although regional erosion has long been detected, no consensus was reached as regards whether the CD as a whole has changed from net sedimentation to erosion so far. It is partially because the bathymetric data used in past studies were not consistent and the spatial range of the data rarely covered the entire delta. Even though, the delta erosion risk and the subsequent impact on the safety of dikes, flooding risk, sustainability of the tidal marshes merits future study and management awareness.

6. Integration and management perspectives

6.1. *An integrated picture of the system*

The CD is a river-tide mixed-energy, fluvio-deltaic composite system in which river and tidal forcing plays a dominant role in shaping hydro-morphodynamics. Regionally, fluvial forcing dominates in the tidal river, whereas tides and river jointly control the dynamic regime in the tidal estuary (Fig. 11). In the tidal river, the mean water level is highly elevated by river discharge and the incident tides are largely dissipated (Guo et al., 2015). The daily-averaged mean water levels are higher at

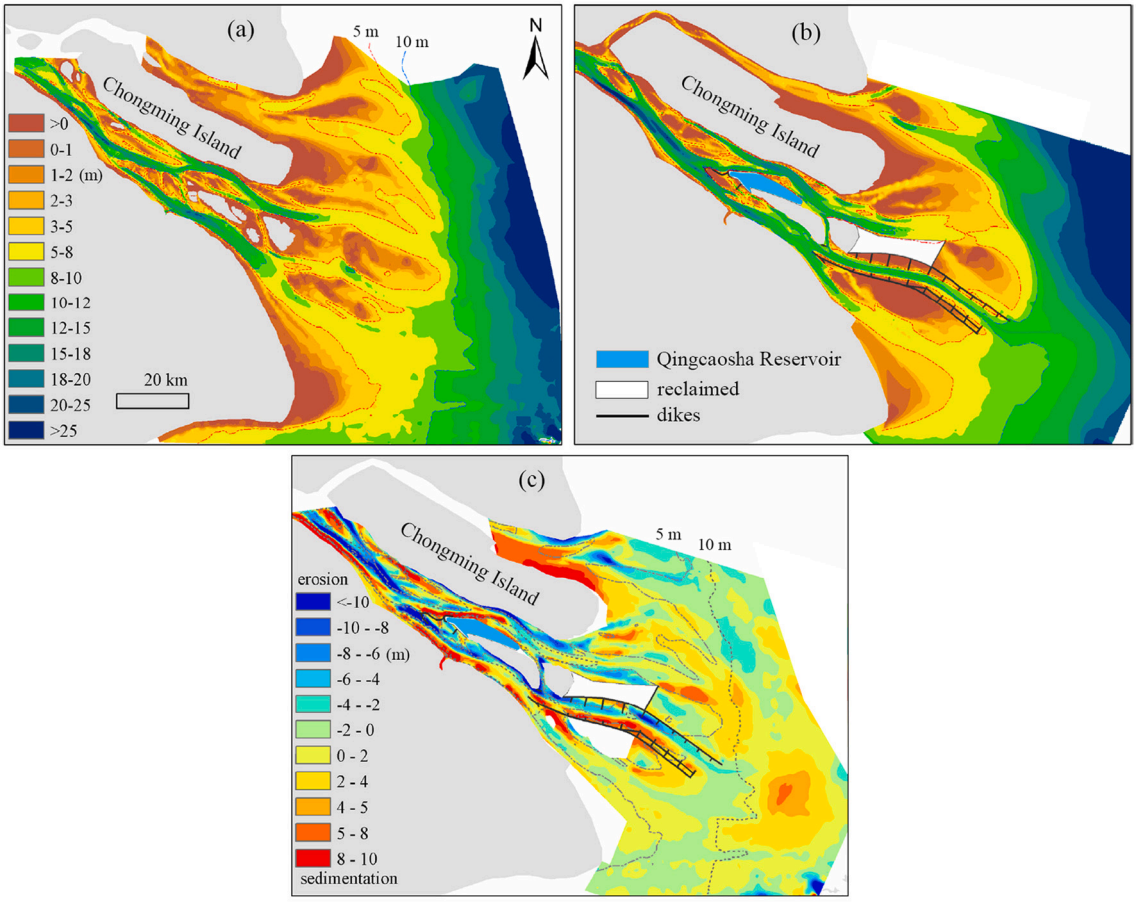

Fig. 10. Bathymetry of region seaward of Xuliujing in CD in (a) 1958 and (b) 2016, and (c) the erosion and sedimentation pattern between 1958 and 2016. Depth in panels (a) and (b) is referenced to the lowest low water. Positive and negative values in (c) indicate sedimentation and erosion, respectively. The isobath lines in 1958 were showed in panel (c). Bathymetry data was not available for the white cut-out areas in panel (b) and (c) because those regions were reclaimed or tidal flats with elevations high above the lowest low tide, thus can not be surveyed by conventional multibeam echosounder.

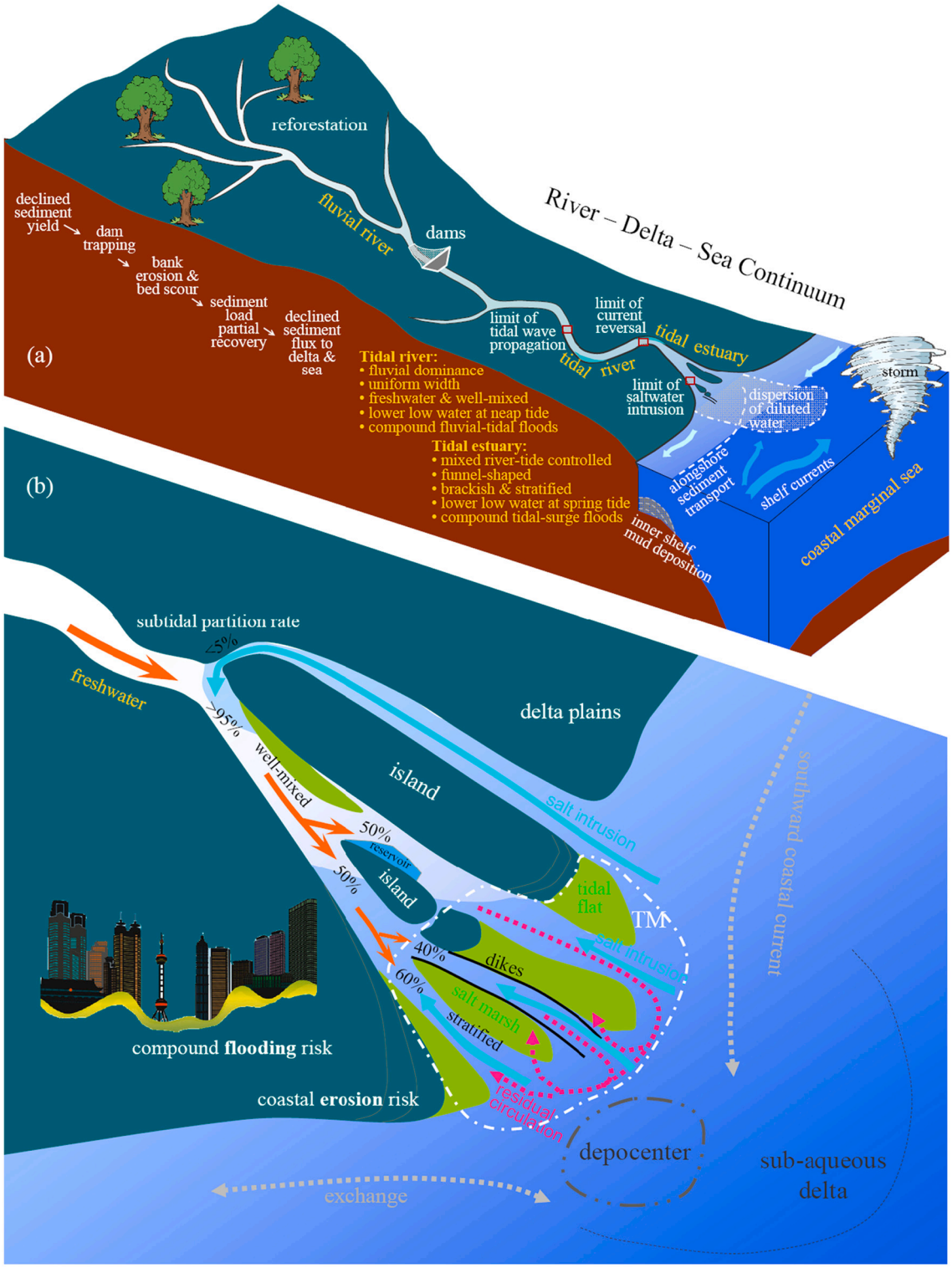

Fig. 11. Sketches of (a) the river-delta-sea continuum with spatial variations and divisions between tidal river and tidal estuary, and (b) a zoom-in view of the branched, saltwater-influenced tidal estuary segment showing subtidal flow partition rates, salt intrusion path, residual circulations in the turbidity maximum (TM) zone, the position of the depocenter, and the influence of coastal currents.

spring tides than neap tides, which tends to exacerbate the highest water levels and induce fluvial-tidal compound flooding risk (Guo et al., 2020). Accordingly, the lowest low water occurs during neap tides in tidal rivers, likely reducing the water depth for navigation and ecosystem services (Hoitink and Jay, 2016). In the tidal estuary, the river influence on the currents is still considerable but the seaward increase in channel width alleviates the river impact in dissipating the tides. The short-term influence of wind, waves, and storms is detectable in the seaward part of the tidal estuary, likely inducing tidal-surge compound flooding and altering nearshore sediment transport. The tidal currents are predominantly unidirectional in the tidal river, bi-directional in the tidal estuary, and exhibit a rotating pattern out of

the delta (Figs. 11a and S4). The major part of the delta is well-mixed, other than the ~60 km long mouth zone where a salt wedge develops. Morphologically, the tidal river part of deltas is characterized by nearly uniform channel width, relatively high sinuosity, and seaward-increasing depth (Gugliotta and Saito, 2019). Intertidal flat is little along tidal rivers owing to smaller tidal range, while the majority of the intertidal flats are found in the mouth zone (Zhang et al., 2016). The tidal estuary has a convergent planform, seaward-decreasing depth, and the ebb channels develop at a larger spatial scale compared with the flood channels. Seaward sediment flux prevails in tidal rivers, whereas landward sediment transport may occur in tidal estuaries, leading to sediment transport convergence in between. These distinctive hydro-morphodynamic differences between the tidal river and tidal estuary in large deltas like the CD mandate specific examination and management awareness (Hoitink and Jay, 2016; Gugliotta and Saito, 2019).

The tidal estuary part of the CD is overall a very wide and shallow environment (see Fig. 1c). The South Branch has a bankfull width of ~15 km and a cross-sectionally averaged depth of <15 m, i.e., a depth-to-width ratio ~ 1/1000. The depth-to-width ratio is even smaller in the mouth zone, i.e., ~1/4000, which is much smaller than their fluvial counterpart is (e.g., >1/500). The sand bars and shoals in the mouth zone are also large in size, e.g., the Jiuduan shoal stretches ~10 km laterally and ~ 50 km longitudinally. The wide and shallow nature of the channels benefits the development of lateral tidal straining and significant horizontal and lateral circulations, other than the vertical density stratification and gravitational circulations. The fully 3-dimensional dynamics were hardly captured in traditional point-based field surveys over tidal cycles, while long time-series of data and usage of numerical modeling have enhanced the scientific understandings (Wu et al., 2010; Zhu et al., 2018).

Large spatial and long time scales are lined up for deltaic hydro-morphodynamics (Fig. 12). The time scale effect is an issue meriting careful consideration in studying sediment transport and large-scale morphodynamic adaptation. By employing tracer age to track water motion, Wang et al. (2010) quantified that the residence time of water was ~23 and ~ 35 days in the CD in the wet and dry seasons, respectively, as regards the water particles released at Xuliujing. Sediment transport lags behind water motion, although the exact sediment transport time scale has not been quantified. Predominantly seaward sediment flushing leads to stepwise development and migration of sand bars in the seaward direction, e.g., the cyclic morphodynamic changes of the Biandan shoal in the South Branch at the time scale of decades (Fig. S8). Accordingly, the occurrence of shifting changes from net deposition to erosion in the mouth zone of the CD (since ~2010) lagged riverine sediment decline (since ~1980s) at a time scale of approximately 30 years (Zhao et al., 2018; Zhu et al., 2019). It is noteworthy that the deltaic morphodynamic adaptation time scale is likely much longer than decades. As a reference, the morphodynamic time scales of the Humber Estuary in the UK and the western Scheldt Estuary in the Netherlands were estimated to be ~40 and 110 years, respectively (Jeuken et al., 2003). These two tide-dominated estuaries are much smaller in size than the CD; therefore, the morphodynamic adaptation time scale of the CD is likely larger than ~100 years. Overall, the hydrodynamic adaptation time scale is essentially smaller compared with that of morphodynamic adjustment (Fig. 12). The large morphodynamic adaptation time scale suggests the necessity of long-term perspectives in management and planning.

Another explanation of the above-mentioned morphodynamic response time lag is the delta system's inherent buffering capacity. One evidence is that the intertidal flats in the mouth zone continued to accrete and increase in elevation and areas while the riverine sediment source has declined (Zhu et al., 2019), although the subtidal flat areas

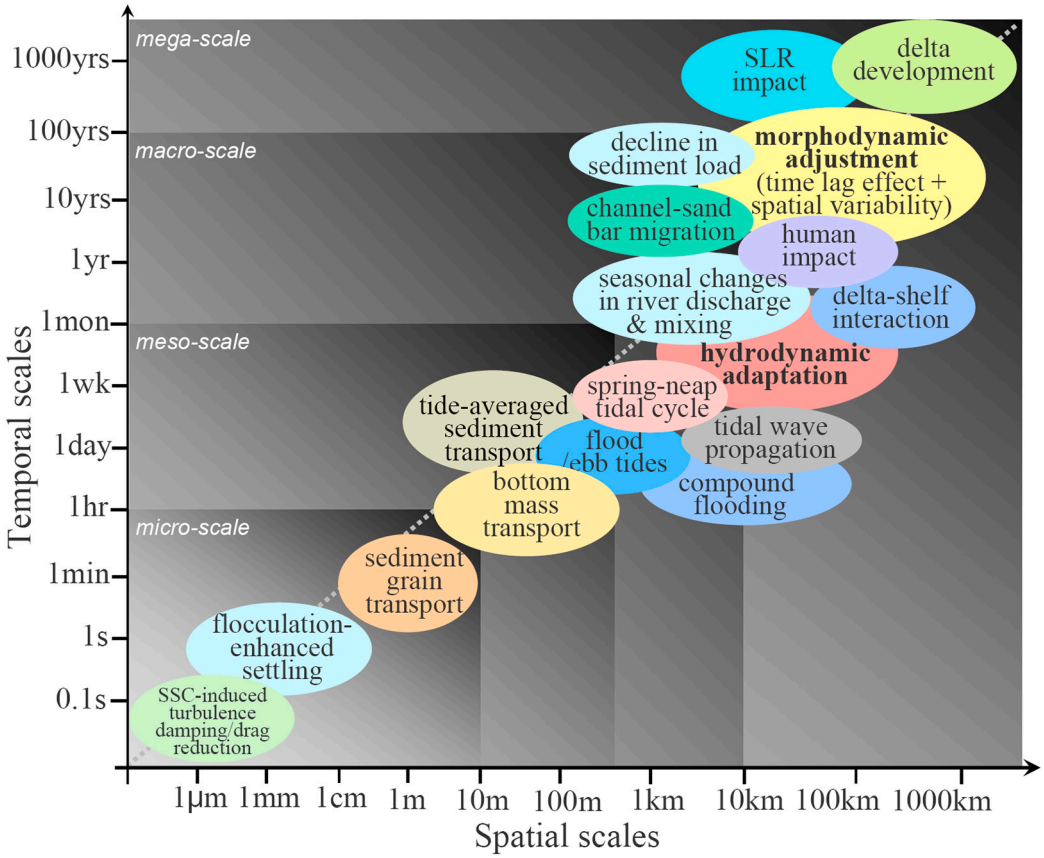

Fig. 12. Multi-space-time-scale hydro-morphodynamic processes involved in the CD, with distinctive time scale differences between hydrodynamic adaptation and morphodynamic adjustment in response to external changes in terms of SLR, sediment decline, and human activities.

were decreasing. Yang et al. (2020a, b, Yang et al., 2021) reported that the sediment eroded from the subaqueous delta front zones can be a source supply in sustaining accretion of the eastern Chongming flat, although the driving mechanisms were not elaborated. The sediment resuspended in the mud bank zone outside the South Passage may also be transported back into the delta (Liu et al., 2010a; Zhu et al., 2018), particularly given the occurrence of a net landward water flux and flood dominance in the seaward parts of the South Passage (Wu et al., 2010). These evidences suggest the role of sediment redistribution within the delta in counteracting riverine sediment decline. This buffering capacity is explainable considering the abundance of previously deposited while less compacted subsurface sediment and the sustained strength of tidal currents and waves in reworking and driving sediment resuspension. Similarly, the importance of sediment redistribution was documented in the San Francisco Bay, in which sediment exchange between its sub-embayments was expected to control the deposition/erosion pattern in the coming century as watershed sediment loads continued to decrease (Ganju and Schoellhamer, 2010).

We identify four phases of hydro-morphodynamic changes at the decadal to centennial time scales. In the pre-1958 period (phase I), the CD underwent constructive morphodynamic development that was featured by the initial formation of the 3-bifurcation-4-branch configuration. Anthropogenic influences are relatively minor at that time. Following that, the CD with a 4-branch configuration started to adjust towards stability between 1958 and ~2000 (phase II). It was characterized by realigned channels, accreted tidal flats, and a matured channel-shoal structure. Human activities like reclamation started to increase in this period and the influence of sediment source decline was not yet detected. Since the early 2000s (phase III), human activities had largely intensified and the morphodynamic impact of sediment load reduction emerge. The deltaic morphodynamic activity reduces owing to increasing hard engineering structures. Reduction in suspended sediment concentrations and regional erosion were detected, e.g., in the South Branch, while the tidal flat accretion rate in the mouth zone slowed down with an emerging shift to erosion. This period was taken as a transitional phase during which the deltaic hydro-morphodynamics were substantially disrupted and struggled to adapt and restore. Considering the coming decades to century (phase IV), the continuously changing conditions may overwhelm the deltaic hydro-morphodynamic buffering capacity, therefore more erosion is expected along the main channels, marsh edges, and delta front regions, and the delta as a whole is likely to enter into a destructive phase.

6.2. *The CD in the Anthropocene*

Intensified human activities since the 1950s rendered the CD as an ideal case for discussion and interpretation of anthropogenic influences (see Fig. S10). On the one hand, human activities in terms of waterway regulation, port development, land reclamation, and reservoir construction etc. have supported regional socio-economical development in the recent six decades, making the CD one of the most significant economical hotspots in China. It is obliged to acknowledge the benefit of the engineering projects in making new land, supplying freshwater resources for millions of people, and facilitating waterway transportation. On the other hand, it raises concerns that human activities have become a fundamental driving forcing affecting the deltaic hydro-morphodynamics (Fig. 13). Understanding the impact of human activities is necessary to minimize the negative impact and prepare for future sustainable development.

Anthropogenic influences in the river watershed in terms of land-use

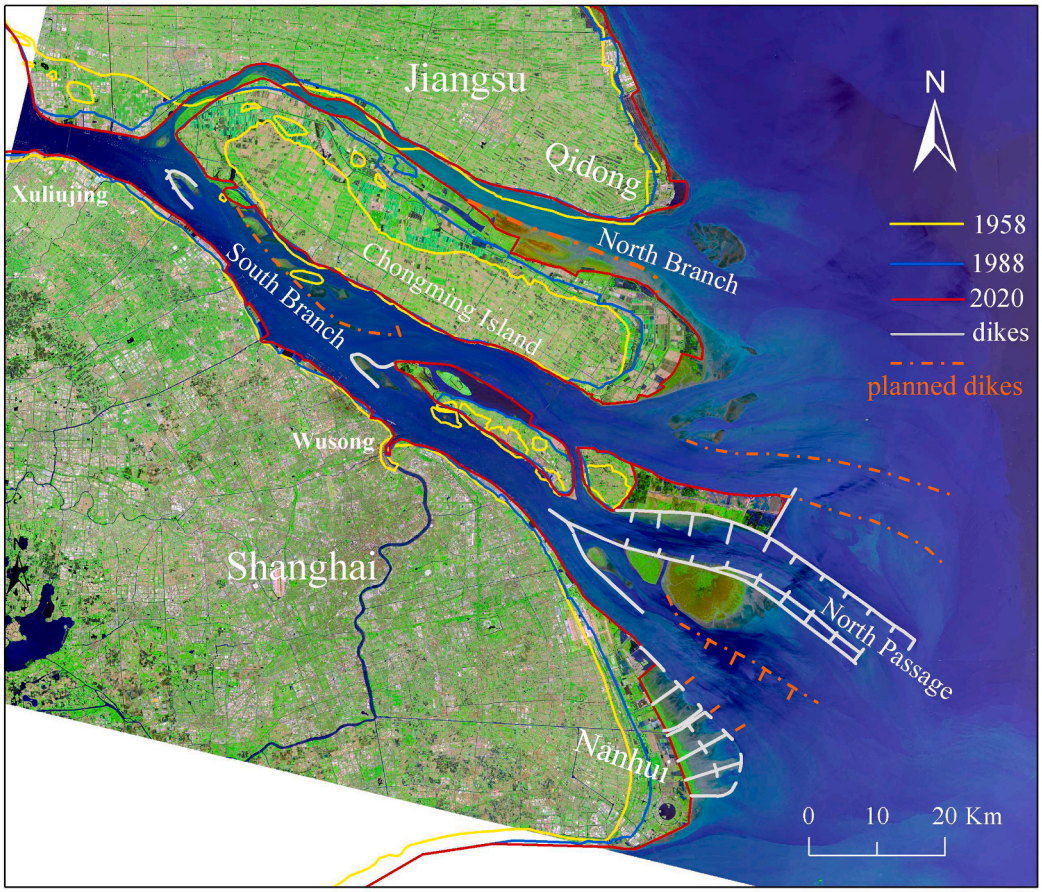

Fig. 13. Coastline changes since 1958 and human activities over the last century based on the satellite images in 2020 during a low tide, with regulation dikes possibly imposed in future identified.

changes (altering sediment yield), construction of hydropower dams (altering both river flow and sediment delivery), and sand mining (extracting sediment from river channel) have substantially modulated the river discharge hydrograph and/or reduced sediment supply to the delta (see Section 3.1). The increased low river discharge in the dry season and reduced high river discharge in the wet season alter saltwater intrusion and sediment deposition and erosion balance at the seasonal time scale in the delta, although the yearly mean river discharge remains stable. The profound reduction in fluvial sediment supply is a primary changing condition in the Anthropocene that initiates a shift from constructive development towards destructive shrinkage. This trend is likely irreversible and tends to persist for centuries given the huge reservoir storage capacity and limited sediment recovery downstream of the dams (Guo et al., 2019). Delta erosion and the subsequent impact on dike safety, wetland, and flooding risk become serious management challenges in the densely populated CD.

In the delta locally, dikes and reclamation of tidal flats are the largest human intervention that profoundly affecting the deltaic hydro-morphodynamics (Figs. 13 and S11). The earliest dikes dated back to 713 CE in the CD, implying a long history of human activities (Chen and Li, 2002). Human settlement was first seen in the emerged mid-channel sand bars since the 7th century when the Chongming Island started to develop (Chen et al., 1979; Yun, 2004). The position of the southern bank along the South Branch changed little in the past century thanks to the historically built dikes and the constraints of harbors and docks. Reclamation of low-lying tidal flats in the North Branch significantly reduced the channel width and volume, accelerating the shifting change towards a convergent, flood-dominated tidal branch (Guo et al., 2021a, 2021b). Tidal flat embankments had largely accelerated the growth of the Chongming, Changxing and Hengsha Islands (Chen, 1957; Yun, 2004). Successive reclamation of tidal flats over the eastern Chongming flat and Nanhui flat since the 1960s stimulated shoreline advance at a rate of 100 m yr^{-1} (Chen et al., 1999; Yang et al., 2001; Yun, 2010). Ongoing reclamation of the inter- and even sub-tidal flats over the eastern Hengsha flat and Nanhui flat further increased the subaerial delta area (Yun, 2010; Tian et al., 2015; Fig. 13). Analyses of satellite images suggested that 40% of the tidal flats have been lost since 1980 in the CD, and a cumulated reclamation area of ~1520 km^2 was achieved between 1950s and 2020 (Li et al., 2020; Fig. S10e). The dikes and shoreline protections have stabilized a major portion of the coastlines and narrowed the channels in the CD.

Large-scale engineering projects exerted strong influences on the deltaic hydro-morphodynamics. A giant reservoir, the Qingcaosha Reservoir with a storage capacity of 380 million m^3 (Fig. 10b), was constructed to store and supply freshwater to Shanghai since 2010 by reclaiming a sand bar to the north of Changxing Island. It reduced the width of the upper North Channel by half and may have affected the flow and sediment partition between the North and South Channels. To overcome the barrier effect of the mouth bars and to facilitate navigation, two long jetties and dozes of groins were constructed between 1998 and 2012 in the selected main waterway, the North Passage. The long jetties, with an elevation of 2.5 m above the Wusong Datum, largely blocked the inter-channel horizontal water and sediment circulations (Zhu et al., 2016). Together with a huge amount of maintenance dredging up to 50–100 million m^3 per year along the 350-m wide and 60-km long navigation channel, the North Passage became narrower and deeper, and its subtidal flow partition rate has decreased from 50% to 40% (Zhu et al., 2019). Stratification and gravitational circulations were enhanced in the seaward part of the North Passage (Wang et al., 2010; Zhu et al., 2018; Chen et al., 2020), which may enhance near-bottom sediment trapping and increase the demand for maintenance dredging. The jetties and groins provided sheltering effect for the adjacent Hengsha flat and Jiuduan shoal and stimulated their accretion (Tian et al., 2015; Zhu et al., 2019; Li et al., 2020). Dumping of the dredged sediment over the landward part of the Hengsha flat and following embankment measures accelerated the sedimentation and flat accretion therein. Moreover, the jetties in the North Passage also play a role in modulating the Changjiang plume (Wu et al., 2018b) and large-scale residual circulation pattern in the mouth and nearshore regions (Zhu et al., 2016; Chen et al., 2020), suggesting the far-field impact of large-scale engineering projects. While the short-term and local impact of human activities has been well studied, their long-term and large-scale impact was largely unknown and mandates future study.

The widely present dikes, jetties, and groins have collectively led to substantially increased shoreline stability and channel-shoal structure, and reduced deltaic morphodynamic activities (Fig. 14). An increase in the stability of channel-shoal structure is beneficial to coastal development, whereas the reduction in morphodynamic activities means a decline in system resilience to external changes like sediment decline and SLR. Considering the cumulative human activities and their fundamental impact on the hydro-morphodynamics, the CD has entered an Anthropocene Epoch and is undergoing dramatic transitional changes in three aspects: a shift from net sedimentation to erosion, a role change of the delta as a sediment sink to a sediment transport conduit, and a change from naturally slow morphodynamic adaptation to human-driven radical hydro-morphodynamic adjustment. Coping with deltas in transition poses a global management challenge and requires strategic planning with longer-term perspectives.

6.3. The CD in a global context

River deltas and estuaries were traditionally classified according to the relative strength of the primary forcing conditions such as river, tides, and waves (Galloway, 1975; Davis and Hayes, 1984). The topography of the CD is characterized by composite features observed in the Mekong Delta and Fly River estuary etc., whereas wave-controlled morphological elements such as sand spits and barrier islands in the Mississippi and Nile River deltas are absent. The CD is overall a river-tide mixed-energy system that is in some way comparable with the Amazon, Mekong, Fly, and Ganges-Brahmaputra estuaries and deltas in terms of driving forces, sedimentary facies, and delta development processes (Hori et al., 2002), and the knowledge obtained in the CD potentially inform study and management of these similar estuaries and deltas (Fig. 15).

Strong river flow plays an important role in damping the incoming tidal waves, constraining landward saltwater intrusion, and flushing sediment seaward. At the longer-term scale, high river flow and associated sediment supply stimulate the formation of a large low-lying delta in the land-ocean interface. This low-lying relief benefits inland tidal wave propagation, which explains why tidal wave propagation is much more inland in the Changjiang and Amazon deltas, although the river discharge is extremely large (Gallo and Vinzon, 2005; Guo et al., 2015). Long-distance tidal wave propagation and deformation under highly variable river discharge highlights the role of large estuaries and deltas as frequency filters for long tidal and surge waves (Guo et al., 2020). Moreover, the river discharge is so large in the Changjiang and Amazon deltas that the river plume extends significantly offshore in the coastal oceans, and saltwater intrusion is constrained in the utmost seaward regions of the river mouths. Landward tidal penetration is comparably shorter in the Ganges-Brahmaputra-Meghna delta, which is ascribed to the higher relief and larger bed gradients in its fluvial-to-tidal transitional regions (Wilson and Goodbred Jr., 2015).

Tides play another important role in water mixing and sediment transport. Seaward dissipation of river influence and landward tidal damping lead to distinctive hydro-morphodynamics between the tidal river and tidal estuary, and similar spatial variations are detected in other large estuaries such as the Columbia (Jay et al., 2015) and Amazon estuaries (Gallo and Vinzon, 2005; Fricke et al., 2018). The CD displays longitudinal changes in channel width, sinuosity, water depth, and bottom sediment composition that are consistent with the Mekong Delta and Fly Estuary (Dalrymple and Choi, 2007; Gugliotta and Saito, 2019; Kästner et al., 2019). In the longer-term, strong tides may favor the

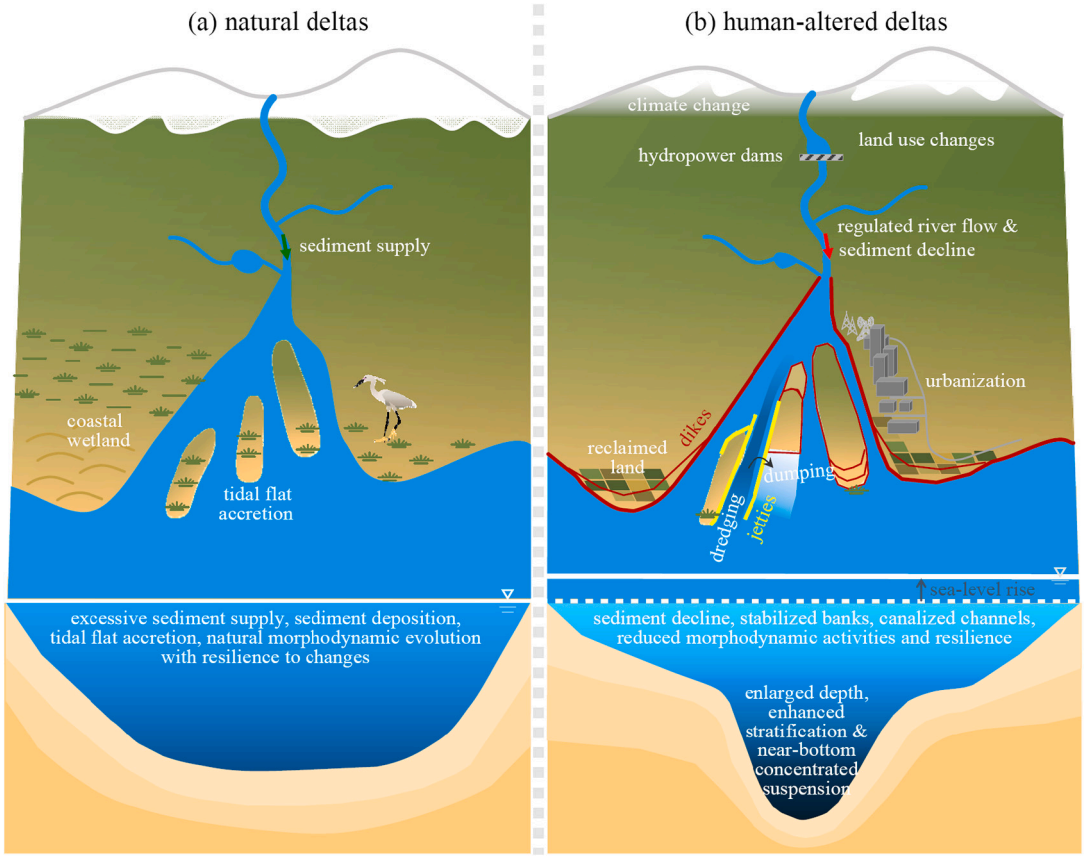

Fig. 14. Sketches of (a) natural deltas and (b) deltas under significant anthropogenic interventions with conditions mimicking the CD.

deposition of river-supplied sediment within the incised valley (Uehara et al., 2002; Chen and Zhu, 2012). However, as the valley was filled to some degree and distributary channels took shape and matured, strong tides and large tidal prism help to maintain wide and shallow channels, which then act as transport passages in flushing river-supplied sediment to the sea.

Geomorphologically, the CD is an alluvial fluvio-deltaic system with relatively few boundary constraints in the lower river course. The incised valley was infilled to a larger degree owing to a high river-borne sediment supply, compared with the less infilled valley in the Pearl and the Fly estuaries. However, the subaerial CD is less advanced into the coastal ocean compared with the Yellow and Mississippi deltas (Saito et al., 2001), even given a high riverine sediment supply for thousands of years. Development of sub-delta lobes and migration of river courses observed in river-dominated deltas did not occur in the CD (Hori et al., 2002). These differences from river-dominated deltas are ascribed to the strong tidal currents and their interaction with river flow, which enhance seaward sediment transport (Guo et al., 2014). The sediment flushed outside the delta is then transported away by alongshore coastal and shelf currents, which partially explains the <68% sediment trapping efficiency in the CD.

The broad and shallow morphology of the ECS shapes the shelf currents and circulations, which in turn influence the morphodynamic development of the CD. The shelf-slope of ECS is comparably smaller than that seaward the Mississippi and Nile deltas, but is similar to that outside the Amazon Estuary and Ganges-Brahmaputra Delta (Wright and Coleman, 1972; Hori et al., 2002). The landward shallowing shelf morphology enhances the dissipation of wind waves but an amplification of long tidal waves, reinforcing tidal influence on the CD. The shallow shelf also benefits nearshore sedimentation, rather than rapid transport and loss into deep trenches and seas as that along leading edge coasts (Inman and Nordstrom, 1971). This shallow-water sedimentation leads to the formation of a broad subaqueous delta over which the temporally deposited and accumulated sediment could be reworked and partially transported back into the delta as a second-hand marine sediment source (Yang et al., 2020a, 2020b; Yang et al., 2021). The importance of this marine sediment source may stand out more clearly in the Anthropocene given a large decline in riverine sediment supply. The majority of the sediment flushed out of the CD was transported southward along the coasts, leading to the formation of distal mud deposition in the inner shelf zone. Similar sediment dispersion and alongshore deposition are observed off the Pearl (Gao et al., 2015) and Amazon estuaries (Anthony et al., 2010). In the latter case, the northward coastal currents transport the sediment as far as to the Guiana and Surinam coasts, resulting in the formation of a thick layer of mud deposition in the inner shelf and along the coasts (Anthony et al., 2010; Nittrouer et al., 2021).

Strong impact of human activities is ubiquitous in many river deltas and tidal estuaries as that in the CD. For instance, the leveed channels in the Mississippi Delta induced pipeline effects that enhance sediment transport and loss to deep waters in the Gulf of Mexico (Paola et al., 2011). Similarly, stabilized river courses in the Yellow River delta reduced the possibility and frequency of channel avulsion, resulting in sediment transport towards the deep waters through the active channels, whereas the adjacent abandoned lobes underwent erosion (Fu et al., 2021). Human-initiated navigational improvements (construction of jetties, dredged channels, and pile dikes) and diking and filling of wetlands overruled the natural shoaling and erosion processes in the Columbia Estuary in the USA, where the tidal prism had decreased by 15% (Sherwood et al., 1990). In the Mersey Estuary in the U.K., training wall construction and dredging activity in the sea approach channels was one of the dominant causes of channel volume reduction by 10% in the past century owing to fine sediment import (Thomas et al., 2002; Lane, 2004; Blott et al., 2006). The Seine Estuary in France was another

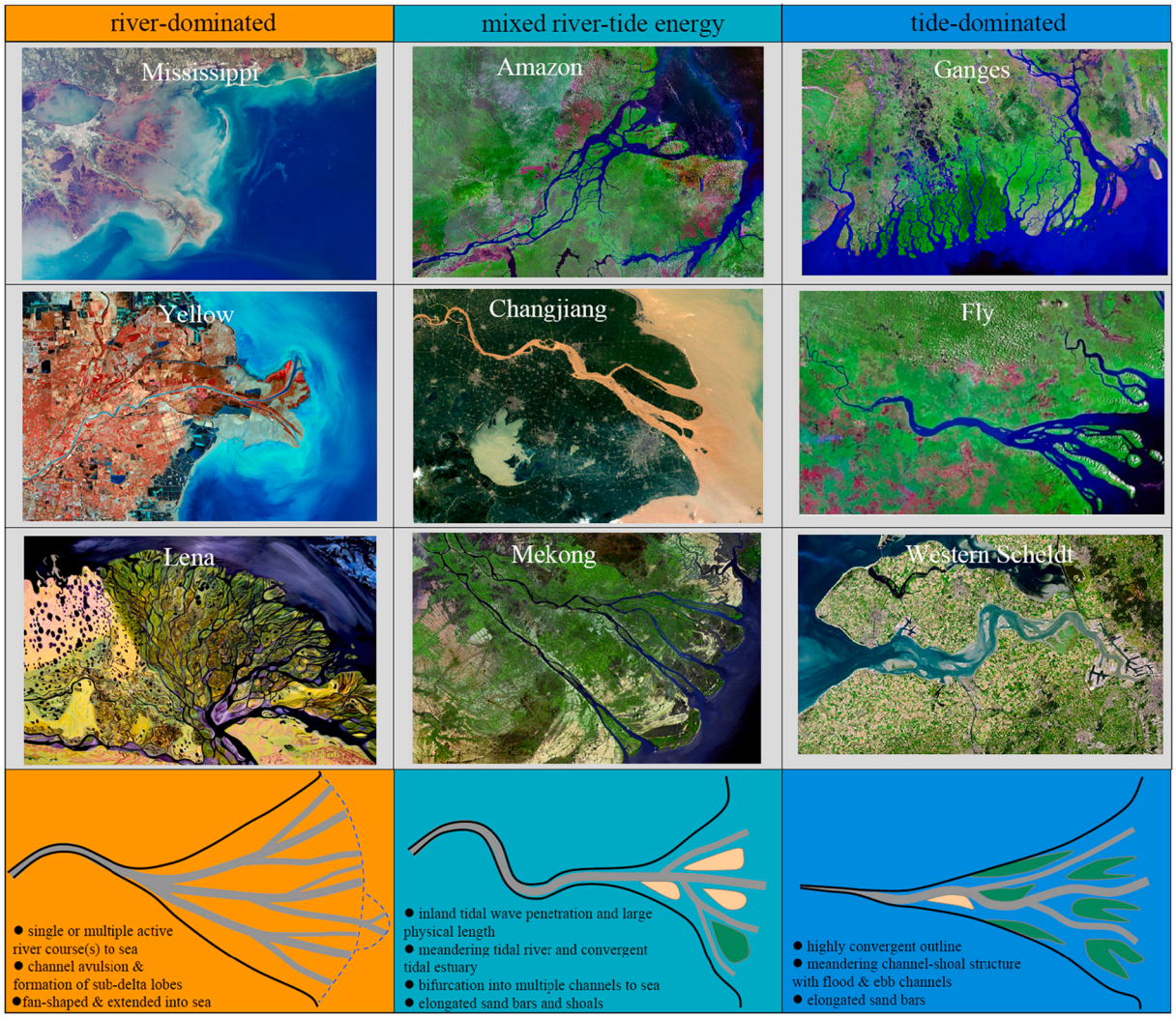

Fig. 15. Satellite images of typical river-dominated, tide-dominated, and mixed-energy estuaries and deltas, with associated sketches of their hydro-morphodynamic features.

example where human activities such as landfill, marsh reclamation, jettying and dredging in the past 130 years had led to a narrow, deep, and jettied channel exit to the sea, and reduced estuarine volume and areas available for sedimentation of fluvial sediments. The amplified seaward transport of fluvial material changed the geologic role of the Seine Estuary from a sink for fluvial and marine sediments, to a source of fluvial sediment for the shelf (Avoine, 1986). Intensive dredging in the Ems Estuary had induced positive feedback changes featured by increased channel depth, enhanced tidal amplification, increased sediment concentration and consequently reduced bottom drag and furthermore tidal amplification (Winterwerp and Wang, 2013). These studies collectively highlight the fundamental impacts of human activities on estuarine and deltaic hydro-morphodynamics (Fig. 14), while the driving and feedback mechanisms between human activities and natural hydro-morphodynamic adaptation were underestimated.

6.4. Hazards and management perspectives

The CD is currently in a critical transition phase given the continuously changing boundary forcing conditions and the conflicting interest between delta development and ecosystem conservation. The delta is vulnerable and exposed to multiple natural hazards that urgently need integrated management strategies. In this section, we mainly elaborate on the geophysical hazards, including saltwater intrusion, land subsidence, flooding risk, and coastal erosion, while other concerns such as water pollution, eutrophication, and ecosystem degeneration are left for a separate discussion.

Saltwater intrusion is a big issue in the CD because it affects the freshwater resource supply for >10 million people in Shanghai. Changjiang water resource supply to Shanghai mainly relies on the Qingcaosha Reservoir and another two small reservoirs (Dongfengxisha and Chenhang); all of them are under the threats of saltwater intrusion. The dynamics and the governing mechanisms of saltwater intrusion in the CD have been well studied based on numerical modeling, e.g., the controlling impact of river discharge, the influence of the TGD-regulated river discharge, bathymetric changes, strong northerly wind, and SLR (Wu et al., 2010; Zhu et al., 2020). The remained problems include extreme saltwater intrusion in the North Channel driven by persistent northerly strong wind in the dry season, and the intrusion in the North Branch and overspill to the South Branch. Possible solutions include real-time operation of the TGD by releasing more river flow to counteract saltwater intrusion in the dry seasons and regulation of the North Branch to mitigate overspill etc. Saltwater intrusion in the North Branch was alleviated in the recent decade owing to channel aggradations and reduced channel volume and tidal prism. There was a plan to construct a barrier at the mouth of North Branch, but the impact on the branch and the delta system as whole remains an open question. Another long-term solution of water supply is to plan a new reservoir, e.g., at the place of

the Biandan shoal (Fig. 1c), which may fundamentally increase water supply capacity and the resilience to saltwater intrusion under SLR.

The CD undergoes land subsidence predominantly owing to past groundwater extraction. Tectonic subsidence was ~1 mm yr^{-1} in the late Pleistocene (Zhao et al., 2008). The mean land subsidence rate was approximately 3.9 mm yr^{-1} between 1921 and 1965 (Wang et al., 2012; He et al., 2019). Groundwater extraction was strictly regulated and recharge was implemented since 1966, and the afterward subsidence rate decreased to 0.9 mm yr^{-1}. Rapid urbanization and intensive construction of high buildings and underground infrastructures again resulted in an increased subsidence rate to 10.2 mm yr^{-1} between 1986 and 1997. The maximum cumulated subsidence in the downtown regions of Shanghai was 6.04 m between 1980 and 2005, i.e., a rate of 24 mm yr^{-1} (Wang et al., 2012; see Fig. S12). Land subsidence, combined with SLR, is to increase the vulnerability of CD to pluvial and coastal flooding.

The CD is exposed to multiple sources of flooding risk and their compound effect, including high river discharge, king tide, storm surge, and SLR. The subaerial CD and the Shanghai city, with a mean elevation of 3–4 m, are on the top of the list of deltas and mega-cities that are subject to severe flooding risk (Balica et al., 2012; Tessler et al., 2015). The TGD has regulated the frequency and magnitude of extremely high river discharge, but high river discharge may still occur, e.g., the large flood in July 2020 with the extreme river discharge reaching 84,500 m^3/s at Datong (Wei et al., 2020). The compound flooding risk resulting from concurrent occurrence of high river discharge, king tide, and storm surge (typhoon events) in the summer season poses extreme threats on delta safety (Balica et al., 2012; Wang et al., 2012; Yin et al., 2020). Land subsidence, SLR and coastal erosion would further exacerbate the flooding risk. The coastal dikes surrounding Shanghai have a protection standard for floods with recurrence interval over 100–200 years (Wang et al., 2012). Raising dikes in response to SLR has become increasingly unsustainable given the costs and the risk of dike failure. Future flooding risk management needs an in-depth knowledge of the compound effect of multiple flood drivers and their covariate occurrence possibility, improved forecast of river floods and typhoon path and associated managed retreat etc. Preserving and restoring waterfront tidal wetlands, instead of reclaiming them, can help to dissipate waves and surges and mitigate flooding risk.

Coastal erosion and land loss due to sediment shortage is another severe problem in the CD as that had occurred in many other estuaries and deltas worldwide (Syvitski et al., 2009; Giosan et al., 2014). The impact of SLR in inducing erosion was relatively less obvious in the past century owing to a high riverine sediment supply (Wang et al., 2009), but its impact is expected to stand out in the future as sediment availability has reduced to a large degree. The initial decline in riverine sediment supply since the mid-1980s, followed by the accelerated reduction since the early 2000s, has reduced tidal flat accretion as to 2016 (Luan et al., 2016; Zhao et al., 2018), while a shifting change from sedimentation to erosion is expected in future. Instead of worrying about the irreversible sediment decline that is to persist for centuries, it would be more practically useful to focus on managing the remained sediment supply and ensure that more sediment is retained within or close to the delta. Lessons learned from the restoration of the Mississippi Delta (Day et al., 2007) etc. have implications for management of the CD. For instance, land-building sediment diversion by breaching dikes and opening barrier gates were proved effective and beneficial in sustaining natural resilience in the Mississippi Delta (Day et al., 2007; Xu et al., 2019). Sediment diversion stimulates sediment deposition in regions close to coasts, rather than allowing the river-supplied sediment flushed along the canalized channels and lost to deeper water. Usage of the dredged sediment to make new marshes and wetlands can also counteract habitat loss due to sediment deficiency. In the Rhine-Meuse Delta, dikes and barriers were traditionally constructed as flood-control defense measures, while opening the barrier gates to let tides do their constructive job in promoting tidal flat accretion is proved successful in conserving tidal wetlands and habitats (Smit et al., 1997). Instead of fighting against nature, living and building with nature and managed retreat to adapt SLR are options to mitigate coastal erosion and increase resilience to flooding hazards, which in the meantime benefits ecosystem restoration (Temmerman et al., 2013). These lessons have implications for management of CD and other deltas.

Overall, sustainable management of the CD needs to take account of multiple needs including the safety of shoreline and infrastructure, coastal flooding defense, ecosystems conservation, and freshwater supply. The multi-objective management strategy need to promote knowledge transfer, involve more stakeholders and cope with interest conflict, and understand the tradeoffs in decision-making and strategic planning. The past strategy in managing the CD was constructing dikes, jetties, groins, and embankments to increase its morphodynamic stability and promote infrastructure development, e.g., fixing the division of the branches, reducing channel migration and sand bar movement, and reclaiming tidal flats. Now it is time to reevaluate this stabilization strategy, its benefits and long-term impacts on the system behavior, and figure out more sustainable and resilient measures. As the delta becomes increasingly constrained, the tidal prism may decrease and the delta probably becomes more efficient in flushing sediment to the sea, i.e., a decline in sediment residence time and sediment trapping efficiency. It means a larger portion of the river-supplied sediment tends to be lost to the sea due to the pipeline effect, instead of depositing within the delta in building up tidal flats and marshes as usual, as that had occurred in the Mississippi Delta (Paola et al., 2011). This trend is worsened by the decline in riverine sediment supply and SLR. Tidal wetlands and ecosystems were growingly valued in coastal management community, and there is an ongoing mindset change from coastal development to ecosystem conservation throughout the Changjiang river-delta continuum. For instance, tidal flat reclamation and embankment are legally restricted in the delta region since 2016. After all, hazard mitigation and multi-objective management of the CD require integrated system thinking and long-term perspectives based on improved interdisciplinary scientific understanding of the deltaic hydro-morphodynamics and their coupled interaction with human and the ecosystem, as well as the responses and feedback mechanisms.

6.5. *Knowledge gaps*

Advanced monitoring and modeling studies have prompted scientific understanding of the hydro-morphodynamics in the CD; however, there are challenges and knowledge gaps that remained. The deltaic hydro-morphodynamic evolution is continuously disrupted by changes in boundary conditions and progressive human activities, increasing the difficulty in sorting out the inherent natural processes and human impact. Based on the foregoing synthesis, we identify five key knowledge gaps that merit future research effort, not only for the CD, but also possibly of implications for other estuaries and deltas in general.

(1) **The dynamic interactions within the river-delta-sea continuum**: As a large system locating at the land-to-ocean transition region, the CD is strongly affected by what happens in the watershed and the marginal sea, making it more than a local but a grand system involving many larger-scale processes. The impact of the river and oceanic forcing on the present-day delta hydrodynamics has been well understood, whereas their interactions and impact on the long-term morphodynamics remains an open question, e.g., how do the river and marine forcing affect the infilling processes of the incised valley and shape delta development towards an asymmetric branching pattern. Our long-term morphodynamic modeling experiences suggest that it may not fully capture the long-term delta development processes when considering river and tidal forcing only. Wu (2021) modeled that the southward Zhe-Min Coastal Currents may not exist if removing the nearshore mud deposition, implying the morphological control on the inner shelf currents. It remains unknown how could the Changjiang River-supplied sediment being flushed to the sea in forming the inner shelf mud

deposition before the incised river valley was filled since the mid-Holocene (Jiang et al., 2021). Further study of the river-delta-ocean interactions would help to better interpret the sedimentation and morphodynamic evolution of the delta, to identify the controls of the distinctive development pattern between the northern and southern delta plains, and to quantify the alongshore and inner shelf sediment transport regime and the governing mechanisms.

(2) **Hydro-morphodynamics in tidal rivers**: Previous studies mainly focused on the tidal estuary part of larger estuaries and deltas where salinity and stratification are profound. Increasing research interest in tidal rivers emerges in recent years (Sassi and Hoitink, 2013; Guo et al., 2015; Zheng et al., 2018b; Fricke et al., 2018; Gugliotta and Saito, 2019), but there is still a lot unknowns that merit future study (Hoitink and Jay, 2016). The tidal river in the CD is ~405 km in length, which is longer than the tidal estuary. Knowledge of the non-stationary tidal dynamics in tidal rivers is necessary to inform tidal prediction and tidal discharge estimation and management of compound flooding risk, wetlands, fish habitat, and navigation channels (Talke and Jay, 2020). Hydro-morphodynamic equilibrium in tidal rivers was rarely discussed compared with numerous studies in fluvial rivers and tidal estuaries. The sediment flux at the limit of tidal wave propagation is conventionally used to represent the flux to the delta or ocean. However, it may be misleading for large deltas like the Changjiang and Amazon, because erosion and deposition along tidal rivers induce extra sediment gain or loss (Nittrouer et al., 2021). Better quantification and update of the global terrestrial sediment flux to oceans need an advanced understanding of the hydro-morphodynamics along tidal rivers.

(3) **Fine sediment transport dynamics and their feedback impact**: The fine sediment transport dynamics are relevant to saltmarsh development, transport of organic matter and pollutants, and siltation of the navigational channels and maintenance dredging. High SSC has a feedback impact on the flow dynamics by enhancing turbulence damping, reducing the effective bottom drag and possibly on saltwater intrusion (Lin et al., 2021; Zhu et al., 2021). It explains why a very low bottom friction coefficient is needed (e.g., a Manning coefficient of 0.012 s $m^{-1/3}$) in order to numerically reproduce tidal wave propagation correctly in the CD (Hu et al., 2009). Dredging-induced increase in channel depth has led to amplified tides, increased SSC and drag reduction in tidal estuaries like the Ems and Loir estuaries (Winterwerp and Wang, 2013). By contrast, the decrease in SSC in the CD, as a result of sediment decline, is likely to alleviate the drag reduction effect, thus leading to increased effective friction and possibly more tidal damping inside the delta. Such feedback changes have not been revealed in the CD and similar estuaries and deltas undergoing significant sediment decline.

Sediment transport dynamics are important for process-based morphodynamic modeling. Previous morphodynamic modeling of the CD as a sandy system does not work well (Guo, 2014) while including mud transport improves model performance (Luan et al., 2017). It has been aware that large-scale deltaic morphodynamic behaviors are largely different under muddy environment compared with sandy counterparts, e.g., formation of less braided channels (Edmonds and Slingerland, 2010; Geleynse et al., 2010; Caldwell and Edmonds, 2014), but the inherent mechanisms are poorly explained. Moreover, as the CD is subject to erosion, it is of practical interest to understand the erodability of bottom sediment, the critical shear stress for erosion and its spatial variations and changes over time for the sake of more accurate sediment transport and morphodynamic modeling. Field measurement of the critical bed shear stress is time-consuming for such a large system; indirect interpretation of the erosion threshold based on sediment composition and water content (reflecting the degree of the compaction of bottom sediment) provides alternated options.

Another important yet understudied topic is the bio-physical interactions, i.e., the mutual influences between hydro-morphodynamics and vegetation. Vegetation widely present in muddy systems affects attenuation of wave energy, sediment trapping and deposition, and modifying large-scale morphodynamics. For instance, *Spartina* was introduced to the Jiuduan shoal in the late 1990s and since then tidal flat accretion gained a larger rate, particularly over the supra-tidal flats (Li et al., 2016; Zhu et al., 2019). Tidal flat elevation increase was followed by an increase in vegetation-occupied areas (Li et al., 2016; Zhu et al., 2019), suggesting a positive feedback mechanism between vegetation and flat accretion. A similar phenomenon was detected in the eastern Chongming flat where tidal flats accreted and advanced at a large rate (Yang et al., 2011; Schwarz et al., 2014). Vegetation also affects large-scale morphodynamic development, e.g., formation of channels and tidal creek networks, leading to new topics like eco-morphodynamic or bio-geomorphology, particularly regarding its implication for conservation and restoration of tidal flats and saltmarshes (Murray et al., 2008; Fagherazzi et al., 2012). In the CD, sediment cohesiveness and the bio-physical processes probably play a role in controlling channel bifurcation and the formation of large-scale shoals and sand bars, a hypothesis meriting future verification.

(4) **The cumulative impact of anthropogenic activities** at the decadal to centennial time scales: Extensive human disturbances are present in worldwide coasts and deltas in the Anthropocene, and human impact merits study in both case-specific situation and universal circumstances. Many previous studies have examined the impact of single human interference at the regional scales, e.g., dredging, embankment, and jetty constructions, whereas the cumulative and long-term impact is insufficiently understood (Chen et al., 2020). One example is the large-scale and long-term impact of the jetties and groins in the North Passage. The satellite images suggest that the subaerial land did not extend more seaward than the shoreline between Qidong and Nanhui (see Figs. 13 and S11). The jetties in the North Passage, however, extend farther seaward compared with the northern and southern delta plains. The jetties have modified the circulation pattern in the mouth zone and the plume to the sea (Zhu et al., 2018; Wu et al., 2018b). In addition, the jetties provide important sheltering effects that benefit sediment deposition over surrounding tidal flats and seaward delta progradation. More jetties and groins are proposed to regulate the South Passage and North Channel and to achieve deeper navigational waterways (see Fig. 13). The dikes, jetties, groins, together with extensive tidal flat reclamations, tend to canalize the deltaic channels, creating pipeline effects and making them highly efficient transport passages for the river-supplied sediment. The cumulative impact of human activities may worsen the situation of sediment deficiency and exacerbate the consequent flooding and erosion risks in the delta.

(5) **The delta erosion risk** under the combined influences of sediment decline, human activities and SLR: Sediment flux reduction to estuaries and deltas and consequent coastal erosion is an urgent global management concern (Milliman and Meade, 1983; Giosan et al., 2014). This is further aggravated by land subsidence and SLR (Syvitski et al., 2009). The role of episodic but energetic events like extreme river discharge and typhoons on the medium- to long-term estuarine morphodynamic adaptation is unknown either. As to the mixed-energy CD, its hydro-morphodynamic adaptation to sediment decline may be more complicated compared with other river-dominated deltas and tidal estuaries, because of: 1) the large spatial scale and strong spatial variations in the erosion and deposition patterns, and the large morphodynamic adaptation time scale; 2) sediment load recovery from erosion in the tidal river, which offset sediment flux to the tidal estuary; and 3) the buffering capacity arising from sediment resuspension and redistribution within the delta (see Section 5.2). Considering these dynamic variations and complexity, a sediment supply threshold that maintains current morphology of CD as a whole may not exist.

Long-term hydro-morphodynamic models provide a potential approach to project future evolution under the changing boundary conditions (van der Wegen, 2010; Luan et al., 2017). Morphodynamic modeling approaches have been successfully employed to study initial channel formation and impact of SLR etc. in tidal estuaries and river deltas (van der Wegen, 2013). It is noteworthy that the uncertainty in

hindcasting historical morphodynamic evolution remains high, because of the strong spatial and temporal variability in physical processes, the uncertainty in sediment transport modeling (particularly cohesive sediment transport and their erosion dynamics), limited knowledge of morphodynamic adaptation time scale, and coupled impact of human activities. Even though, long-term morphodynamic models can be used to explore the governing mechanisms and the hydro-morphodynamic sensitivity to sediment load decline, SLR, and human activities.

7. Concluding remarks

This work provides a synthesis of the multi-scale hydro-morphodynamics of the large-scale CD, which is classified as a river-tide mixed-energy, fluvio-deltaic system. The river supplies a huge amount of sediment that fills an incised valley formed during low sea level condition, building up a mega-delta, and provides a persistent force flushing sediment seaward. Strong tidal currents interact with river flow, creating significant stratification and gravitational circulations in the mouth zone, which creates sediment transport convergence and stimulates sediment trapping. This river-tide interaction controls the formation of a turbidity maximum zone and associated submerged transverse mouth bars. Fair weather wind and waves are of secondary importance, but strong wind and big waves during stormy condition exert considerable impact on saltwater intrusion, formation of fluid mud, and tidal flat erosion. Outside the CD, the coastal and shelf currents play a role in controlling the river plume and sediment dispersion over the wide and shallow marginal shelf sea. Moreover, the fluvial and marine forcing conditions exhibit strong variations at the fortnight (spring-neap), seasonal (dry-wet), and inter-annual time scales, leading to associated multi-scale changes in the hydrodynamics and sediment transport. The dynamic processes in the CD also exhibit significant spatial variations, leading to division into a single-channel fluvial-dominated tidal river of nearly uniform length, and a multi-bifurcated, funnel-shaped tidal estuary, and a nearshore zone with marine forcing dominant.

The CD is a highly muddy system with a persistent turbidity maximum zone where the near-bottom sediment concentration is up to 100 kg m^{-3}. Flocculation and enhanced settling of fine sediment is observed throughout the river-delta-sea continuum. Mass transport of bed material plays a role inside the delta, inducing frequent sand bar movement and channel migration. Strong deposition-resuspension, formation of near-bottom sediment hyper-concentration, and fluid mud transport prevail in the energetic mouth zone. A nearshore depocenter to the southern part of the subaqueous delta is characterized by strong seasonal erosion and deposition and high exchange rates between suspended and bed sediment. Sediment budget analysis implies that nearly 40–68% of the river-supplied sediment deposited in the river mouth in building up the delta in the long-term, and the remained portion was delivered to the shelf sea. The sediment trapping efficiency may reduce as the deltaic morphodynamic matures and the channels become narrower, deeper and constrained, which is more efficient in flushing sediment to the sea.

The CD develops through infilling of an incised deep valley and is characterized by meandering channels inside the delta and bifurcated channels in the mouth zone. The overall channel-shoal structure takes shape since the late 1950s and persists until nowadays. The centennial hydro-morphodynamic evolution of the CD is classified into a constructive configuration-formation phase, a mature development phase, a transitional period, and a future erosion phase. Collectively, the strong river and tidal forcing, high sediment supply, low-relief of the coastal plain, gentle shelf slope, and the influence of coastal currents exert a joint control on the long-term development of the CD, while human activities like reclamation and construction of jetties have played an increasingly important modulating role in the recent decades. Under the combined influence of sediment decline, human activities and SLR, the CD is facing high erosion and flooding risks and challenges to meet multiple management objectives.

Although knowledge of the deltaic hydro-morphodynamics has accumulated profoundly in the past 70 years, future studies based on long-time series of data, integrated analyses combining field data, conceptual and numerical modeling approaches, and inter-disciplinary investigation between estuarine physicists, coastal oceanographers, geomorphologists, and biologists are still very much needed. We identify five key knowledge gaps for future study, i.e., river-delta-ocean interactions, tidal river dynamics, fine sediment transport dynamics, the cumulated impact of human activities, and long-term erosion risk. Moreover, knowledge transfer, multi-objective management and long-term perspectives, and a mindset change towards nature-based solutions would provide a better opportunity for sustainable development in the future.

Disclosure statement

The authors are not aware of any affiliations, memberships, funding, or financial holdings that might be perceived as affecting the objectivity of this review.

Declaration of Competing Interest

The authors declare that they have no known competing financial interests or personal relationships that could have appeared to influence the work reported in this paper.

Acknowledgements

This work is financed by the Ministry of Science and Technology, P. R. China (MOST) (No. 2017YFE0107400; 2016YFE0133700) and Royal Netherlands Academy of Arts and Sciences (KNAW) (No. PSA-SA-E-02). Financial support from Natural Science Foundation of China (Nos. 51739005; U2040216; 41876091) and Science and Technology Commission of Shanghai Municipality (Nos. 19QA1402900; 20DZ1204700) is also acknowledged.

Appendix A. Supplementary data

Supplementary data to this article can be found online at https://doi.org/10.1016/j.earscirev.2021.103850.

References

Anthony, E.J., Gardel, A., Gratiot, N., Proisy, C., Allison, M.A., Dolique, F., Fromard, F., 2010. The Amazon-influenced muddy coast of South America: a review of mud-bank-shoreline interactions. Earth Sci. Rev. 103 (3–4), 99–121.

Avoine, J., 1986. Sediment exchanges between the Seine Estuary and its adjacent shelf. J. Geol. Soc. 144, 135–148.

Balica, S.F., Wright, N.G., van der Meulen, F., 2012. A flood vulnerability index for coastal cities and its use in assessing climate change impacts. Nat. Hazards 64, 73–105.

Beardsley, R.C., Limeburner, R., Yu, H., Cannon, G.A., 1985. Discharge of the Changjiang into the East China Sea. Cont. Shelf Res. 4 (1/2), 57–76.

Blott, S.J., Pye, K., van der Wal, D., Neal, A., 2006. Long-term morphological change and its causes in the Mersey Estuary, NW England. Geomorphology 81, 185–206.

Blum, M.D., Roberts, H.H., 2012. The Mississippi Delta Region: past, present, and Future. Annu. Rev. Earth Planet. Sci. 40, 655–683.

Cai, H.Y., Savenije, H.H.G., Toffolon, M., 2014. Linking the river to the estuary: influence of river discharge on tidal damping. Hydrology and Earth System Science 18, 287–304.

Caldwell, R.L., Edmonds, D.A., 2014. The effects of sediment properties on deltaic processes and morphologies: a numerical modeling study. Journal of Geophysical Research: Earth Surface 119. https://doi.org/10.1002/2013JF002965.

Chang, P.H., Isobe, A., 2003. A numerical study on the Changjiang diluted water in the Yellow and East China Seas. J. Geophys. Res. 108, 1510–1517.

Chang, P.H., Isobe, A., Kang, K.R., Ryoo, S.B., Kang, H.S., Kim, Y.H., 2014. Summer behavior of the Changjiang diluted water to the East/Japan Sea: a modeling study in 2003. Cont. Shelf Res. 81, 7–18.

Chao, S.Y., 1991. Circulation of the East China Sea, a numerical study. Journal of the Oceanographical Society of Japan 46, 273–295.

Chen, J.Y., 1957. Notes on the development of the Yangtze Estuary. Acta Geograph. Sin. 23 (3), 241–253 (in Chinese with an abstract in English).

Chen, X.Q., 1991. Sea-level changes since the early 1920's from the long records of two tidal gauges in Shanghai, China. Journal of Coastal Research 7 (3), 787–799.
Chen, S.L., 2003. Tidal Bore in the North Branch of the Changjiang Estuary. In: Proceedings of the International Conference on Estuaries and Coasts, Hangzhou, China, pp. 233–239.
Chen, J.Y., Li, D.J., 2002. Regulation of the Changjiang Estuary: past, present and future. In: Chen, J.Y., Eisma, D., Hotta, K., Walker, H.J. (Eds.), Engineered Coasts. Kluwer Academic Publishers, the Netherlands, pp. 185–196.
Chen, J.Y., Xu, H.G., 1981. Developmental processes of south Branch channel of Changjiang Estuary. Journal of East China Normal University (Natural Science Edition) 2, 93–108 (in Chinese).
Chen, Z.Y., Yang, D.Y., 1991. Quaternary Paleogeography and Paleoenvironment of Changjiang River Estuarine Region, 46(4), pp. 436–448.
Chen, Q.Q., Zhu, Y.R., 2012. Holocene evolution of bottom sediment distribution on the continental shelves of the Bohai Sea, Yellow Sea and East China Sea. Sediment. Geol. 273–274, 58–72.
Chen, J.Y., Yun, C.X., Xu, H.G., Dong, Y.F., 1979. The developmental model of the Changjiang River Estuary during last 2000 years. Acta Oceanologia Sinica 1 (1), 103–111 (in Chinese with English abstract).
Chen, J.Y., Zhu, H.F., Dong, Y.F., Sun, J.M., 1985. Development of the Changjiang estuary and its submerged delta. Cont. Shelf Res. 4 (1/2), 47–56.
Chen, J.Y., Li, D.J., Chen, B.L., Hu, F.X., Zhu, H.F., Liu, C.Z., 1999. The processes of dynamic sedimentation in the Changjiang Estuary. J. Sea Res. 41, 129–140.
Chen, S.L., Zhang, G.A., Yang, S.L., Shi, Z., 2006. Temporal variation of fine suspended sediment concentration in the Changjiang River estuary and adjacent coastal waters, China. J. Hydrol. 331, 137–145.
Chen, H.Q., Chen, J.Y., Chen, Z.J., Ruan, R.L., Xu, G.Q., Zeng, G., Zhu, J.R., Dai, Z.J., Chen, X.Y., Gu, S.H., Zhang, X.L., Wang, H.M., 2018. Mapping Sea level rise behavior in an estuarine delta system: a case study along the Shanghai coast. Engineering 4 (1), 156–163.
Chen, Y., He, Q., Shen, J., Du, J.B., 2020. The alteration of lateral circulation under the influence of human activities in a multiple channel system, Changjiang Estuary. Estuar. Coast. Shelf Sci. 106823 https://doi.org/10.1016/j.ecss.2020.106823.
China Water Resources Committee (CWRC), 2010. China River Sediment Bulletin. Ministry of Water Resources of China. China Water Power Press, Beijing, China (in Chinese).
China Water Resources Committee (CWRC), 2020. China River Sediment Bulletin. Ministry of Water Resources of China. China Water Power Press, Beijing, China (in Chinese).
Dalrymple, R.W., Choi, K.S., 2007. Morphologic and facies trends through the fluvial-marine transition in tide-dominated depositional systems: a systematic framework for environmental and sequence-stratigraphic interpretation. Earth-Sci. Rev. 81, 135–174.
Davis, R.A., Hayes, M.O., 1984. What is a wave-dominated coast? Mar. Geol. 60, 313–329.
Day, J.W., Boesch, D.F., Clairain, E.J., Kemp, G.P., Laska, S.B., Mitsch, W.J., Orth, K., Mashriquie, H., Reed, D.J., Shabman, L., Simenstad, C.A., Streever, B.J., Twilley, R. R., Watson, C.C., Wells, J.T., Whigham, D.F., 2007. Restoration of the Mississippi Delta: lessons from Hurricanes Katrina and Rita. Science 315, 1679–1684.
DeMaster, D.J., McKee, B.A., Nittrouer, C.A., Qiang, J.C., Cheng, G.D., 1985. Rates of sediment accumulation and particle reworking based on radiochemical measurements from continental shelf deposits in the East China Sea. Cont. Shelf Res. 4, 143–158.
Deng, B., Wu, H., Yang, S.L., Zhang, J., 2017. Longshore suspended sediment transport and its implications for submarine erosion off the Yangtze River Estuary. Estuar. Coast. Shelf Sci. 190, 1–10.
Deng, Z.R., He, Q., Safar, Z., Chassagne, C., 2019. The role of algae in fine sediment flocculaton: In-situ and laboratory measurements. Mar. Geol. 413, 71–84.
Deng, Z.R., He, Q., Chassagne, C., Wang, Z.B., 2021. Seasonal variation of floc population influenced by the presence of algae in the Changjiang (Yangtze River) Estuary. Mar. Geol. 440, 106600 https://doi.org/10.1016/j.margeo.2021.106600.
Division of Marine Monitoring and Warning (DMMW) State Oceanic Administration of China, 2021. Bulletin of Sea Level Changes in China 2020. http://gi.mnr.gov.cn/202104/P020210426570276410847.pdf.
Earth Science Division of Chinese Academy of Sciences, 1994. Impact of Sea Level Rise on the Deltaic Regions of China and its Mitigation. Science Press, Beijing, China (355p).
Edmonds, D.A., Slingerland, R.L., 2010. Significant effect of sediment cohesion on delta morphology. Nat. Geosci. https://doi.org/10.1038/NGEO730.
Eisma, D., Ji, Z., Chen, S., Chen, M., van der Gaast, S.J., 1995. Clay mineral composition of recent sediments along the China coast, in the Yellow Sea and the East China Sea. NIOZ-Report 4, 1–13.
Fagherazzi, S., Kirwan, M.L., Mudd, S.M., Guntenspergen, G.R., Temmerman, S., D'Alpaos, A., van de Koppel, J., Rybczyk, J.M., Reyes, E., Craft, C., Clough, J., 2012. Numerical models of salt marsh evolution: ecological, geomorphic, and climatic factors. Rev. Geophys. 50, RG1002. https://doi.org/10.1029/2011RG000359.
Fan, D.D., Guo, X., Wang, P., Shi, Z., 2006. Cross-shore variations in the morphodynamic processes of an open-coast mudflat in the Changjiang Delta, China: with an emphasis on storm impacts. Cont. Shelf Res. 26, 517–538.
Fricke, A.T., Nittrouer, C.A., Ogston, A.S., Nowacki, D.J., Asp, N.E., Souza Filho, P.W.M., 2018. Morphology and dynamics of the inter-tidal floodplain along the Amazon tidal river. Earth Surf. Process. Landf. 44, 204–218.
Fu, Y.T., Chen, S.L., Ji, H.Y., Fan, Y.S., Li, P., 2021. The modern Yellow River Delta in transition: causes and implications. Mar. Geol. 436, 106476 https://doi.org/10.1016/j.margeo.2021.106476.
Gallo, M.N., Vinzon, S.B., 2005. Generation of overtides and compound tides in the Amazon Estuary. Ocean Dyn. 55, 441–448.
Galloway, W.E., 1975. Process framework for describing the morphologic and stratigraphic evolution of deltaic depositional systems. In: Broussard, M.L. (Ed.), Deltas: Models for Exploration. Houston Geological Society, Houston, TX, pp. 87–98.
Ganju, N.K., Schoellhamer, D.H., 2010. Decadal-timescale estuarine geomorphic change under future scenarios of climate and sediment supply. Estuar. Coasts 33, 15–29.
Gao, S., Liu, Y.L., Yang, Y., Liu, P.J., Zhang, Y.Z., Wang, Y.P., 2015. Evolution status of the distal mud deposit associated with the Pear River, northern South China Sea continental shelf. J. Asian Earth Sci. 114, 562–573.
Gao, J.H., Shi, Y., Sheng, H., Kettner, A.J., Yang, Y., Jia, J.J., Wang, Y.P., Li, J., Chen, Y. N., Zou, X.Q., Gao, S., 2019. Rapid response of the Changjiang (Yangtze) river and East China Sea source-to-sink conveying system to human induced catchment perturbations. Mar. Geol. 414, 1–17.
Ge, J.Z., Shen, F., Guo, W.Y., Chen, C.S., Ding, P.X., 2015. Estimation of critical shear stress for erosion in the Changjiang Estuary: a synergy research of observation, GOCI sensing and modeling. J. Geophys. Res. 120, 8439–8465.
Ge, J.Z., Chen, C.S., Wang, Z.B., Ke, K.T., Yi, J.X., Ding, P.X., 2020. Dynamic response of the fluid mud to a tropical storm. Journal of Geophysical Research: Oceans 125 (3), 1–27.
Geleynse, N., Storms, J.E.A., Stive, M.J.F., Jagers, H.R.A., Walstra, D.J.R., 2010. Modelling of a mixed-load fluvio-deltaic system. Geophys. Res. Lett. 37, L05402. https://doi.org/10.1029/2009GL042000.
Giosan, L., Syvitski, J., Constantinescu, S., Day, J., 2014. Climate change: Protect the world's deltas. Nature 516, 31–33.
Godin, G., 1999. The propagation of tides up rivers with special consideration of the upper Saint Lawrence River. Estuar. Coast. Shelf Sci. 48, 307–324.
Gugliotta, M., Saito, Y., 2019. Matching trends in channel width, sinuosity, and depth along the fluvial to marine transition zone of tide-dominated river deltas: the need for revision of depositional and hydraulic models. Earth Sci. Rev. 191, 93–113.
Guo, L.C., 2014. Modeling Estuarine Morphodynamics under Combined River and Tidal Forcing. PhD dissertation of. Delft University of Technology and UNESCO-IHE, Delft, the Netherlands.
Guo, L.C., He, Q., 2011. Freshwater flocculation of suspended sediments in the Changjiang River, China. Ocean Dynamics 61 (2–3), 371–386.
Guo, Z.G., Yang, Z.S., Fan, D.J., Pan, Y.J., 2003. Seasonal variation of sedimentation in the Changjiang Estuary mud area. J. Geogr. Sci. 13 (3), 348–354.
Guo, L.C., Roelvink, J.A., van der Wegen, M., He, Q., 2011. Modeling the Long-Term Morphodynamic Behavior of the Changjiang Estuary, China. Proceeding of the 7th River, Coastal and Estuarine Morphodynamics, Beijing, China.
Guo, L.C., van der Wegen, M., Roelvink, D., He, Q., 2014. The role of river flow and tidal asymmetry on 1D estuarine morphodynamics. Journal of Geophysical Research: Earth Surface 119, 2315–2334. https://doi.org/10.1002/2014JF003110.
Guo, L.C., van der Wegen, M., Jay, D.A., Matte, P., Wang, Z.B., Roelvink, D., He, Q., 2015. River-tide dynamics: exploration of nonstationary and nonlinear tidal behavior in the Yangtze River estuary. Journal of Geophysical Research: Oceans 120, 3499–3521. https://doi.org/10.1002/2014JC010491.
Guo, C., He, Q., Guo, L.C., Winterwerp, J.C., 2017. A study of in-situ sediment flocculation in the turbidity maxima of the Yangtze Estuary. Estuar. Coast. Shelf Sci. 191, 1–9.
Guo, L.C., Su, N., Zhu, C.Y., He, Q., 2018. How have the river discharges and sediment loads changed in the Changjiang River basin downstream of the three Gorges Dam? J. Hydrol. 560, 259–274.
Guo, L.C., Su, N., Townend, T., Wang, Z.B., Zhu, C.Y., Zhang, Y.N., Wang, X.Y., He, Q., 2019. From the headwater to the delta: a synthesis of the basin-scale sediment load regime in the Changjiang River. Earth Sci. Rev. 197, 102900 https://doi.org/10.1016/j.earscirev.2019.102900.
Guo, L.C., Zhu, C.Y., Wu, X.F., Wan, Y.Y., Jay, D.A., Townend, T., Wang, Z.B., He, Q., 2020. Strong inland propagation of low-frequency long waves in river estuaries. Geophys. Res. Lett. 47 https://doi.org/10.1029/2020GL089112 e2020GL089112.
Guo, L.C., Xie, W.M., Xu, F., Wang, X.Y., Zhu, C.Y., Meng, Y., Zhang, W.G., He, Q., 2021a. A histroical review of sediment export-import shift in the North Branch of Changjiang Estuary. Earth Surface Landforms and Processes. https://doi.org/10.1002/esp.5084.
Guo, X.J., Fan, D.D., Zheng, S.W., Wang, H.M., Zhao, B.C., Qin, C.J., 2021b. Revisited sediment budget with latest bathymetric data in the highly altered Yangtze (Changjiang) Estuary. Geomorphology 391, 107873. https://doi.org/10.1016/j.geomorph.2021.107873.
He, X.C., Yang, T.L., Shen, S.L., Xu, Y.S., Arulrajah, A., 2019. Land subsidence control zone and policy for the environmental protection of Shanghai. Int. J. Environ. Res. Public Health 16, 2729. https://doi.org/10.3390/ijerph16152729.
Hoitink, A.J.F., Jay, D.A., 2016. Tidal river dynamics: implications for deltas. Rev. Geophys. 54, 240–272.
Hori, K., Saito, Y., Zhao, H., Cheng, X., Wang, P., Saito, Y., Li, C., 2001. Sedimentary facies and Holocene progradation rates of the Changjiang (Changjiang) Delta, China. Geomorphology 41 (2–3), 233–248.
Hori, K., Saito, Y., Zhao, Q.H., Wang, P.X., 2002. Architecture and evolution of the tide-dominated Changjiang (Changjiang) river delta, China. Sediment. Geol. 146, 249–264.
Hu, D.X., Yang, Z.S., 2001. Key Processes of the East China Sea Flux. China Ocean Press, Beijing (204 pp. in Chinese, with English Summary).
Hu, K.L., Ding, P.X., Wang, Z.B., Yang, S.L., 2009. A 2D/3D hydrodynamic and sediment transport model for the Changjiang Estuary, China. Journal of Marine System 77, 114–136.
Inman, D.L., Nordstrom, C.E., 1971. On the tectonic and morphologic classification of coasts. The Journal of Geology 79, 1–21.

Jay, D.A., Leffler, K., Diefenderfer, H.L., Borde, A.B., 2015. Tidal-fluvial and estuarine processes in the lower Columbia River: I. along-channel water level variations, Pacific Ocean to Bonneville Dam. Estuar. Coasts 38, 415–433.
Jeuken, M.C.J.L., Wang, Z.B., Keiller, D., Townend, I., Liek, G.A., 2003. Morphological response of estuaries to nodal tide variations. In: Proceedings of the International Conference on Estuaries and Coasts, Hangzhou, China, pp. 166–173.
Jia, J.J., Gao, J.H., Cai, T.L., Li, Y., Yang, Y., Wang, Y.P., Xia, X.M., Li, J., Wang, A.J., Gao, S., 2018. Sediment accumulation and retention of the Changjiang (Yangtze River) subaqueous delta and its distal muds over the last century. Mar. Geol. 401, 2–16.
Jiang, C.J., de Swart, H.E., Li, J.F., Liu, G.F., 2013. Mechanisms of along-channel sediment transport in the North Passage of the Changjiang Estuary and their response to large-scale interventions. Ocean Dyn. 63, 283–305.
Jiang, F., Zhao, X.S., Chen, J., Liu, Y., Sun, Q.L., Chen, J., Chen, Z.Y., 2020. Depocenter shift and en-echelon shoal development in the pre-Holocene incised valley of the Yangtze Delta, China. Marine Geology 426, 106212. https://doi.org/10.1016/j.margeo.2020.106212.
Jiang, F., Wang, Y.N., Zhao, X.S., Liu, Y., Chen, J., Sun, Q.L., Li, M.T., Finlason, B., Chen, Z.Y., 2021. Reconstruction of the Holocene sedimentary-ecological complex in the incised valley of the Yangtze Delta, China. Paleogeogrphy, Paleoclimatology, Paleoecology 571, 110387. https://doi.org/10.1016/j.palaeo.2021.110387.
Kästner, K., Hoitink, A.J.F., Torfs, P.J.J.F., Deleersnijder, E., Ningsih, N.S., 2019. Propagation of tides along a river with a sloping bed. J. Fluid Mech. 872, 39–73.
Katayama, H., Watanabe, Y., 2003. The Huanghe and Changjiang contribution to seasonal variability in terrigenous particulate load to the Okinawa Trough. Deep-Sea Research II 50, 475–485.
Lai, X.H., Yin, D.W., Finlayson, B.L., Wei, T.Y., Li, M.T., Yuan, W.H., Yang, S.L., Dai, Z.J., Gao, S., Chen, Z.Y., 2017. Will river erosion below the three Gorges Dam stop in the middle Yangtze? J. Hydrol. 554 (24–3).
Lane, A., 2004. Bathymetric evolution of the Mersey Estuary, UK, 1906-1997: causes and effects. ECSS 249–263.
Lee, H.J., Chao, S.Y., 2003. A climatological description of circulation in and around the East China Sea. Deep Sea Research II 50, 1065–1084.
Lee, H.J., Moon, I.-J., Moon, J.-H., Kim, S.-H., Jeong, Y.Y., Koo, J.-H., 2017. Impact of typhoons on the Changjiang plume extension in the Yellow and East China Sea. Journal of Geophysical Research: Oceans 122, 4962–4973.
Li, J.F., Zhang, C., 1998. Sediment resuspension and implications for turbidity maximum in the Changjiang Estuary. Mar. Geol. 148, 117–124.
Li, C.X., Chen, Q.Q., Zhang, J.Q., Yang, S.Y., Fan, D.D., 2000. Stratigraphy and paleoenvironmental changes in the Changjiang Delta during the late quaternary. J. Asian Earth Sci. 18, 452–469.
Li, C.X., Wang, P., Sun, H.P., Zhang, J.Q., Fan, D.D., Deng, B., 2002. Late Quaternary incised-valley fill of the Changjiang delta (China): its stratigraphic framework and evolution. Sediment. Geol. 152, 133–158.
Li, M.T., Chen, Z.Y., Yin, D.W., Chen, J., Wang, Z.H., Sun, Q.L., 2011. Morphodynamic characteristics of the dextral diversion of the Yangtze River mouth, China: tidal and the Coriolis force controls. Earth Surf. Process. Landf. 36, 641–650.
Li, L., Zhu, J.R., Wu, H., 2012a. Impacts of wind stress on saltwater intrusion in the Yangtze Estuary. Science China Earth Sciences 55, 1178–1192.
Li, P., Yang, S.L., Milliman, J.D., Xu, K.H., Qin, W.H., Wu, C.S., Chen, Y.P., Shi, B.W., 2012b. Spatial, temporal and human-induced variations in suspended sediment concentration in the surface waters of the Changjiang Estuary and adjacent coastal areas. Estuar. Coasts 35 (5), 1316–1327.
Li, X., Liu, J.P., Tian, B., 2016. Evolution of the Jiuduansha wetland and the impact of navigation works in the Yangtze Estuary, China. Geomorphology 253, 328–339.
Li, S.Z., Yang, Y.P., Zhang, M.J., Sun, Z.H., Zhu, L.L., You, X.Y., Li, K.Y., 2017. Coarse and fine sediment transportation patterns and causes downstream of the three Gorges Dam. Frontiers of Earth Science 12, 750–764.
Li, X., Zhang, X., Qiu, C.Y., Duan, Y.Q., Liu, S.A., Chen, D., Zhang, L.P., Zhu, C.M., 2020. Rapid loss of tidal flats in the Yangtze River Delta since 1974. Int. J. Environ. Res. Public Health 17, 1636. https://doi.org/10.3390/ijerph17051636.
Lin, J.L., van Prooijen, B.C., Guo, L.C., Zhu, C.Y., He, Q., Wang, Z.B., 2021. Regime shifts in the Changjiang (Yangtze River) Estuary: the role of concentrated benthic suspensions. Mar. Geol. 433, 106403 https://doi.org/10.1016/j.margeo.2020.106403.
Liu, H., 2009. Sediment Mixing and Exchange Processes in the Changjiang Estuary. PhD. Dissertation of East. China Normal University, Shanghai, China (in Chinese with English abstract).
Liu, C.Z., Walker, H.J., 1989. Sedimentary characteristics of cheniers and the formation of the chenier plains of East China. J. Coast. Res. 5 (2), 353–368.
Liu, J.P., Li, A.C., Xu, K.H., Velozzi, D.M., Yang, Z.S., Milliman, J.D., DeMaster, D.J., 2006. Sedimentary features of the Changjiang River-derived along-shelf clinoform deposit in the East China Sea. Cont. Shelf Res. 26, 2141–2156.
Liu, J.P., Xu, K.H., Li, A.C., Milliman, J.D., Velozzi, D.M., Xiao, S.B., Yang, Z.S., 2007. Flux and fate of the Changjiang River sediment delivered to the East China Sea. Geomorphology 85, 208–224.
Liu, H., He, Q., Wang, Z.B., Weltje, G.J., Zhang, J., 2010a. Dynamics and spatial variability of near-bottom sediment exchange in the Changjiang Estuary, China. Estuar. Coast. Shelf Sci. 86, 322–330.
Liu, J., Saito, Y., Kong, X.H., Wang, H., Xiang, L.H., Wen, C., Nakashima, R., 2010b. Sedimentary record of environmental evolution off the Changjiang River estuary, East China Sea, during the last 13,000 years, with special reference to the influence of the Yellow River on the Changjiang River delta during the last 600 years. Quat. Sci. Rev. 29, 2424–2438.
Liu, X.Y., Liu, Y.G., Guo, L., Rong, Z.R., Gu, Y.Z., Liu, Y.H., 2010c. Interannual changes of sea level in the two regions of East China Sea and different responses to ENSO. Global and Planetary Changes 72, 215–226.
Liu, G.F., Zhu, J.R., Wang, Y.Y., Wu, H., Wu, J.X., 2011. Tripod measured residual currents and sediment flux: impacts on the silting of the Deepwater Navigation Channel in the Changjiang Estuary. Estuar. Coast. Shelf Sci. 93 (3), 192–201.
Liu, Z.Q., Gan, J.P., Wu, H., Hu, J.Y., Cai, Z.Y., Deng, Y.F., 2021. Advances on coastal and estuarine circulations around the Changjiang Estuary in the recent decades (2000−2020). Front. Mar. Sci. 8, 615929 https://doi.org/10.3389/fmars.2021.615929.
Luan, H.L., Ding, P.X., Wang, Z.B., Ge, J.Z., Yang, S.L., 2016. Decadal morphological evolution of the Yangtze Estuary in response to river input changes and estuarine engineering projects. Geomorphology 265, 12–23.
Luan, H.L., Ding, P.X., Wang, Z.B., Ge, J.Z., 2017. Process-based morphodynamic modeling of the Yangtze Estuary at a decadal time scale: controls on estuarine evolution and future trend. Geomorphology 290, 347–364.
Luan, H.L., Ding, P.X., Yang, S.L., Wang, Z.B., 2021. Accretion-erosion conversion in the subaqueous Yangtze Delta in response to fluvial sediment decline. Geomorphology 382, 107680. https://doi.org/10.1016/j.geomorph.2021.107680.
Luo, X.X., Yang, S.L., Zhang, J., 2012. The impact of the three Gorges Dam on the downstream distribution and texture of sediments along the middle and lower Changjiang River and its estuary, and subsequent sediment dispersal in the East China Sea. Geomorphology 179, 126–140.
Mao, H.L., Gan, Z.J., Lan, S.F., 1963. A preliminary study of the Changjiang diluted water and its mixing processes. Oceanologia Et Limnologia Sinica 5 (3), 183–206.
McKee, B.A., Nittrouer, C.A., DeMaster, D.J., 1983. Concepts of sediment deposition and accumulation applied to the continental shelf near the mouth of the Changjiang River. Geology 11 (11), 631–633.
Mei, X.F., Dai, Z.J., Darby, S.E., Zhang, M., Cai, H.Y., Wang, J., Wei, W., 2021. Landward shifts of the maximum accretion zone in the tidal reach of the Changjiang estuary following construction of the three Gorges Dam. J. Hydrol. 592, 125789 https://doi.org/10.1016/j.jhydrol.2020.125789.
Milliman, J.D., Meade, R.H., 1983. World-wide delivery of river sediment to the oceans. Geology 91 (1), 1–21.
Milliman, J.D., Shen, H.T., Yang, Z.S., Meade, R.H., 1985. Transport and deposition of river sediment in the Changjiang Estuary and adjacent continental shelf. Cont. Shelf Res. 4 (1/2), 37–45.
Milliman, J.D., Qin, Y.S., Park, Y.A., 1989. Sediments and sedimentary processes in the Yellow and East China Seas. In: Taira, Asahiko, Masuda, Fujio (Eds.), Sedimentary Facies in the Active Plate Margin. Terra Scientific Publishing, Tokyo, Japan, pp. 233–249.
Muis, S., Verlaan, M., Winsemius, H.C., Aerts, J.C.J.H., Ward, P.J., 2016. A global reanalysis of storm surge and extreme sea levels. Nat. Commun. 7, 11969. https://doi.org/10.1038/ncomms11969.
Murray, A.B., Knaapen, M.A.F., Tal, M., Kirwan, M.L., 2008. Biomorphodynamics: Physical-biological feedbacks that shape landscape. Water Resour. Res. 44, W11301. https://doi.org/10.1029/2007WR006410.
Nakaegawa, T., Kitoh, A., Hosaka, M., 2013. Discharge of major global rivers in the 21st century climate projected with the high horizontal resolution MRI-AGCSMs. Hydrol. Process. 27, 3301–3318.
Niino, H., Emery, K.O., 1961. Sediments of shallow portions of East China Sea and South China Sea. Geol. Soc. Am. Bull. 72 (5), 731–762.
Nittrouer, C.A., DeMaster, D.J., McKee, B.A., 1984. Fine-scale stratigraphy in proximal and distal deposits of sediment dispersal systems in the East China Sea. Mar. Geol. 61, 13–24.
Nittrouer, C.A., DeMaster, D.J., Kuehl Jr., S.A., Figueiredo, A.G., Sternberg, R.W., Faria, L.E.C., Silveira, O.M., Allison, M.A., Kineke, G.C., Ogston, A.S., Souza Filho, P.W.M., Asp, N.E., Nowacki, D.J., Fricke, A.T., 2021. Amazon sediment transport and accumulation along the continuum of the mixed fluvial and marine processes. Annu. Rev. Mar. Sci. 13 (6.1–6.36).
Paola, C., Twilley, R.R., Edmonds, D.A., Kim, W., Mohrig, D., Parker, G., Viparelli, E., Voller, V.R., 2011. Natural processes in delta restoration: Application to the Mississippi Delta. Annual Reviews of Marine Science 3, 67–91.
Pawlowicz, R., Beardsley, B., Lentz, S., 2002. Classical tidal harmonic analysis including error estimates in MATLAB using T_TIDE. Comput. Geosci. 28, 929–937.
Qiao, Y., 2019. Erodibility of Bed Sediments in the Yangtze Estuary. MSc Thesis of East. China Normal University, Shanghai, China.
Qin, Z.H., Li, Y.P., 1997. Discussion of the sea-level variations and its long-term projection methods in Shanghai. Acta Oceanol. Sin. 19, 1–7.
Ren, J.B., Xu, F., He, Q., Shen, J., Guo, L.C., Xie, W.M., Zhu, L., 2021. The role of a remote tropical cyclone in sediment resuspension over the subaqueous delta front in the Changjiang Estuary. China. Geomorphology 377, 107564. https://doi.org/10.1016/j.geomorph.2020.107564.
Saito, Y., Yang, Z.S., Hori, K., 2001. The Huanghe (Yellow River) and Changjiang (Changjiang River) deltas: a review on their characteristics, evolution and sediment discharge during the Holocene. Geomorphology 41 (2–3), 219–231.
Sassi, M.G., Hoitink, A.J.F., 2013. River flow controls on tides and tide-mean water level profiles in a tidal freshwater river. J. Geophys. Res. 118, 1–3. https://doi.org/10.1002/jgrc.20297.
Schwarz, C., Ye, Q.H., van der Wal, D., Zhang, L.Q., Bouma, T., Ysebaert, T., Herman, P.M.J., 2014. Impacts of salt marsh plants on tidal channel initiation and inheritance. Journal of Geophysical Research: Earth Surface 119. https://doi.org/10.1002/2013JF002900.
Shang, Y., Nian, X.M., Zhang, W.G., Wang, F., 2021. Yellow River's contribution to the building of Yangtze Delta during the last 500 years- Evidences from detrital zircon U-

Pb geochronology. Geophys. Res. Lett. 48 https://doi.org/10.1029/2020GL091896 e2020GL091896.
Shen, H.T. (Ed.), 2001. Material Flux of the Changjiang Estuary. China Ocean Press, Beijing, China (in Chinese).
Shen, H.T., Pan, D.A., 2001. Turbidity Maximum in the Changjiang Estuary. China Ocean Press, Beijing, China (in Chinese).
Shen, H.T., Gu, G.C., Li, J.F., 1989a. 1988a. Characteristics of the tidal wave propagation and its effect on channel evolution in the Changjiang Estuary. In: Chen, J.Y., Shen, H. T., Yun, C.X. (Eds.), Dynamic Process and Geomorphic Development of Changjiang Estuary. Shanghai Scientific and Technological Press, Shanghai, pp. 73–79 (in Chinese).
Shen, H.T., Pan, D.A., Li, J.F., Gu, G.Z., 1989b. 1988b. The relationship of channel evolution with the characteristics of residual currents in the Changjiang Estuary. In: Chen, J.Y., Shen, H.T., Yun, C.X. (Eds.), Dynamic Process and Geomorphic Development of Changjiang Estuary. Shanghai Scientific and Technological Press, Shanghai, pp. 102–107 (in Chinese).
Shen, H.T., Mao, Z.C., Zhu, J.R., 2003. Saltwater Intrusion in the Changjiang Estuary. China Ocean Press, Beijing, China (in Chinese).
Shen, F., Zhou, Y.X., Li, J.F., He, Q., Verhoef, W., 2013. Remotely sensed variability of the suspended sediment concentration and its response to decreased river discharge in the Changjiang Estuary and its adjacent coast. Cont. Shelf Res. 69, 52–61.
Sherwood, C.R., Jay, D.A., Harvey, R.B., Hamilton, P., Simenstad, C.A., 1990. Historical changes in the Columbia River Estuary. Prog. Oceanogr. 25, 299–352.
Shi, W., Wang, M.H., 2012. Satellite views of the Bohai Sea, Yellow Sea, and East China Sea. Prog. Oceanogr. 104, 30–45.
Shi, Z., Zhou, H.J., 2004. Controls on effective settling velocities on mud flocs in the Changjiang Estuary, China. Hydrological Processes 18 (15), 2877–2892.
Smit, H., Smits, R., van der Velder, G., Coops, H., 1997. Ecosystem responses in the Rhine-Meuse Delta during two decades after enclosure and step toward estuary restoration. Estuaries 20, 504–520.
Song, B., Li, Z., Saito, Y., Okuno, J., Li, Z., Lu, A.Q., Hua, D., Li, J., Li, Y.X., Nakashima, R., 2013a. Initiation of the Changjiang (Changjiang) delta and its response to the mid-Holocene Sea level change. Paleogeography, Paleoclimatology, Paleoecology 388, 81–97.
Song, D.H., Wang, X.H., Cao, Z.Y., Guan, W.B., 2013b. Suspended sediment transport in the Deepwater Navigation Channel, Changjiang River Estuary, China, in the dry season 2009: 1. Observations over spring and neap tidal cycles. Journal of Geophysical Research: Oceans 118. https://doi.org/10.1002/jgrc.20410.
Song, D.H., Wang, X.H., Zhu, X.M., Bao, X.W., 2013c. Modeling studies of the far-field effects of tidal flat reclamation on tidal dynamics in the East China Seas. Estuarine, Coastal and Shelf Sciences 133, 147–160.
State Oceanic Administration People''s Republic of China (SOA), 2020. China Sea Level Rise Bulletin 2019. China Ocean Press, Beijing, China.
Sternberg, R.W., Larsen, L.H., Miao, Y.T., 1985. Tidally driven sediment transport on the East China Sea continental shelf. Cont. Shelf Res. 4 (1/2), 105–120.
Su, J.F., Fan, D.D., Liu, J.P., Wu, Y.J., 2020. Anotomy of the transgressive depositional system in a sediment-rich tide-dominated estuary: the paleo-Yangtze estuary. China. Marine and Petroleum Geology 121, 104588. https://doi.org/10.1016/j.marpetgeo.2020.104588.
Syvitski, J.P.M., Kettner, A.J., Overeem, I., Hutton, E.W.H., Hannon, M.T., Brakenridge, G.R., 2009. Sinking deltas due to human activities. Nat. Geosci. 2 (10), 681–686.
Syvitski, J., Waters, C.N., Day, J., Milliman, J.D., Summerhayes, C., Steffen, W., Zalasiewicz, J., Cearreta, A., Galuszka, A., Hajdas, I., Head, M.J., Leinfelder, R., McNeill, J.R., Poirier, C., Rose, N.L., Shotyk, W., Wagreich, M., Williams, M., 2020. Extraordinary human energy consumption and resultant geological impacts beginning around 1950 CE initiated the proposed Anthropocene Epoch. Nature Communications Earth & Environement 1, 32. https://doi.org/10.1038/s43247-020-00029-y.
Talke, S.A., Jay, D.A., 2020. Changing tides: the role of natural and anthropogenic factors. Annual Review of Marine Sciences 12 (14.1–14.31).
Tang, J.H., 2007. Characteristics of Fine Cohesive sediment's Flocculation in the Changjiang Estuary and its Adjacent Sea Area. MSc Thesis of East. China Normal University, Shanghai, China (in Chinese with English abstract).
Temmerman, S., Meire, P., Bouma, T.J., Herman, P.M.J., Ysebaert, T., de Vriend, H.J., 2013. Ecosystem-based coastal defense in the face of global change. Nature 504, 79–83.
Tessler, Z.D., Vorosmarty, C.J., Grossberg, M., Gladkova, I., Aizenman, H., Syvitski, J.P. M., Foufoula-Georgiou, E., 2015. Profiling risk and sustainability in coastal deltas of the world. Science 349, 638–643.
Thomas, C.G., Spearman, J.R., Turnbull, M.J., 2002. Historical morphological change in the Mersey Estuary. Cont. Shelf Res. 22, 1775–1794.
Tian, B., Zhou, Y.X., Thom, R.M., Diefenderfer, H.L., Yuan, Q., 2015. Detecting wetland changes in Shanghai, China using FORMOSAT and Landsat TM imagery. J. Hydrol. 529, 1–10.
Tian, Q., Xu, K.H., Dong, C.M., Yang, S.L., He, Y.J., Shi, B.W., 2021. Declining sediment discharge in the Yangtze River from 1956 to 2017: Spatial and temporal changes and their causes. Water Resour. Res. https://doi.org/10.1029/WR028645.
Tolhurst, T.J., Black, K.S., Paterson, D.M., Mitchener, H.J., Termaat, G.R., Shayler, S.A., 2000. A comparison and measurement standardization of four in situ devices for determining the erosion shear stress of intertidal sediments. Cont. Shelf Res. 20 (10–11), 1397–1418.
Uehara, K., Saito, Y., Hori, K., 2002. Paleotidal regime in the Changjiang (Changjiang) estuary, the East China Sea, and the Yellow Sea at 6 ka and 10 ka estimated from a numerical model. Mar. Geol. 183, 179–192.
van der Wegen, M., 2010. Modeling morphodynamic evolution in alluvial estuaries. In: PhD. Dissertation of Delft University of Technology and UNESCO-IHE, Delft, the Netherlands.
van der Wegen, M., 2013. Numerical modeling of the impact of sea level rise on tidal basin morphodynamics. Journal of Geophysical Research: Earth Surface 118, 1–14. https://doi.org/10.1002/jgrf.20034.
van Maren, D.S., Yang, S., He, Q., 2013. The impact of silt trapping in large reservoirs on downstream morphology: the Changjiang River. Ocean Dyn. 63 (6), 691–707.
Wan, Y.Y., Roelvink, J.A., Li, W.H., Qi, D.M., Gu, F.F., 2014. Observation and modeling of the storm-induced fluid mud dynamics in a muddy-estuarine navigational channel. Geomorphology 217, 23–36.
Wang, H.J., Yang, Z.S., Wang, Y., Saito, Y., Liu, J.P., 2008. Reconstruction of sediment flux from the Changjiang (Yangtze River) to the sea since 1860s. J. Hydrol. 349, 318–332.
Wang, J., Bai, S.B., Liu, P., Li, Y.Y., Gao, Z.R., Qu, G.X., Cao, G.J., 2009. Channel sedimentation and erosion of the Jiangsu reach of the Yangtze River during the last 44 years. Earth Surf. Process. Landf. 34, 1587–1593.
Wang, Y., Shen, J., He, Q., 2010. A numerical model study of the transport timescale and change of estuarine circulation due to waterway constructions in the Changjiang Estuary, China. J. Mar. Syst. 82, 154–170.
Wang, Z.H., Li, M.T., Zhang, R.H., Zhuang, C.C., Liu, Y., Saito, Y., Xie, J.L., Zhao, B.C., 2011. Impacts of human activity on the late Holocene development of the subaqueous Yangtze delta, China, as shown by magnetic properties and sediment accumulation rates. The Holocene 21 (3), 393–408.
Wang, J., Gao, W., Xu, S.Y., Yu, L.Z., 2012. Evaluation of the combined risk of sea level rise, land subsidence, and storm surges on the coastal areas of Shanghai, China. Clim. Chang. 115, 537–558.
Wang, H.J., Yang, Z.S., Bi, N.S., 2013a. Changjiang (Yangtze) and Huanghe (Yellow) Rivers: Historical reconstruction of land-use change and sediment load to the sea. In: Bianchi, T.S., Allison, M.A., Cai, W.-J. (Eds.), Biogeochemical Dynamics at Major River-Coastal Interfaces: Linkages with Global Change. Cambridge University Press, pp. 118–137.
Wang, Y.H., Dong, P., Oguchi, T., Chen, S.L., Shen, H.T., 2013b. Long-term (1842-2006) morphological change and equilibrium state of the Changjiang (Changjiang) Estuary, China. Cont. Shelf Res. 56, 71–81.
Wang, J., Yi, S., Li, M.Y., Wang, L., Song, C.C., 2018a. Effects of sea level rise, land subsidence, bathymetric change and typhoon tracks on storm flooding in the coastal areas of Shanghai. Sci. Total Environ. 621, 228–234.
Wang, Q.S., Pan, C.H., Zhang, G.Z., 2018b. Impact of and adaptation strategies for sea-level rise on Yangtze River Delta. Adv. Clim. Chang. Res. 9, 154–160.
Wang, Z.H., Saito, Y., Zhan, Q., Nian, X.M., Pan, D.D., Wang, L., Chen, T., Xie, J.L., Li, X., Jiang, X.Z., 2018c. Three-dimensional evolution of the Yangtze River mouth, China during the Holocene: impacts of sea level, climate and human activity. Earth Sci. Rev. 185, 938–955.
Wang, F., Zhang, W.G., Nian, X.M., Roberts, A.P., Zhao, X., Shang, Y., Ge, C., Dong, Y., 2020. Magnetic evidences for Yellow River sediment in the late Holocene deposit of the Yangtze River Delta. China. Marine Geology 106274. https://doi.org/10.1016/j.margeo.2020.106274.
Watanabe, M., 2007. Simulation of temperature, salinity and suspended matter distributions induced by the discharge into the East China Sea during the 1998 flood of the Yangtze River. Estuar. Coast. Shelf Sci. 71, 81–97.
Waters, C.N., Zalasiewicz, J., Summerhayes, C., Barnosky, A.D., Poirier, C., Galuszka, A., Cearreta, A., Edgeworth, M., Ellis, E.C., Ellis, M., Jeandel, C., Leinfelder, R., McNeill, J.R., Richter, D., Steffen, W., Syvitsky, J., Vidas, D., Wagreich, M., Williams, M., An, Z.S., Grinevald, J., Odada, E., Oreskes, N., Wolfe, A.P., 2016. The Anthropocene is functionally and stratigraphically distinct from the Holocene. Science 351, aad2622.
Wei, K., Ouyang, C.J., Duan, H.T., Li, Y.L., Chen, M.X., Ma, J., An, H.C., Zhou, S., 2020. Reflections on the catastrophic 2020 Yangtze River basin flooding in southern China. The Innovation 1 (2), 100038. https://doi.org/10.1016/j.xinn.2020.100038.
Wilson, C.A., Goodbred Jr., S.L., 2015. Construction and maintenance of the Ganges-Brahmaputra-Meghna delta: linking process, morphology, and stratigraphy. Annu. Rev. Mar. Sci. 7, 67–88.
Winterwerp, J.C., Wang, Z.B., 2013. Man-induced regime shifts in small estuaries- I: theory. Ocean Dyn. 63, 1279–1292.
Winterwerp, J.C., van Kesteren, W.G.M., van Prooijen, B., Jacobs, W., 2012. A conceptual framework for shear flow-induced erosion of soft cohesive sediment beds. J. Geophys. Res. 117, C10020. https://doi.org/10.1029/2012JC008072.
Wright, L.D., Coleman, J.M., 1972. River delta morphology: wave climate and the role of the subaqueous profile. Science 176, 282–284.
Wright, L.D., Friedrichs, C.T., 2006. Gravity-driven sediment transport on continental shelves: a status report. Cont. Shelf Res. 26, 2092–2107.
Wu, H., 2015. Cross-shelf penetrating fronts: a response of buoyant coastal water to ambient pycnocline undulation. Journal of Geophysical Research: Oceans 120, 5101–5119.
Wu, H., 2021. Beta-plane arrested topographic wave as a linkage of open ocean forcing and mean shelf circulation. J. Phys. Oceanogr. https://doi.org/10.1175/JPO-D-20-0195.1.
Wu, H., Zhu, J.R., 2010. Advection scheme with 3rd high-order spatial interpolation at the middle temporal level and its application to saltwater intrusion in the Changjiang Estuary. Ocean Model. 33, 33–51.
Wu, H., Zhu, J.R., Choi, B.H., 2010. Links between salt water intrusion and subtidal circulation in the Changjiang Estuary: a model guide study. Cont. Shelf Res. https://doi.org/10.1016/j.csr.2010.09.001.
Wu, J.X., Ren, J., Liu, H., Qiu, C.H., Cui, Y.S., Zhang, Q.J., 2016. Trapping and escaping processes of Yangtze River-derived sediments to the East China Sea. In: Clift P.D.,

Harff J., Wu J.X., Qiu Y. (eds). River-dominated shelf sediments of East Asian Seas, Geological Society, London, Special Publications 429, 153–169.
Wu, H., Gu, J., Zhu, P., 2018a. Winter counter-wind transport in the inner southwestern Yellow Sea. Journal of Geophysical Research: Oceans 123, 411–436.
Wu, H., Wu, T., Bai, M., 2018b. Mega estuarine constructions modulate the Changjiang River plume extension in adjacent seas. Estuar. Coasts 41, 1234–1252.
Xu, G., 1995. Evolution and Development of the Changjiang River Estuarine delta and its Impact on the Adjacent Sea Water. PhD. Dissertation of East. China Normal University, Shanghai, China.
Xu, S.Y., Chen, Z.Y., 1995. Similarity and discrepancy of major delta processes, on eastern coast of China. Acta Oceanologia Sinica 62 (6), 481–490 (in Chinese).
Xu, K.H., Milliman, J.D., 2009. Seasonal variations of sediment discharge from the Yangtze River before and after impoundment of the three Gorges Dam. Geomorphology 104 (3–4), 276–283.
Xu, K.H., Li, A.C., Liu, J.P., Milliman, J.D., Yang, Z.S., Liu, C.S., Kao, S.J., Wan, S.M., Xu, F.J., 2012. Provenance, structure, and formation of the mud wedge along inner continental shelf of the East China Sea: a synthesis of the Yangtze dispersal system. Mar. Geol. 291–294, 176–191.
Xu, K.H., Bentley, S.J., Day, J.W., Freeman, A.M., 2019. A review of sediment diversion in the Mississippi River Deltaic plain. Estuar. Coast. Shelf Sci. 225, 106241 https://doi.org/10.1016/j.ecss.2019.05.023.
Xue, P.F., Chen, C.S., Ding, P.X., Beardsley, R.C., Lin, H.C., Ge, J.Z., Kong, Y.Z., 2009. Saltwater intrusion into the Changjiang River: a model-guided mechanism study. Journal of Geophysical Research: Ocean 114, C02006. https://doi.org/10.1029/2008JC004831.
Yang, Z.S., Guo, Z.G., Wang, Z.X., Xu, J.P., Gao, W.B., 1992. A macro-scale regime of the offshore transport of suspended material in the Yellow Sea and East China Sea. Acta Oceanol. Sin. 14, 81–90 (in Chinese).
Yang, S.L., Ding, P.X., Chen, S.L., 2001. Changes in progradation rate of the tidal flats at the mouth of the Changjiang (Changjiang) Rive, China. Geomorphology 38, 167–180.
Yang, Z.S., Wang, H.J., Saito, Y., Milliman, J.D., Xu, K.H., Qiao, S., Shi, G., 2006. Dam impacts on the Changjiang (Changjiang) river sediment discharge to the sea: the past 55 years and after the three Gorges Dam. Water Resour. Res. 42, W04407. https://doi.org/10.1029/2005WR003970.
Yang, S.L., Milliman, J.D., Li, P., Xu, K.H., 2011. 50000 dams later: erosion of the Changjiang River its delta. Glob. Planet. Chang. 75, 14–20.
Yang, S.L., Shi, B.W., Bouma, T.J., Ysebaert, T., Luo, X.X., 2012. Wave attenuation at a salt marsh margin: a case study of an exposed coast on the Changjiang Estuary. Estuar. Coasts 35, 169–182.
Yang, S.L., Fan, J.Q., Shi, B.W., Bouma, T.J., Xu, K.H., Yang, H.F., Zhang, S.S., Zhu, Q., Shi, X.F., 2019. Remote impacts of typhoons on the hydrodynamics, sediment transport and bed stability of an intertidal wetland in the Yangtze Delta. J. Hydrol. 575, 755–766.
Yang, H.F., Li, B.C., Zhang, C.Y., Qiao, H.J., Liu, Y.T., Bi, J.F., Zhang, Z.L., Zhou, F.N., 2020a. Recent spatial-temporal variations of suspended sediment concentrations in the Yangtze Estuary. Water 12, 818. https://doi.org/10.3390/w12030818.
Yang, S.L., Luo, X.X., Temmerman, S., Kirwan, M., Bouma, T., Xu, K.H., Zhang, S.S., Fan, J.Q., Shi, B.W., Yang, H.F., Wang, Y.P., Shi, X.F., Gao, S., 2020b. Role of delta-front erosion in sustaining salt marshes under sea-level rise and fluvial sediment decline. Limnol. Oceanogr. 65 (9), 1990–2009.
Yang, H.F., Yang, S.L., Li, B.C., Wang, Y.P., Wang, J.Z., Zhang, Z.L., Xu, K.H., Huang, Y. G., Shi, B.W., Zhang, W.X., 2021. Different fates of the Yangtze and Mississippi deltaic wetlands under similar riverine sediment decline and sea-level rise. Geomorphology 381, 107646. https://doi.org/10.1016/j.geomorph.2021.107646.
Yin, D.W., Chen, Z.Y., 2009. The Changjiang sediment flux into the seas: measurability and predictability. Frontier of Earth Science in China 3 (2), 146–153.
Yin, J., Jonkman, S., Lin, N., Yu, D.P., Aert, J., Wilby, R., Pan, M., Wood, E., Bricker, J., Ke, Q., Zeng, Z.Z., Zhao, Q., Ge, J.Z., Wang, J., 2020. Flood risks in sinking delta cities: Time for reevaluation? Earth's. Future 8. https://doi.org/10.1029/2020EF001614 e2020EF001614.
Yun, C.X., 2004. Recent Evolution of the Changjiang Estuary and its Mechanism, 2004. China Ocean Press, Beijing (in Chinese).
Yun, C.X., 2010. Illustrated Evolution of the Changjiang River Estuary, 2010. China Ocean Press, Beijing (in Chinese).
Zhang, E.F., Chen, X.Q., Wang, X.L., 2003. Water discharge changes of the Changjiang River downstream Datong during dry season. Journal of Geographical Research 13 (3), 355–362.
Zhang, M., Townend, I., Zhou, Y.X., Cai, H.Y., 2016. Seasonal variations of river and tide energy in the Yangtze Estuary, China. Earth Surf. Process. Landf. 41, 98–116.
Zhao, X.T., Han, S.Y., Li, P.R., 1996. Regional coastal evolution and sea level variations with geological records. In: Zhao, X.T. (Ed.), Sea Level Variations in China. Shangdong Science and Technology Press, Jinan, China, pp. 44–150.
Zhao, B.C., Wang, Z.H., Chen, J., Chen, Z.Y., 2008. Marine sediment records and relative sea level change during late Pleistocene in the Changjiang Delta area and adjacent continental shelf. Quat. Int. 186, 164–172.
Zhao, J., Guo, L.C., He, Q., Wang, Z.B., van Maren, D., Wang, X.Y., 2018. An analysis on half century morphological changes in the Changjiang Estuary: spatial variability under natural processes and human intervention. J. Mar. Syst. 181, 25–36.
Zheng, S.W., Cheng, H.Q., Shi, S.Y., Xu, W., Zhou, Q.P., Jiang, Y.H., Zhou, F.N., Cao, M. X., 2018a. Impact of anthropogenic drivers on subaqueous topographical change in the Datong to Xuliujing reach of the Yangtze River. Science China Earth Sciences 61, 940–950.
Zheng, S.W., Xu, Y.J., Cheng, H.Q., Wang, B., Xu, W., Wu, S.H., 2018b. River bed erosion of the final 565 kilometers of the Yangtze River (Changjiang) following construction of the three Gorges Dam. Sci. Rep. 8, 11917. https://doi.org/10.1038/s41598-018-30441-6.
Zhou, L.Y., Liu, J., Saito, Y., Zhang, Z.X., Chu, H.S., Hu, G., 2014. Coastal erosion as a major sediment supplier to continental shelves: example from the abandoned Old Huanghe (Yellow River) delta. Cont. Shelf Res. 82, 43–59.
Zhou, Z.Y., Ge, J.Z., Wang, Z.B., van Maren, D.S., Ma, J.F., Ding, P.X., 2019. Study of lateral flow in a stratified tidal channel-shoal system: the importance of intratidal salinity variation. Journal of Geophysical Research: Oceans 124, 6702–6719.
Zhu, H.F., Yun, C.X., Mao, Z.C., Wang, S.M., 1984. Characteristics and empiric relationships of wind generated wave in the Changjiang Estuary. Journal of East China Normal University 1, 74–85.
Zhu, Q., Yang, S.L., Ma, Y.X., 2014. Intra-tidal sedimentary processes associated with combined wave-current action on an exposed, erosional mudflat, southeastern Changjiang River Delta, China. Mar. Geol. 347, 95–106.
Zhu, L., He, Q., Shen, J., Wang, Y., 2016. The influence of human activities on morphodynamics and alteration of sediment source and sink in the Changjiang Estuary. Geomorphology 273, 52–62.
Zhu, L., He, Q., Shen, J., 2018. Modeling lateral circulation and its influence on the along-channel flow in a branched estuary. Ocean Dyn. 68, 177–191.
Zhu, C.Y., Guo, L.C., van Maren, D.S., Tian, B., Wang, X.Y., He, Q., Wang, Z.B., 2019. Decadal morphological evolution of the mouth zone of the Yangtze Estuary in response to human interventions. Earth Surf. Process. Landf. 44, 2319–2332.
Zhu, J.R., Chen, X.Y., Li, L.J., Wu, H., Gu, J.H., Lyu, H.H., 2020. Dynamics mechanism of an extremely severe saltwater intrusion in the Changjiang Estuary in February 2014. Hydrology Earth System Science 24, 1–14.
Zhu, C.Y., Guo, L.C., van Maren, D.S., Wang, Z.B., He, Q., 2021. Exploration of decadal tidal evolution in response to morphological and sedimentary changes in the Yangtze Estuary. Journal of Geophysical Research: Oceans 126. https://doi.org/10.1029/2020JC017019 e2020JC017019.